INTERIM REPORT

on

EXAMINATION, TESTING, AND EVALUATION OF IRRADIATED PRESSURE VESSEL SURVEILLANCE SPECIMENS FROM THE MONTICELLO NUCLEAR GENERATING PLANT

to

NORTHERN STATES POWER COMPANY

April 18, 1983

by

L. M. Lowry, M. P. Landow, J. S. Perrin,
A. M. Walters, R. G. Jung, and R. S. Denning

BATTELLE
Columbus Laboratories
505 King Avenue
Columbus, Ohio 43201

Battelle is not engaged in research for advertising, sales promotion, or publicity purposes, and this report may not be reproduced in full or in part for such purposes.

8308190358 830810
PDR ADOCK 05000263
P PDR

TABLE OF CONTENTS

	Page
SUMMARY	1
INTRODUCTION	3
SPECIMEN PREPARATION	6
CAPSULE RECOVERY AND DISASSEMBLY	10
EXPERIMENTAL PROCEDURES	17
Neutron Dosimetry	17
Charpy Impact Properties	22
Tensile Properties	24
Chemical Analysis	25
RESULTS AND DISCUSSION	27
Neutron Dosimetry	27
Charpy Impact Properties	39
Tensile Properties	57
Chemical Analysis	66
CONCLUSIONS	70
REFERENCES	72

APPENDIX A

INSTRUMENTED CHARPY EXAMINATION	A- 1
REFERENCES	A-27

LIST OF TABLES

		Page
TABLE 1.	INVENTORY OF CHARPY AND TENSILE SPECIMENS FROM THE TWO MONTICELLO 30 DEGREE SURVEILLANCE CAPSULE BASKETS	14
TABLE 2.	CALIBRATION DATA FOR THE HOT LABORATORY CHARPY IMPACT MACHINE USING AMMRC STANDARDIZED SPECIMENS	22
TABLE 3.	CROSS SECTIONS FOR THE IRRADIATED FLUX MONITORS (E> 1MeV) IN RADIALLY CENTERED TWO CAPSULE MESHES (MONTICELLO SURVEILLANCE CAPSULE) 30 DEGREE	32
TABLE 4.	CONSTANTS USED IN DOSIMETRY CALCULATIONS FOR THE MONTICELLO 30 DEGREE SURVEILLANCE CAPSULE	32
TABLE 5.	FLUX AND FLUENCE VALUES AT THE MONTICELLO SURVEILLANCE CAPSULE (30 DEGREE AZIMUTHAL LOCATION)	34
TABLE 6.	FLUX AND FLUENCE BEHIND THE MONTICELLO SURVEILLANCE CAPSULE AND AT THE MAXIMUM VESSEL WALL POSITION	35
TABLE 7.	CHARPY V-NOTCH IMPACT RESULTS FOR IRRADIATED BASE METAL SPECIMENS FOR THE MONTICELLO 30 DEGREE SURVEILLANCE CAPSULE	41
TABLE 8.	CHARPY V-NOTCH IMPACT RESULTS FOR IRRADIATED WELD METAL SPECIMENS FOR THE MONTICELLO 30 DEGREE SURVEILLANCE CAPSULE	42
TABLE 9.	CHARPY V-NOTCH IMPACT RESULTS FOR IRRADIATED HAZ METAL SPECIMENS FOR THE MONTICELLO 30 DEGREE SURVEILLANCE CAPSULE	43
TABLE 10.	SUMMARY OF CHARPY IMPACT PROPERTIES FOR IRRADIATED MATERIALS FROM THE MONTICELLO 30 DEGREE SURVEILLANCE CAPSULE	56
TABLE 11.	TENSILE PROPERTIES OF IRRADIATED MATERIALS FROM THE MONTICELLO 30 DEGREE SURVEILLANCE CAPSULE	59
TABLE 12.	CHEMICAL ANALYSIS RESULTS FOR IRRADIATED WELD METAL SPECIMENS FROM THE MONTICELLO SURVEILLANCE CAPSULE	68

LIST OF TABLES
(Continued)

Page

TABLE A-1. INSTRUMENTED CHARPY IMPACT RESULTS FOR IRRADIATED BASE METAL SPECIMENS FROM THE MONTICELLO 30 DEGREE SURVEILLANCE CAPSULE .....A- 7

TABLE A-2. INSTRUMENTED CHARPY IMPACT RESULTS FOR IRRADIATED WELD METAL SPECIMENS FROM THE MONTICELLO 30 DEGREE SURVEILLANCE CAPSULE .....A- 8

TABLE A-3. INSTRUMENTED CHARPY IMPACT RESULTS FOR IRRADIATED HAZ METAL SPECIMENS FROM THE MONTICELLO 30 DEGREE SURVEILLANCE CAPSULE .....A- 9

LIST OF FIGURES

		Page
FIGURE 1.	MONTICELLO CORE MIDPLANE SHOWING THE LOCATION OF THE 30 DEGREE, 120 DEGREE, AND 300 DEGREE SURVEILLANCE CAPSULES	5
FIGURE 2.	CHARPY V-NOTCH IMPACT SPECIMEN	8
FIGURE 3.	TENSILE SPECIMEN	9
FIGURE 4.	MONTICELLO 30 DEGREE SURVEILLANCE CAPSULE CONTAINING TWO BASKETS	11
FIGURE 5.	PHOTOGRAPH SHOWING BURST OPEN TENSILE TUBE G5 FROM THE MONTICELLO 30 DEGREE SURVEILLANCE CAPSULE	15
FIGURE 6.	TYPICAL CHARPY PACKET WITH CHARPY SPECIMEN	16
FIGURE 7.	TYPICAL TENSILE TUBE WITH TENSILE SPECIMEN	16
FIGURE 8.	MONTICELLO CORE, INTERNAL VESSEL STRUCTURES, AND VESSEL WALL GEOMETRY USED IN THE DOT CALCULATION	29
FIGURE 9.	COMPARISON OF DOT SPECTRUM WITH FISSION SPECTRUM AT THE MONTICELLO 30 DEGREE SURVEILLANCE CAPSULE	30
FIGURE 10.	CALCULATED FLUX (E > 1 MeV) AT THE MONTICELLO 30 DEGREE CAPSULE, INNER WALL, 1/4 THICKNESS, AND 3/4 THICKNESS AS A FUNCTION OF AZIMUTHAL ANGLE	36
FIGURE 11.	FLUENCE AT 1/4T and 3/4T POSITIONS AS A FUNCTION OF TIME FOR THE MONTICELLO NUCLEAR GENERATING REACTOR VESSEL	38
FIGURE 12.	CHARPY V-NOTCH IMPACT ENERGY VERSUS TEST TEMPERATURE FOR IRRADIATED BASE METAL SPECIMENS FROM THE MONTICELLO 30 DEGREE SURVEILLANCE CAPSULE	44
FIGURE 13.	CHARPY V-NOTCH LATERAL EXPANSION VERSUS TEST TEMPERATURE FOR IRRADIATED BASE METAL SPECIMENS FROM THE MONTICELLO 30 DEGREE SURVEILLANCE CAPSULE	45
FIGURE 14.	CHARPY V-NOTCH PERCENT DUCTILE SHEAR VERSUS TEST TEMPERATURE FOR IRRADIATED BASE METAL SPECIMENS FROM THE MONTICELLO 30 DEGREE SURVEILLANCE CAPSULE	46

LIST OF FIGURES
(Continued)

Page

FIGURE 15. CHARPY V-NOTCH IMPACT ENERGY VERSUS TEST TEMPERATURE FOR IRRADIATED WELD METAL SPECIMENS FROM THE MONTICELLO 30 DEGREE SURVEILLANCE CAPSULE 47

FIGURE 16. CHARPY V-NOTCH LATERAL EXPANSION VERSUS TEST TEMPERATURE FOR IRRADIATED WELD METAL SPECIMENS FROM THE MONTICELLO 30 DEGREE SURVEILLANCE CAPSULE 48

FIGURE 17. CHARPY V-NOTCH PERCENT DUCTILE SHEAR VERSUS TEST TEMPERATURE FOR IRRADIATED WELD METAL SPECIMENS FROM THE MONTICELLO 30 DEGREE SURVEILLANCE CAPSULE 49

FIGURE 18. CHARPY V-NOTCH IMPACT ENERGY VERSUS TEST TEMPERATURE FOR IRRADIATED HAZ METAL SPECIMENS FROM THE MONTICELLO 30 DEGREE SURVEILLANCE CAPSULE 50

FIGURE 19. CHARPY V-NOTCH LATERAL EXPANSION VERSUS TEST TEMPERATURE FOR IRRADIATED HAZ METAL SPECIMENS FROM THE MONTICELLO 30 DEGREE SURVEILLANCE CAPSULE 51

FIGURE 20. CHARPY V-NOTCH PERCENT DUCTILE SHEAR VERSUS TEST TEMPERATURE FOR IRRADIATED HAZ METAL SPECIMENS FROM THE MONTICELLO 30 DEGREE SURVEILLANCE CAPSULE 52

FIGURE 21. CHARPY IMPACT SPECIMEN FRACTURE SURFACES FOR IRRADIATED BASE METAL SPECIMENS FROM THE MONTICELLO 30 DEGREE SURVEILLANCE CAPSULE 53

FIGURE 22. CHARPY IMPACT SPECIMEN FRACTURE SURFACES FOR IRRADIATED WELD METAL SPECIMENS FROM THE MONTICELLO 30 DEGREE SURVEILLANCE CAPSULE 54

FIGURE 23. CHARPY IMPACT SPECIMEN FRACTURE SURFACES FOR IRRADIATED HAZ METAL SPECIMENS FROM THE MONTICELLO 30 DEGREE SURVEILLANCE CAPSULE 55

FIGURE 24. BASE METAL YIELD AND ULTIMATE TENSILE STRENGTHS VERSUS TEST TEMPERATURE FOR IRRADIATED TENSILE SPECIMENS FROM THE MONTICELLO 30 DEGREE SURVEILLANCE CAPSULE 60

FIGURE 25. BASE METAL TOTAL ELONGATION AND REDUCTION IN AREA VERSUS TEST TEMPERATURE FOR IRRADIATED TENSILE SPECIMENS FROM THE MONTICELLO 30 DEGREE SURVEILLANCE CAPSULE 61

LIST OF FIGURES
(Continued)

Page

FIGURE 26. POSTTEST PHOTOGRAPHS OF IRRADIATED BASE METAL TENSILE SPECIMENS SHOWING BOTH THE REDUCED AREAS AND FRACTURE SURFACES (MONTICELLO 30 DEGREE SURVEILLANCE CAPSULE) 62

FIGURE 27. POSTTEST PHOTOGRAPHS OF IRRADIATED WELD METAL TENSILE SPECIMENS SHOWING BOTH THE REDUCED AREAS AND FRACTURE SURFACES (MONTICELLO 30 DEGREE SURVEILLANCE CAPSULE) 63

FIGURE 28. POSTTEST PHOTOGRAPHS OF IRRADIATED HAZ METAL TENSILE SPECIMENS SHOWING BOTH THE REDUCED AREAS AND FRACTURE SURFACES (MONTICELLO 30 DEGREE SURVEILLANCE CAPSULE) 64

FIGURE 29. TYPICAL TENSILE LOAD-ELONGATION CURVE 65

FIGURE A-1. AN IDEALIZED LOAD-TIME HISTORY FOR A CHARPY IMPACT TEST .....A- 2

FIGURE A-2. GRAPHICAL ANALYSIS OF CHARPY IMPACT DATA .....A- 4

FIGURE A-3. DIAGRAM OF INSTRUMENTATION ASSOCIATED WITH INSTRUMENTED CHARPY EXAMINATION .....A- 5

FIGURE A-4. INSTRUMENTED CHARPY IMPACT DATA FOR IRRADIATED BASE METAL SPECIMENS FROM THE MONTICELLO 30 DEGREE SURVEILLANCE CAPSULE A-10

FIGURE A-5. INSTRUMENTED CHARPY IMPACT DATA FOR IRRADIATED WELD METAL SPECIMENS FROM THE MONTICELLO 30 DEGREE SURVEILLANCE CAPSULE A-14

FIGURE A-6. INSTRUMENTED CHARPY IMPACT DATA FOR IRRADIATED HAZ METAL SPECIMENS FROM THE MONTICELLO 30 DEGREE SURVEILLANCE CAPSULE A-19

FIGURE A-7. THE SIX TYPES OF FRACTURES FOR NOTCHED BAR BENDING A-23

FIGURE A-8. INSTRUMENTED CHARPY LOAD VERSUS TEST TEMPERATURE FOR IRRADIATED BASE METAL SPECIMENS FROM THE MONTICELLO 30 DEGREE SURVEILLANCE CAPSULE A-24

FIGURE A-9. INSTRUMENTED CHARPY LOAD VERSUS TEST TEMPERATURE FOR IRRADIATED WELD METAL SPECIMENS FROM THE MONTICELLO 30 DEGREE SURVEILLANCE CAPSULE A-25

FIGURE A-10. INSTRUMENTED CHARPY LOAD VERSUS TEST TEMPERATURE FOR IRRADIATED HAZ METAL SPECIMENS FROM THE MONTICELLO 30 DEGREE SURVEILLANCE CAPSULE A-26

INTERIM REPORT

on

EXAMINATION, TESTING, AND EVALUATION OF IRRADIATED PRESSURE VESSEL SURVEILLANCE SPECIMENS FROM THE MONTICELLO NUCLEAR GENERATING PLANT

to

NORTHERN STATES POWER COMPANY

from

BATTELLE
Columbus Laboratories

by

L. M. Lowry, M. P. Landow, J. S. Perrin
A. M. Walters, R. G. Jung, and R. S. Denning

April 18, 1983

SUMMARY

A 30-degree azimuthal surveillance capsule assembly was received from the Monticello Reactor. The capsule was visually examined, opened, and the specimens inventoried. The two baskets of this capsule assembly contained twice the number of tensile and Charpy specimens required for testing and evaluation. Each basket contained a complete compliment of eight tensile specimens and 36 Charpy specimens. One set of specimens was stamped with a combination of three digits beginning with the letter J and the other set of specimens was stamped with a combination of three digits beginning with the letter D. It was originally believed that both sets of specimens were from

the Monticello core beltline plates. During disassembly it was noted that one tensile tube had burst open and probably contained two weld specimens beginning with the letter D. Therefore, the complete set of specimens (those beginning with the letter J) were chosen for testing.

However, it has since been found that there presently appears to be a lack of complete traceability for the set of specimens from the Monticello 30-degree surveillance capsule with the letter J designation. Additional actions by Northern States Power, including further record searching and possibly additional chemical analysis, may be required before a complete evaluation can be made. Therefore, this report provides only the results of those tests already performed. Also, because of the apparent present lack of traceability to core beltline plates of the specimens already tested, no comparison of these irradiated properties and baseline unirradiated properties has been made. It is anticipated that this interim report will be finalized after additional information and test data are obtained.

Four iron and four copper neutron monitor wires from Charpy packets G-2, G-6, G-7, and G-8 were analyzed. The capsule specimens received a fast neutron fluence (E > 1 MeV) of 2.98×10^7 n/cm^2. The calculated maximum fast neutron fluence at the 1/4T pressure vessel wall position occurred at about 3 degrees azimuthal and was 7.2×10^{17} n/cm^2 at the time the capsule was removed from the reactor vessel.

Charpy impact specimens were tested to determine the impact behavior, including the impact energy, lateral expansion, fracture appearance, and upper shelf energies for irradiated base metal, weld metal, and heat affected zone (HAZ) metal. The tensile properties of the irradiated specimens were determined, including the yield and ultimate tensile strengths, as well as uniform and total elongations, and reductions in area.

The halves of three broken weld metal Charpy V-notch specimens were analyzed for 10 elemental constituents including copper, phosphorus, nickel, molybdenum, chromium, manganese, vanadium, silicon, sulfur, and carbon.

INTRODUCTION

Irradiation of materials such as pressure vessel steels used in commercial nuclear power reactors cause changes in the mechanical properties of the material. Specimens such as tensile and Charpy V-notch are used to evaluate radiation induced changes in the material tensile, impact, and fracture properties.(1-6)* Tensile properties generally exhibit a decrease in uniform elongation, total elongation, and reduction-in-area accompanied by an increase in yield and ultimate tensile strength with increasing neutron exposure. The impact properties as determined by Charpy V-notch impact tests generally exhibit an increase in the ductile-to-brittle transition temperature and a drop in the upper shelf energy.

A reactor pressure vessel receives neutron irradiation during operation and is simultaneously subject to radiation-induced embrittlement. Because the reactor pressure vessel contains the reactor core and coolant, the changes in fracture properties must be known. Therefore, a pressure vessel surveillance program is required by the U.S. Nuclear Regulatory Commission (NRC) and material surveillance capsules containing appropriate specimens are placed into each commercial nuclear power reactor prior to initial startup. The purpose of the surveillance program associated with each reactor is to monitor the changes in mechanical properties as a function of neutron exposure.

The Northern States Power Company has a surveillance program for its Monticello Nuclear Generating Plant which is described in reports issued by the General Electric Company.(7,16) The program is based on ASTM E185 "Standard Practice for Conducting Surveillance Tests for Light-Water Cooled Nuclear Power Reactor Vessels",(8) and was conducted using numerous other American Society for Testing and Materials (ASTM) and American Society of Mechanical Engineers (ASME) standards.(9-15)

---

* References are listed at the end of the text (pages 72, 73, and 74)

Three surveillance capsules, each containing Charpy and tensile mechanical property test specimens and iron (Fe), copper (Cu), and nickel (Ni) dosimeter wires, were inserted into the reactor pressure vessel prior to the initial startup of the Monticello Nuclear Reactor. Figure 1 shows the position of the three (30, 120, and 300 degree) capsules.

The American Society of Mechanical Engineers (ASME) Boiler and Pressure Vessel Code, Section III, Appendix G for Nuclear Power Plant Components, Division 1 presents a procedure for obtaining allowable loading for ferritic pressure retaining materials to protect against nonductile failure. The procedure is based on the principles of linear elastic fracture mechanics.

The present report includes descriptions of the recovery and disassembly of the Monticello 30-degree surveillance capsule and the examination of the test specimens and dosimetry wires. This report also includes the procedures and results of the tensile and Charpy impact tests and dosimetry and chemical analysis for the Monticello 30-degree surveillance capsule which was removed from the reactor during November of 1981.

The BCL surveillance capsule quality assurance program is a planning, controlling, surveillance, and documentation program to assure that all work is conducted following the basic principles of scientific investigation. The organization of this program follows the requirements of Title 10 CFR Part 50 Appendix B, ASME NA-4000, and ASME Section III NB-2360, "Calibration of Instruments and Equipment", where applicable to testing verification. All tests were conducted in full compliance with the Nuclear Materials Technology Quality Assurance Manual. This manual is responsive to all 18 criteria of a quality assurance program.

Implementation of the quality assurance requirements included the use of technical and quality assurance authorized work instructions, procedures, and work completion forms. The forms were used to document that all data was generated in compliance with the procedures and conformed to requirements of the applicable ASTM specifications. Both Charpy and tensile machines were periodically certified to ensure accurate and reliable results. A system of technical overchecks and independent quality assurance surveillance was used to insure compliance with the procedures and the overall

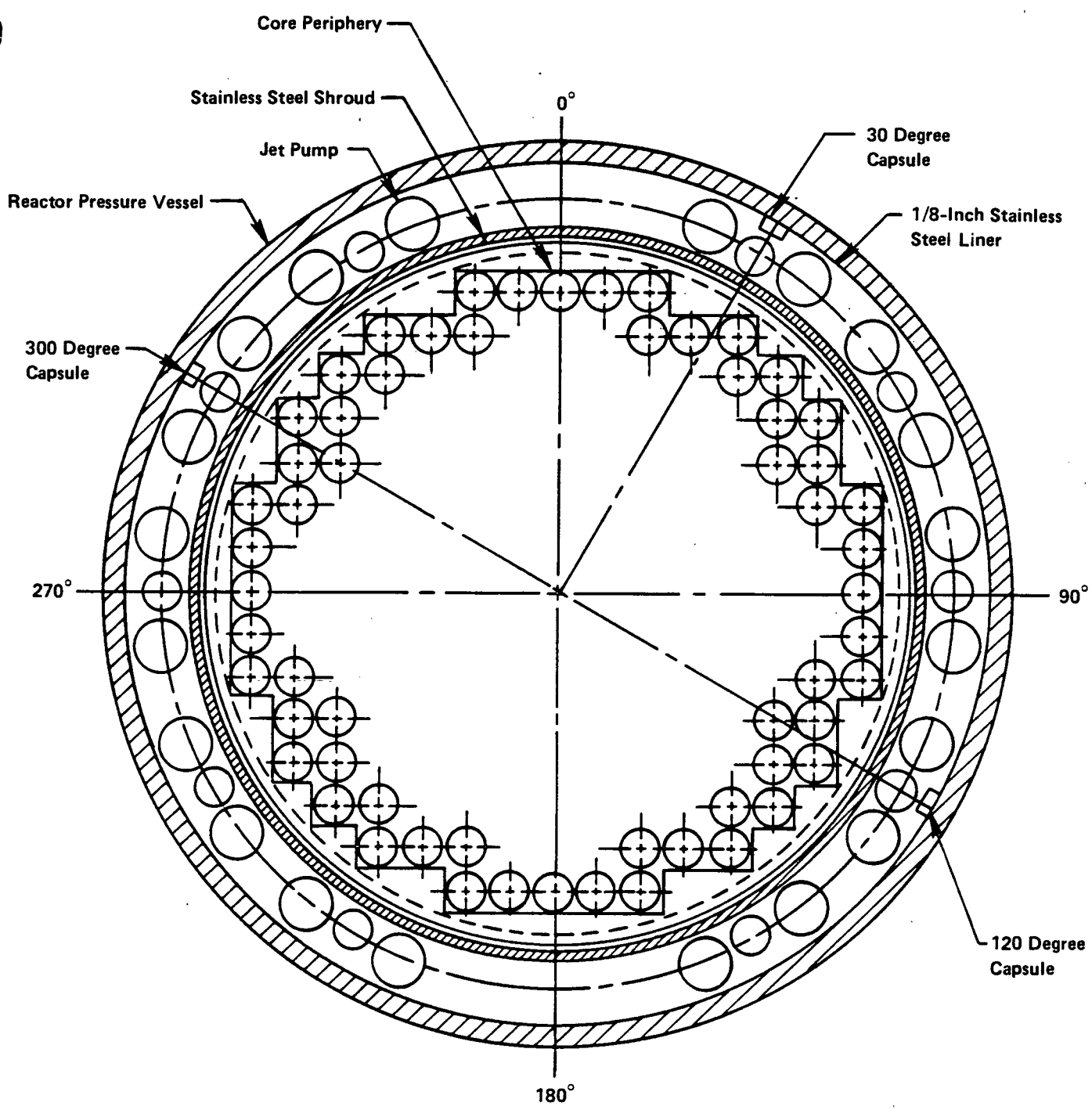

FIGURE 1. MONTICELLO CORE MIDPLANE SHOWING THE LOCATION OF THE 30 DEGREE, 120 DEGREE, AND 300 DEGREE SURVEILLANCE CAPSULES

quality assurance program. All personnel were trained and certified in compliance with ANSI N45.2.6 as being technically qualified for the task being undertaken and were aware of the quality assurance requirements.

All data-generating instruments and apparatus were calibrated by standards traceable to the U.S. Bureau of Standards.

Specimen receipt and the packaging and shipment of wastes for disposal are in accordance with the quality assurance program which is responsive to Title 10 CFR Part 71, Appendix E. All waste material from the capsules was disposed of in containers authorized by the applicable Department of Transportation (DOT) and Nuclear Regulatory Commission (NRC) regulations at a properly licensed waste disposal site. Mechanical property specimens and dosimeter wires are being held for 12 months following receipt of the final technical report.

SPECIMEN PREPARATION

The Monticello reactor pressure vessel was purchased from the Chicago Bridge and Iron Company, Birmingham, Alabama.[16] The vessel was designed and constructed in accordance with the ASME Boiler and Pressure Vessel Code - Section III, 1965 Edition with addenda to and including Summer 1966 addenda in accordance with the General Electric APED specification No. 21A1112, Revision 6. Base metal specimens were cut from flat slabs cut parallel to both the plate surfaces at a depth of one-quarter- and three-quarter-plate thickness. The Charpy and tensile specimens were machined with their longitudinal axes parallel to the plate rolling direction. The Charpy specimen notches were cut perpendicular to the plate surface and designated longitudinal specimens.

The Charpy weld metal specimens were machined in a direction transverse to the weld direction; thus, only the central notched section of the specimen would necessarily be composed of weld-deposited metal. Charpy specimens were taken throughout the weld section to a depth of 0.75 inch from the weld root. The Charpy weld metal specimens long axes were, therefore,

parallel to the plate surface, and the notches were cut perpendicular to the plate surface. The tensile weld metal specimens were composed entirely of weld metal and were obtained by machining the specimens parallel to the weld length and parallel to the plate surface.

The Charpy weld HAZ metal specimens were machined in a direction transverse to the weld length and parallel to the plate surface. The axes of the notches were then cut perpendicular to the plate surface, with the notch located at the intersection of the base metal and weld deposit. The tensile weld HAZ metal specimens were machined transverse to the weld length and parallel to the plate surface. The joint between the base metal and weld deposit was located at the center of the tensile specimen gage length.

A modification of a marking system developed by the U.S. Steel Corporation Applied Research Laboratory (designated FAB Code) was used to mark one end of each surveillance Charpy and tensile specimen for later positive identification.

The Charpy V-notch impact specimen design is shown in Figure 2. This is a standard specimen design recommended in ASTM E23-82 entitled "Standard Methods for Notched Bar Impact Testing of Metallic Materials". The tensile specimen design is shown in Figure 3. This specimen design conforms to recommendations in ASTM E8-81 for small-size specimens. The ASTM E8-81 standard is entitled "Standard Methods for Tension Testing Metallic Materials".

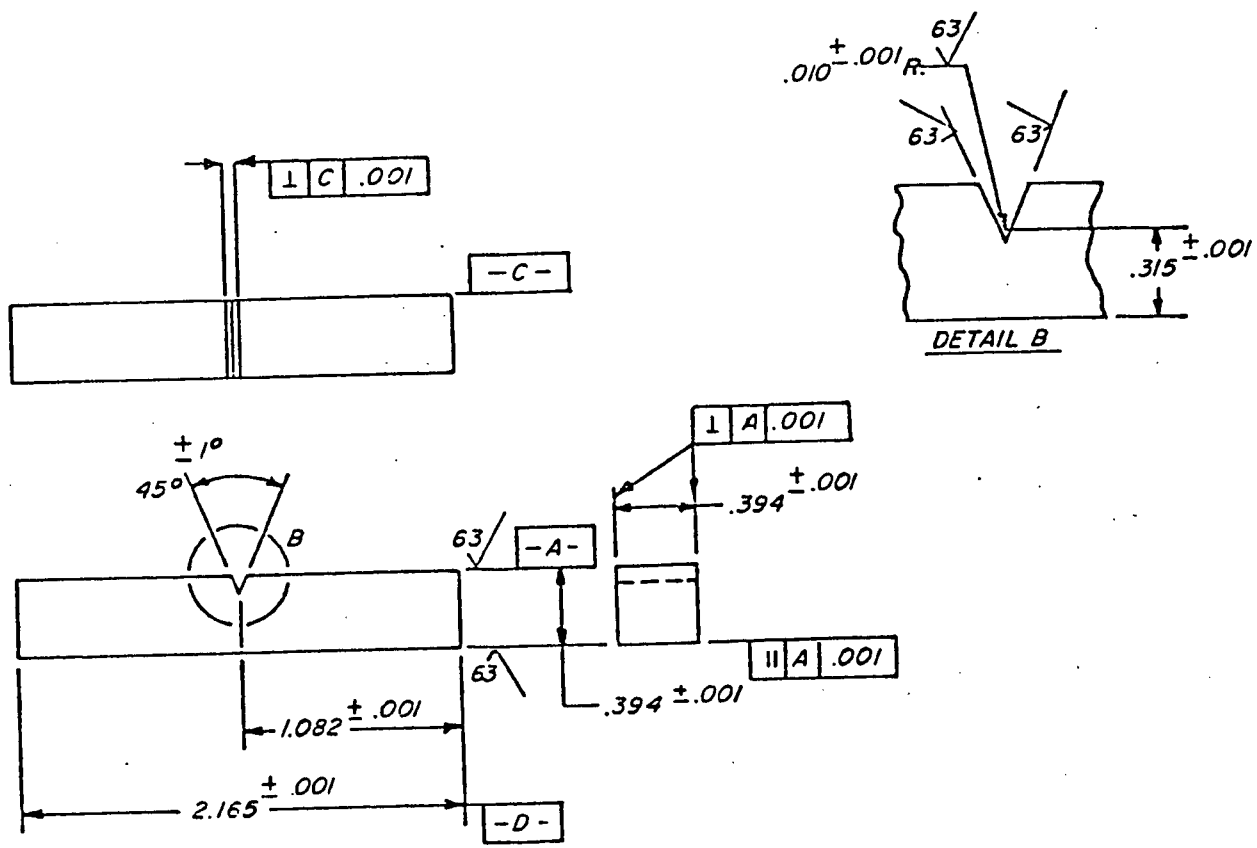

FIGURE 2. CHARPY V-NOTCH IMPACT SPECIMEN

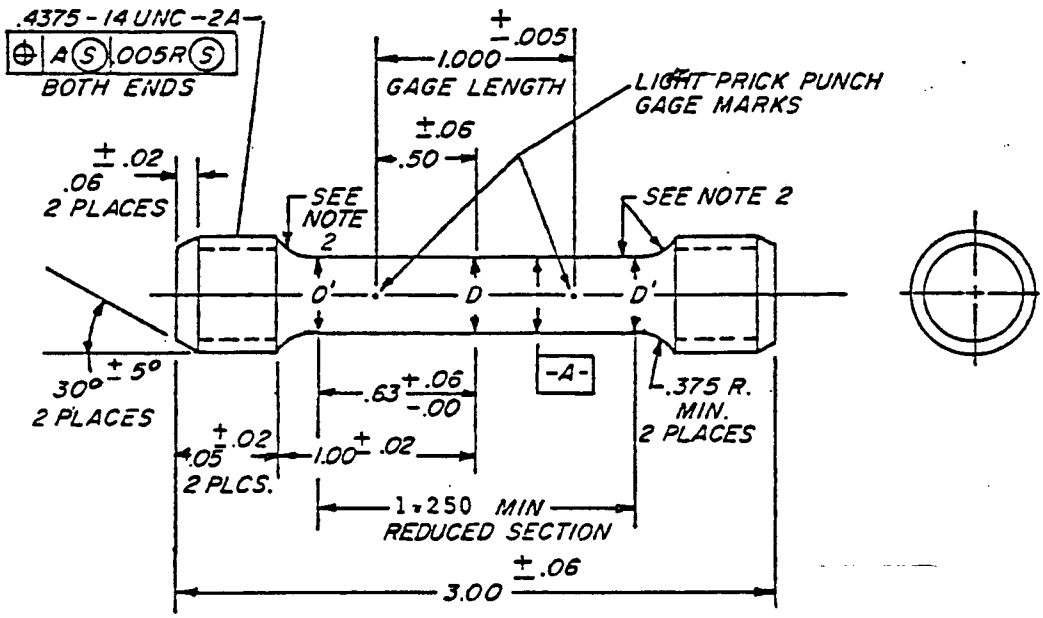

NOTES

1. D = .250 ± .001 DIA. AT CENTER OF REDUCED SECTION. D' = ACTUAL D DIA +.002 TO .005 AT ENDS OF REDUCED SECTION TAPERING TO D AT CENTER

2. GRIND REDUCED SECTION & RADII TO 32/ RADII TO BE TANGENT TO REDUCED SECTION WITH NO CIRCULAR TOOL MARKS AT POINT OF TANGENCY OR WITHIN REDUCED SECTION. POINT OF TANGENCY SHALL NOT LIE WITHIN REDUCED SECTION.

FIGURE 3. TENSILE SPECIMEN

CAPSULE RECOVERY AND DISASSEMBLY

The surveillance capsule assembly was shipped from the Monticello Reactor site to the Battelle Columbus Laboratories (BCL) hot laboratory for postirradiation examination. Upon arrival at BCL on February 2, 1982, the assembly was transferred to a hot cell for visual examination, serial number verification, photography, and disassembly.

The initial visual examination revealed two notable features. The first and most obvious was that the capsule contained two baskets (see Figure 4). From these photographs, it appeared that each basket contained four tensile tubes and three Charpy packets for a total of eight tensile tubes and six Charpy packets. The second and less obvious feature was what appeared to be a burst-open tensile tube. The dark jagged edge of the burst-open tensile tube can be seen through the hole in the containment basket indicated by the arrow in Figure 4. After disassembly the tensile tubes and Charpy packets were again examined. The lower basket bore the serial number 117C 3911 G-1. Both baskets bore the Monticello Reactor code number 19. Both also bore the basket code number 1, which corresponds to the applicable group number, and is the same as the last digit in the basket serial number. The Monticello Reactor code number and basket code number appear as a binary code, and it is explained in Reference 7. The binary code numbers (drilled holes) appeared in the lower corners of the basket surface facing the pressure vessel wall (back face) and the serial number (stamped alphanumeric) appeared in the lower center of the basket surface facing the core (front face).

Both baskets were opened by cutting away the lower (spacer packed) ends using a flexible abrasive cut-off wheel attached to a Mototool*. The upper basket was opened first and contained four intact tensile tubes and three Charpy packets. Identification numbers of the tubes and packets are listed below in the order of their location with the first being located

---

* Mototool is a trademark for a variable, high-speed motor attached to a flexible shaft and chuck for grinding and cutting operations.

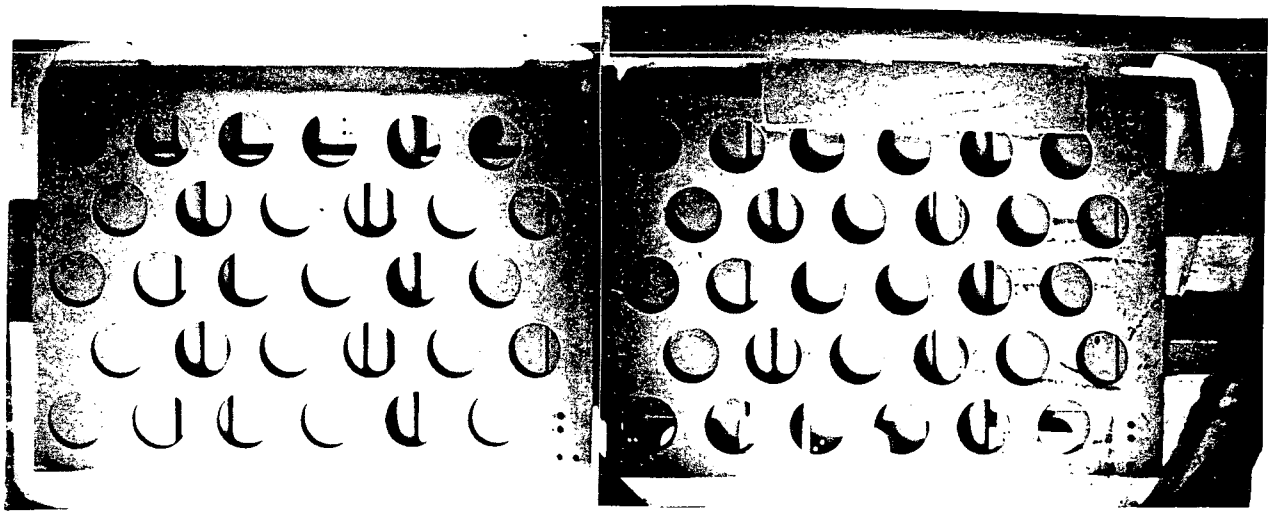

0.3X C-9639 and -9640

CAPSULE BACK SIDE*

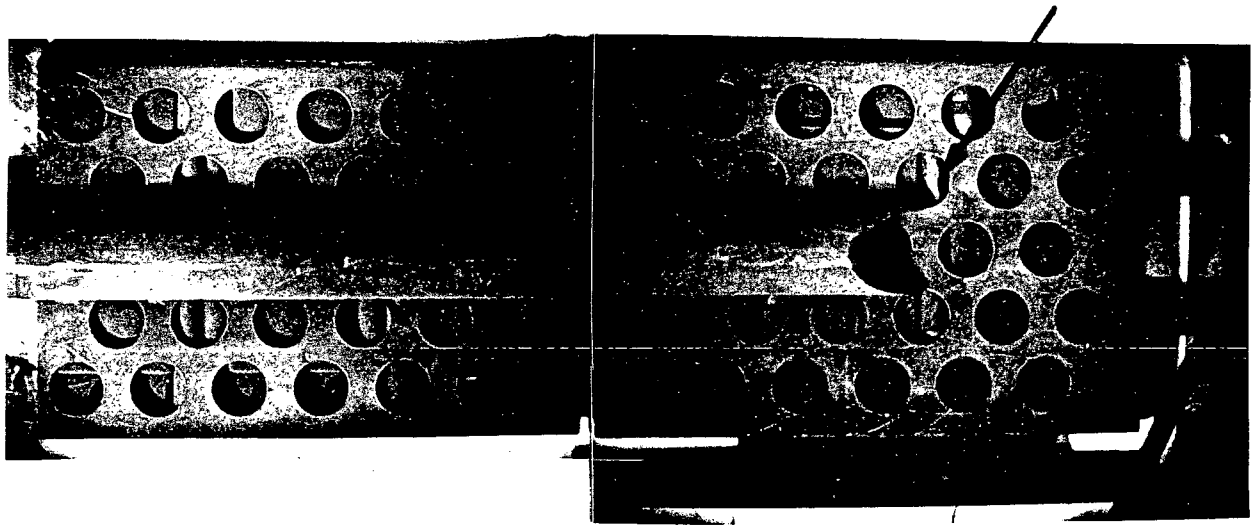

0.3X C-9634 and -9635

CAPSULE FRONT SIDE*

*The capsule front side was facing the core and back side was facing the pressure vessel wall.

FIGURE 4. MONTICELLO 30 DEGREE SURVEILLANCE CAPSULE CONTAINING TWO BASKETS

at the top of upper basket and the last being located at the bottom of the upper basket. The Charpy packets had both the binary code numbers and the alphanumeric identification, whereas the tensile tubes contained only a letter and a number stamped into one end of the plug.

Charpy Packet 6	117C 3913 G-6
Tensile Tube	G6
Tensile Tube	G8
Charpy Packet 8	117C 3913 G-8
Tensile Tube	G9
Tensile Tube	G10
Charpy Packet 7	117C 3913 G-7

Upon consulting with Northern States Power Company personnel, the decision was made to open the second basket. Identification numbers of the tubes and packets are listed below. The list is in order of their location, with the first being located at the top of the lower basket, and the last being located at the bottom of the lower basket. Again, the Charpy packets had both the binary code numbers and alphanumeric identification, whereas the tensile tubes contained only a letter and a number stamped into one end of the plug.

Charpy Packet 1	117C 3913 G-1
Tensile Tube	G1
Tensile Tube	G3
Charpy Packet 2	117C 3913 G-2
Tensile Tube	G4
Tensile Tube	G5
Charpy Packet 3	117C 3913 G-3

The six Charpy packets were also opened using the abrasive cut-off wheel to remove one end of the packet. The specimens were then removed by shaking the packet and allowing the specimens to drop out the open end. Each Charpy packet contained one iron (Fe), one copper (Cu), and one nickel (Ni) dosimeter wire. An inventory of the Charpy specimens is given in Table 1, and a total of 25 base metal, 25 weld metal, and 22 HAZ metal specimens were recovered.

Seven of the tensile tubes were opened using the abrasive cut-off wheel to remove one end of the tube. The specimens were then removed by shaking the tube and allowing the specimens to drop out the open end. An inventory of the tensile specimens is also given in Table 1, and a total of five base metal, four weld metal, and five HAZ metal specimens were recovered.

It was noted that the tensile tube G5 appeared to have burst open, as shown in Figure 5. Note that the tube burst in two positions, near the center of the two tensile specimens. It is unlikely that the burst occurred simultaneously and, therefore, it is postulated that the following sequence of events occurred: (1) the tensile tube G5 was not sealed during fabrication or a leak occurred after insertion into the reactor; (2) water leaked into the tube and reacted with the contents (oxidized the iron and aluminum) and an effective gas tight seal was formed at the center of the tube producing two compartments within the tensile tube; (3) hydrogen pressure produced from the water/metal reaction caused both compartments to burst open. After again consulting with the Northern States Power Company personnel, this tensile tube G5, along with the two contained tensile specimens, were discarded as waste.

A photograph of a typical Charpy packet is shown with a single Charpy impact specimen is Figure 6. Similarly, a photograph of a typical tensile tube is shown with a single tensile specimen in Figure 7.

TABLE 1. INVENTORY OF CHARPY AND TENSILE SPECIMENS FROM THE TWO MONTICELLO 30 DEGREE SURVEILLANCE CAPSULE BASKETS ("FAB" CODE)

Charpy Packets					
G-1[a]	G-2[b]	G-3[c]	G-6[a]	G-7[b]	G-8[c]
D3M	D6A	DBT	JDJ	JEM	JKM
D1C	D5C	D72	JD4	JEK	JKK
D3P	D5B	D7E	JD5	JEY	JLM
D3E	D57	DBU	JDU	JJT	JKT
D3L	D51	D76	JE3	JE7[a]	JK5[b]
D33	D52	DAE	DE5	JEL	JLK
D3Y	D53	D77	JCP	JJ7	JKD
D37	D55	D7A	JD1	JJP	JKA[b]
D3A	D56	D75	JD4	JEV	JL2
D35	D5A	D74	JE4	JJM	JLB
D34	D6B	D73	JDY	JJE	JLE
D36	D5Y	D71	JE1	JEP	JLC

Tensile Tubes						
G1[a]	G3[c]	G4	G6[b]	G8[c]	G9	G10
DC2	DE3	DC5[a]	JC1	JCK	JBM[b]	JC6[c]
DC4	DE3	DDC[b]	JC2	JCM	JB2[a]	JB6[a]

(a) Base metal specimens
(b) Weld metal specimens except as noted
(c) HAZ metal specimens except as noted

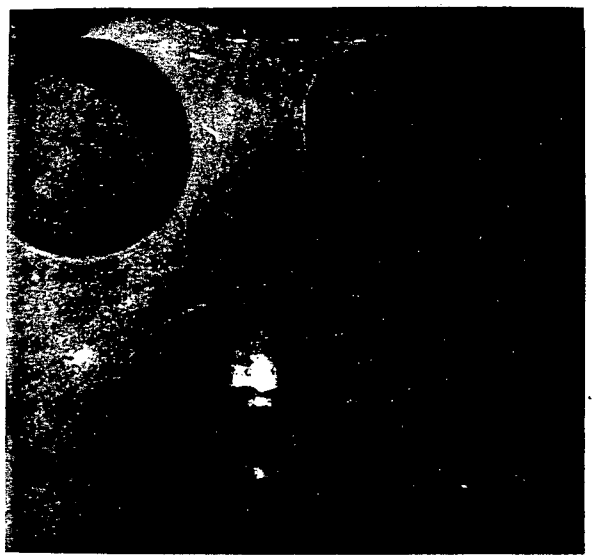

2X C-9637

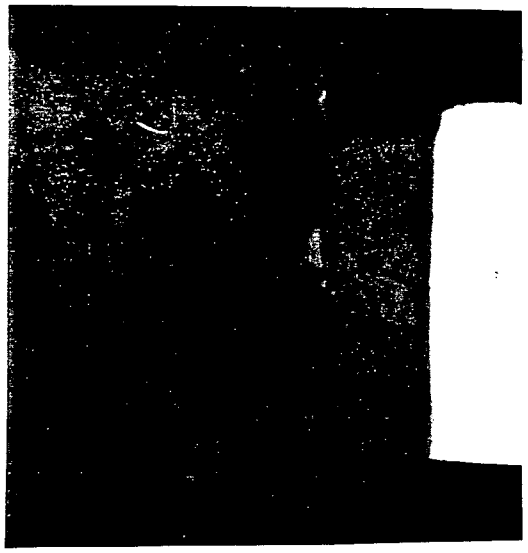

2X C-9636

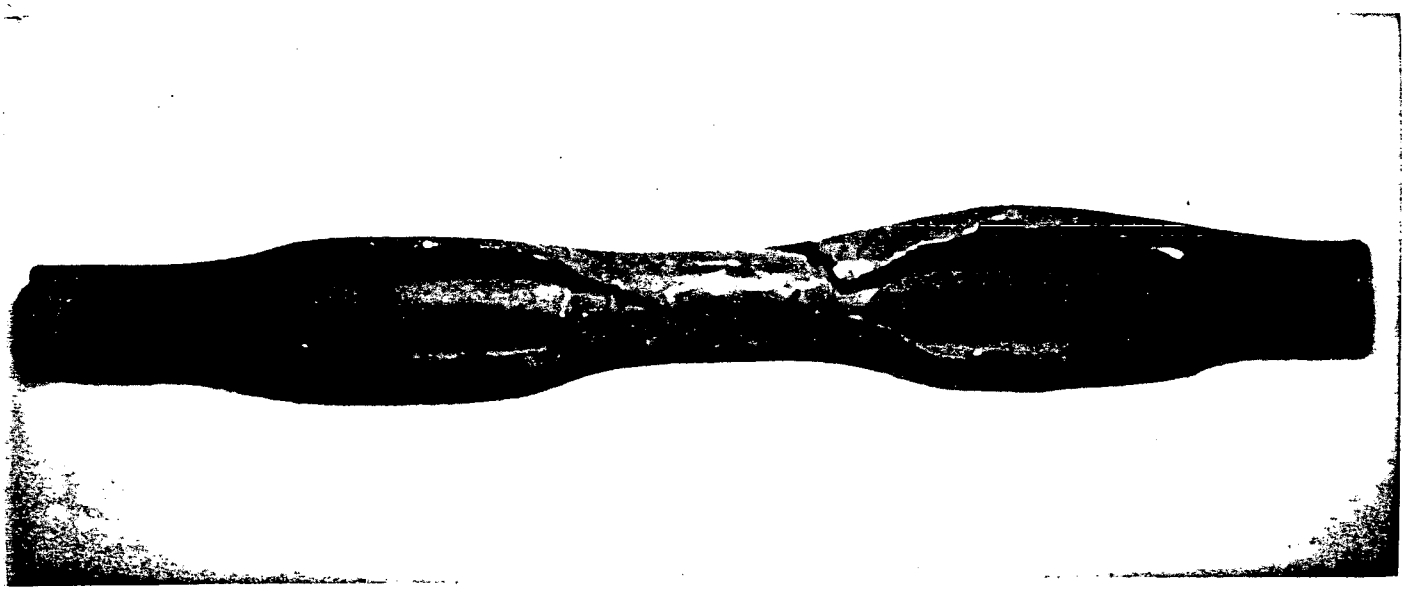

1X C-9828

FIGURE 5. PHOTOGRAPH SHOWING BURST OPEN TENSILE TUBE G5 FROM THE MONTICELLO 30 DEGREE SURVEILLANCE CAPSULE

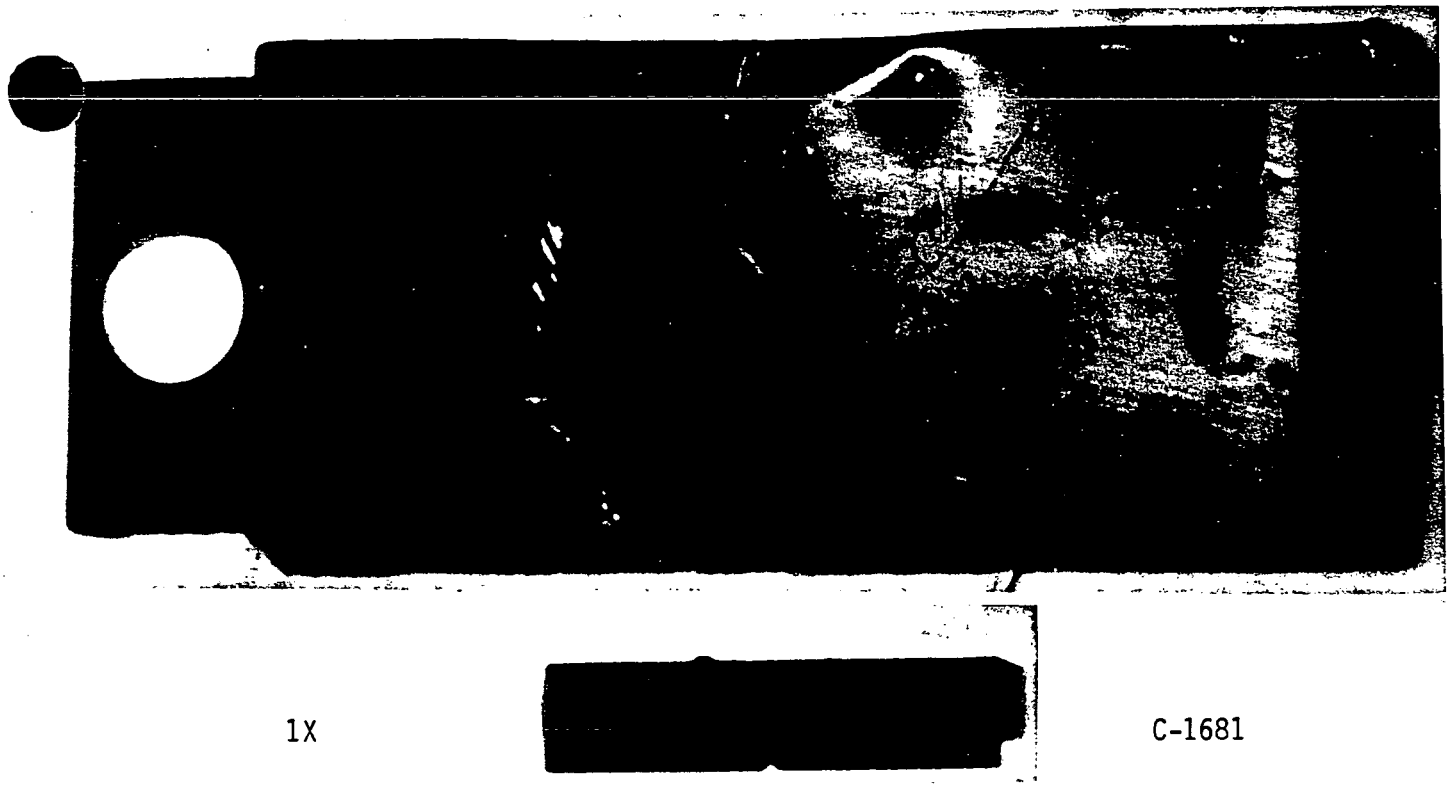

1X C-1681

FIGURE 6. TYPICAL CHARPY PACKET WITH CHARPY SPECIMEN

1X C-1680

FIGURE 7. TYPICAL TENSILE TUBE WITH TENSILE SPECIMEN

EXPERIMENTAL PROCEDURES

This section of the report describes the general procedures used to determine the neutron (>0.1 and >1.0 MeV) flux and fluence and to determine the pressure vessel material impact and tensile properties. The general procedures for chemical analysis are also included. All tests, except those for carbon analysis under Chemical Analysis, were performed at Battelle's Columbus Laboratories (BCL). All data evaluations were performed at BCL and the original data are recorded in Laboratory Record Book 37550.

Neutron Dosimetry

Each of the two Monticello surveillance baskets contained three Charpy specimen packets. The flux monitor wires, one each of iron (Fe), copper (Cu), and nickel (Ni), were recovered from inside each of the Charpy packets. Each wire was identified, placed in a plastic vial, brought out of cell, ultrasonically cleaned in a water/soap solution, placed in a clean vial, and transferred to the radiochemistry area for further cleaning and analysis. The wires were cleaned by wiping using successive swabs containing dilute acid (10 volume percent nitric for Cu and 25 volume percent hydrochloric for Fe), distilled water, and reagent alcohol until a negligible contamination level was reached. Because of the short half-life associated with the ^{58}Ni (n, p) ^{58}Co reaction (71.2 days) the nickel dosimeter wires were not counted and therefore only the iron and copper dosimeter wire data was generated.

Depending on the wire activity, a suitable and representative sample was selected for counting. Four Fe and four Cu dosimeter wires from Charpy packets G-2, G-6, G-7, and G-8 were weighted to an accuracy of $\pm$ 0.0001 g using a calibrated (NBS traceable) analytical balance. The eight wires were then mounted and analyzed by gamma ray spectroscopy. Fast neutron flux and

fluence values with energies greater than 0.1 MeV and greater than 1.0 MeV at the capsule wall, 1/4 T, and 3/4 T locations were calculated. Data used in these determinations included the following:

Dosimeter Material	Reaction	Threshold Energy, MeV	Half-Life
Fe, pure	^{54}Fe (n, p) ^{54}Mn	1.5	312.6 days
Cu, high purity	^{63}Cu (n, α) ^{60}Co	5.0	5.27 years

The ASTM procedures followed in the measurement of the monitor activities and calculation of the neutron flux included:

ASTM E261-77, "Measuring Neutron Flux, Fluence, and Spectra by Radioactivation Techniques"

ASTM E263-82, "Determining Fast-Neutron Flux Density by Radioactivation of Iron"

ASTM E522-78, "Calibration of Germanium Detectors for Measurement of Gamma-Ray Emission Rates of Radionuclides"

ASTM E523-76, "Measuring Fast-Neutron Flux Density by Radioactvation of Copper"

ASTM E482-76, "Application of Neutron Transport Methods for Reactor Vessel Surveillance".

The BCL premium, high resolution 50 cc high-purity germanium detector, capable of 2.0 KeV resolution (full width, half maximum at ^{60}Co 1332 KeV peak) was calibrated with NBS standard reference materials and was used to determine the radioactivity induced in the flux wires. Data handling and reduction were accomplished using an Ortec Model 7010 Multichannel Analyzer (4096 channels).

The integrated neutron fluence at the surveillance location was determined from the radioactivity induced in the irradiated detector materials. The gamma radiation from the dosimeter was measured and used to calculate the flux required to produce this level of activity. The fluence was then calculated from the integrated power output of the reactor during the exposure interval.

The activity A induced into an element irradiated for a time t_i in a constant neutron flux is given by:

$$A = N\left[\int_0^\infty \sigma(E)\,\phi(E)dE\right](1 - e^{-\lambda t_i}) \qquad (1)$$

where

$\sigma(E)$ = the differential cross section for the activation reaction (barns)

$\phi(E)$ = the neutron differential flux ($n/cm^2/sec$)

N = the atom density of the target nuclei (atoms/g)

λ = the decay constant of the product atom (sec^{-1}). If the sample is permitted to decay for a time t_w between exposure and counting, then the activity when counted is:

$$A = N\left[\int_0^\infty \sigma(E)\,\phi(E)dE\right](1-e^{-\lambda t_i})\, e^{-\lambda t_w} \qquad (2)$$

If it is desired to find the flux of neutrons with energies above a given energy level, E_c, the cross section corresponding to this energy level is defined as:

$$\sigma(E>E_c) = \frac{\int_0^\infty \sigma(E)\,\phi(E)dE}{\int_{E_c}^\infty \phi(E)dE}$$

where

$$\phi(E>E_c) = \int_{E_c}^\infty \phi(E)dE$$

Then

$$\int_0^\infty \sigma(E)\,\phi\,dE = \frac{\int_0^\infty \sigma(E)\,\phi\,(E)dE}{\int_{E_c}^\infty \phi(E)dE} \int_{E_c}^\infty \phi(E)dE$$

$$= \sigma(E>E_c)\,\phi\,(E>E_c)$$

and the activity A may be written as:

$$A = N\,\sigma(E>E_c)\,\phi(E>E_c)\,(1 - e^{-\lambda t_i})\,e^{-\lambda t_w} \quad .$$

The flux is then computed from the measured activity as:

$$\phi(E>E_c) = \frac{A}{N\,\sigma(E>E_c)\,(1 - e^{-\lambda t_i})\,e^{-\lambda t_w}} \quad .$$

To correct for fluctuations in power level, the flux is computed as:

$$\phi(E>E_c) = \frac{A}{N\,\sigma(E>E_c)C}$$

where

$$C = \sum_{n=1}^{N} fn\,(1 - e^{-\lambda t_i^n})\,e^{-\lambda t_w^n} \quad ,$$

N = number of time intervals of constant flux

fn = the fractional power level during interval n

t_i^n = the time length of the interval n irradiation

t_w^n = the time between the end of interval n and counting.

In order to determine the effective cross section to be used in the above calculations, the cross section as a function of energy must be known and the neutron flux intensity as a function of energy must be known. A cross section library of this nature is available[18] and a computer code SAND-II[19] was used to retrieve the cross sections desired from this library. The neutron flux and spectrum was calculated with computer code DOT.[20] This code solves the two-dimensional Boltzmann transport equation using the method of discrete ordinates. The reactor geometrical configuration design was modeled to simulate the core structure, intervening structures, and pressure vessel. Calculations were performed in the S_8P_3 approximation using 22 neutron group cross sections from the DLC-23 library.[21] The effective cross sections were generated by the DOT calculation. Coincidental with the calculation of the effective cross sections in the DOT run, the lead factor and neutron flux profile in the reactor vessel wall were also determined.

The neutron fluence was calculated by multiplying the flux (neutrons per square centimeter per second) by the time of operation at full power (using effective full power seconds). To perform the computations, the following information was used:

(1) A description or sketch of the fuel bundle arrangement making up the core, the structures between the core and the pressure vessel, and the pressure vessel itself. This description included materials, thicknesses, and distances between components. The cladding material properties and thickness was also incuded.

(2) The average fast flux distribution in the core. These data included the fuel bundles in one octant of the core and covered the entire time span during which the capsule was in the reactor.

(3) Detailed capsule and capsule holder drawings and the exact position of the capsule relative to other structures.

(4) A complete energy generation history by month (MWH_t per month) for the time during which the capsule was in the reactor, plus a value considered to be full power.

Charpy Impact Properties

Charpy impact tests were conducted using a 264 ft-lb Tinneous-Olsen Model 74 impact machine in accordance with ASTM specifications.[11, 22] The 264 ft-lb range was used for all tests. Velocity of the hammer at impact was 16.87 ft/sec. Calibration of the machine was verified as specified in ASTM E23-82 and proof tested using a set of standard Charpy specimens obtained from the U.S. Army Materials and Mechanics Research Center (AMMRC) of Watertown, Massachusetts. Results of the proof tests are listed in Table 2.

Instrumented impact tests were conducted utilizing a tup (hammer) on the impact machine to which strain gage instrumentation had been added. The instrumented tup in conjunction with a computer controlled, programmable system and a digital storage oscilloscope to record the load-time history of each impact test was used as the data acquisition system.[23] The information stored in the oscilloscope was then recorded using an X-Y plotter to produce hard copies of the test load-time curves. Testing of the irradiated Charpy V-notch specimens from the Monticello capsules followed in general the recommendations of the General Electric document SIL No. 14, Supplement 1.

TABLE 2. CALIBRATION DATA FOR THE HOT LABORATORY CHARPY IMPACT MACHINE USING AMMRC STANDARDIZED SPECIMENS

Group	Average of 5 BCL Energy (ft-lb)	AMMRC Standard Energy[a] (ft-lb)	Variation Between BCL Average And AMMRC Standard Energy	
			Actual	Allowed
Low Energy	14.1 ± 0.4	14.6	-0.5 ft-lb	±1.0 ft.-lb
High Energy	73.7 ± 2.7	72.5	+1.7 percent	±5.0 percent

(a) Established by U.S. Army Materials and Mechanics Research Center.

ASTM procedures for specimen temperature control were utilized.[22] The low temperature bath consisted of a refrigeration unit containing methyl alcohol. The alcohol was agitated by a magnetic stirring bar to minimize temperature variation in the bath. The liquid level of the bath was maintained so that a minimum of 1 inch of liquid over the specimens was maintained. Each Charpy specimen was held at temperature for at least the minimum time (± 1 C for at least 5 minutes) recommended by ASTM E23-82. Tests above room temperature were conducted in a similar manner using a heated oil bath.

Each specimen was transferred from the temperature bath to the anvil of the impact machine by an automatic transfer device. Specimens were removed from the bath and impacted in less than 5 seconds as the testing proceeded. The energy required to break each specimen was recorded and plotted as a function of test temperature.

Lateral expansion was determined from measurements made with a lateral expansion gage.[22] The amount of lateral expansion as a function of test temperature was also plotted. Fracture appearance (percent shear) of the Charpy specimens was estimated from observation of the fracture surface and by comparing the appearance of the specimen to an ASTM fracture appearance chart.[11]

The Battelle's Columbus Laboratory approach was to test each type specimen (base, weld, and HAZ metal) in the approximate temperature range of -50 F to 400 F with the actual test temperature mutually agreed upon prior to testing. The data generated was used to construct conventional Charpy transition curves, which were could then be used to determine the adjusted reference temperature (RT_{NDT}). Emphasis was placed on establishing a 30 ft-lb, 50 ft-lb, and 35 mil lateral expansion index temperatures. Because of the current concern regarding the upper shelf energy level of pressure vessel materials, tests were also conducted in a manner such that the upper shelf was well-defined. Items reported include test temperature, energy abosrbed by the specimen in breaking, lateral expansion, percent ductile fracture, upper shelf energy, 30 ft-lb level nil-ductility transition (NDT) temperature, 50 ft-lb level NDT temperature, and photographs (at least 1X) of each pair of fracture surfaces. The Charpy impact data was prepared and reported in accordance with ASTM E185-82.[8]

Tensile Properties

Tensile tests were conducted using a screw-driven Instron machine having a 20,000 pound capacity. The tensile properties of base metal, weld metal, and HAZ metal specimens were determined following the procedures of ASTM E8-81,[24] "Tension Testing of Metallic Materials", ASTM A370-77,[11] "Mechanical Testing of Steel Products", and ASTM E21-79,[25] "Elevated Temperature Tension Tests of Metallic Materials". The samples of each material were tested at room temperature (∿68 F), 200 F and 550 F. The representative operating temperature of the Monticello Nuclear Generating Plant was 550 F. Temperatures of the specimens tested at elevated temperatures were monitored by two Chromel-Alumel thermocouples attached directly to the gage length. As required by ASTM, temperature control was maintained to ± 5 F of the desired test temperature for 20 minutes prior to start of, as well as during, the tensile test. Tensile specimens were heated by means of a hot air-furnace.

The testing machine crosshead speed was 0.005 in./min from the beginning of the test until well past the 0.2 percent off set yield point. The crosshead speed was then increased to 0.05 in./min and held at this speed to the end of the test. A knife edge extensometer was attached directly to the tensile specimen central one inch gage section. A strain gage unit sensed the differential movement between the two extensometer extension arms which were attached to the specimen gage section by two vee notched knife edge bars. The extension arms are required so that the strain gage can be located outside the furnace hot zone during elevated temperature testing. Elongation of the tensile specimen (at a crosshead speed of 0.005 in./min) was measured to a point beyond the yield point using the strain gage extensometer over a one inch gage section. Once the yield point was passed, the crosshead speed was increased to 0.05 in./min and the specimen elongation determined by multiplying the crosshead speed by the elapse time and dividing by the specimen gage section length (1.0 in.). After testing, each broken tensile specimen was reassembled using a special jig, photographed, and the distance between the punch marks measured. Each specimen was also photographed end-on to show the fracture surface.

Load-elongation data were recorded on the testing machine strip chart. Yield strength, ultimate tensile strength, uniform elongation, and total elongation were determined from these charts. The reduction in area was determined from specimen measurements made using a blade micrometer. Total elongation was also determined from the increase in distance between two punch marks which were made in the gage section prior to testing.

The Instron load cell was calibrated prior to testing using a strain gage tensile bar which had been calibrated against NBS traceable standards. The Instron crosshead speeds were also determined using a calibrated stop watch and a calibrated dial indicator. The extensometer was also calibrated before tensile testing using an Instron high-magnification drum-type extensometer calibrator. The calibrator was calibrated using NBS traceable standards.

Chemical Analysis

The method of X-ray fluorescence (XRF) was used to determine copper (Cu), phosphorus (P), nickel (Ni), molybdenum (Mo), chromium (Cr), manganese (Mn), vanadium (V), silicon (Si), and sulfur (S). Each sample consisted of a separate half of a broken weld metal Charpy specimen which was polished through 600 grit grinding paper to provide a satisfactory surface for analysis. Both tantalum and aluminum masks were used to accommodate the sample. The masked-down samples and NBS standards (with known amounts of each element) were bombarded with primary X-rays to produce measurable characteristic or secondary X-rays of the desired elements. These characteristic or secondary X-rays which result from inner orbital electron jumps of a particular element are produced in proportion to the amount of that element in the sample. Qualification and calibration was achieved by comparing the accummulated intensities and wavelengths of the X-rays from the sample to those from NBS standards possessing a known concentration range for each element.

The procedure for the chemical analysis for the elements listed above involved counting on the major lines and at off-line background positions. Counts were accummulated for up to 200 seconds at least twice for each sample to improve counting statistics. Electronic pulse height analysis (PHA) elimination of excessive background due to the radioactivity of the sample was incorporated for the phosphorous, vanadium, silicon, and sulfur analysis. This PHA provided greater sensitivity in the net intensities for elements of low concentration.

The standards used for this analysis are certified NBS standards. They included low alloy steels standards Numbers 1161 through 1169, and cast steel standards Numbers 1104 through 1183.

The XRF procedures used in this program are those in general use throughout the industry and are described in the literature. Two sources that typify common practice are:

(1) Theory and Practice of X-Ray Fluorescence; Philips Electronic Inst., Mt. Vernon, New York.

(2) Principles and Practices of X-Ray Spectrochemical Analysis; E. P.Bertin; Plenum Press (1969).

In addition to the nine elements listed above, Charpy weld metal specimens were drilled and the chips (between 1 and 2 g) were sent to the Westinghouse Analytical Laboratory at Waltz Mill, Pennsylvania, for carbon analysis. Each sample was analyzed for its carbon content using the combustion gravimetric method according the ASTM E350-82[26] Sections 169 to 174.

RESULTS AND DISCUSSION

Neutron Dosimetry

Introduction

The neutron environment to which a surveillance capsule has been exposed must be known so that the pressure vessel material property changes (tensile and Charpy V-notch property changes) can be related to that environment. However, the exact neutron spectrum is very complicated and varies over the operating history of the reactor. Therefore, the Monticello surveillance program utilizes iron and copper dosimeter wires to yield an integrated flux at the capsule position. The activation process is both time and energy dependent and a computer code is used to establish the neutron energy spectrum at the capsule position. Once the integrated flux at the capsule has been established, the flux or fluence > 0.1 MeV and > 0.1 MeV can be calculated at positions within the pressure vessel wall and at angular positions around the vessel.

Analytical Method

The determination of the neutron flux at the capsule, and subsequently in the pressure vessel wall, requires the completion of three procedures. First, the disintegration rate of the product isotope per unit mass of the flux monitor must be determined. This has been discussed earlier under experimental procedures. Second, in order to find a spectrum-averaged reaction cross section at the capsule location, the neutron energy spectrum must be calculated. Third, the neutron flux at the capsule must be found by calculations involving the counting rate data, the spectrum-averaged cross sections, and the operating history of the reactor.

The energy and spatial distribution of neutron flux in the reactor were calculated using the DOT 3.5 computer program.[20] DOT solves the Boltzman transport equation in two-dimensional geometry using the method of discrete ordinates. Balance equations are solved for the density of particles moving along discrete directions in each cell of a two-dimensional spatial mesh. Anistotropic scattering is treated using a Legendre expansion of arbitrary order.

The two-dimensional geometry that was used to model the Monticello reactor is shown in Figure 8. As seen, there are 17 circumferential meshes and 51 radial meshes. Capsule 1 includes circumferential meshes 7 and 8 and radial meshes 41, 42, and 43. Third order scattering was used (P_3) and 48 angular directions of neutron travel (24 positive and 24 negative) were used (S_8 quadrature). Neutron energies were divided into 22 groups with energies from 14.9 MeV to 0.01 eV. The 22 group structure is that of the RSIC Data Library DLC/CASK[21], and neutron absorption, scattering, and fission cross sections used are those supplied by this library. The core shroud, jet pumps, and liner are Type 304 stainless steel. The capsule is also modeled as a solid piece of 304 stainless steel. The reactor pressure vessel wall is SA533B steel. The reactor core was mocked up as homogenized fuel and water having the densities found in the operating reactor. The water in the core region has a density consistent with the average coolant temperature in the core (550 F) at the operating pressure of 1015 psia. Finally, the fuel was a source of neutrons having a U-235 fission energy spectrum. The relative power in the assemblies nearest the capsule, during the interval the capsule was in the reactor, is shown in Figure 8.[27] A plane view of the Monticello reactor physical geometry at the core midplane is shown in Figure 8 and because of symmetry includes only a 1/8th segment.

The neutron spectrum at the capsule center, as calculated by DOT, is shown in Figure 9. Also shown for comparison is the fission spectrum. Both spectra have been normalized to contain one neutron above 1.0 MeV. As can be seen, the capsule spectrum is considerably harder than the fission spectrum. This is caused by neutron travel through water.

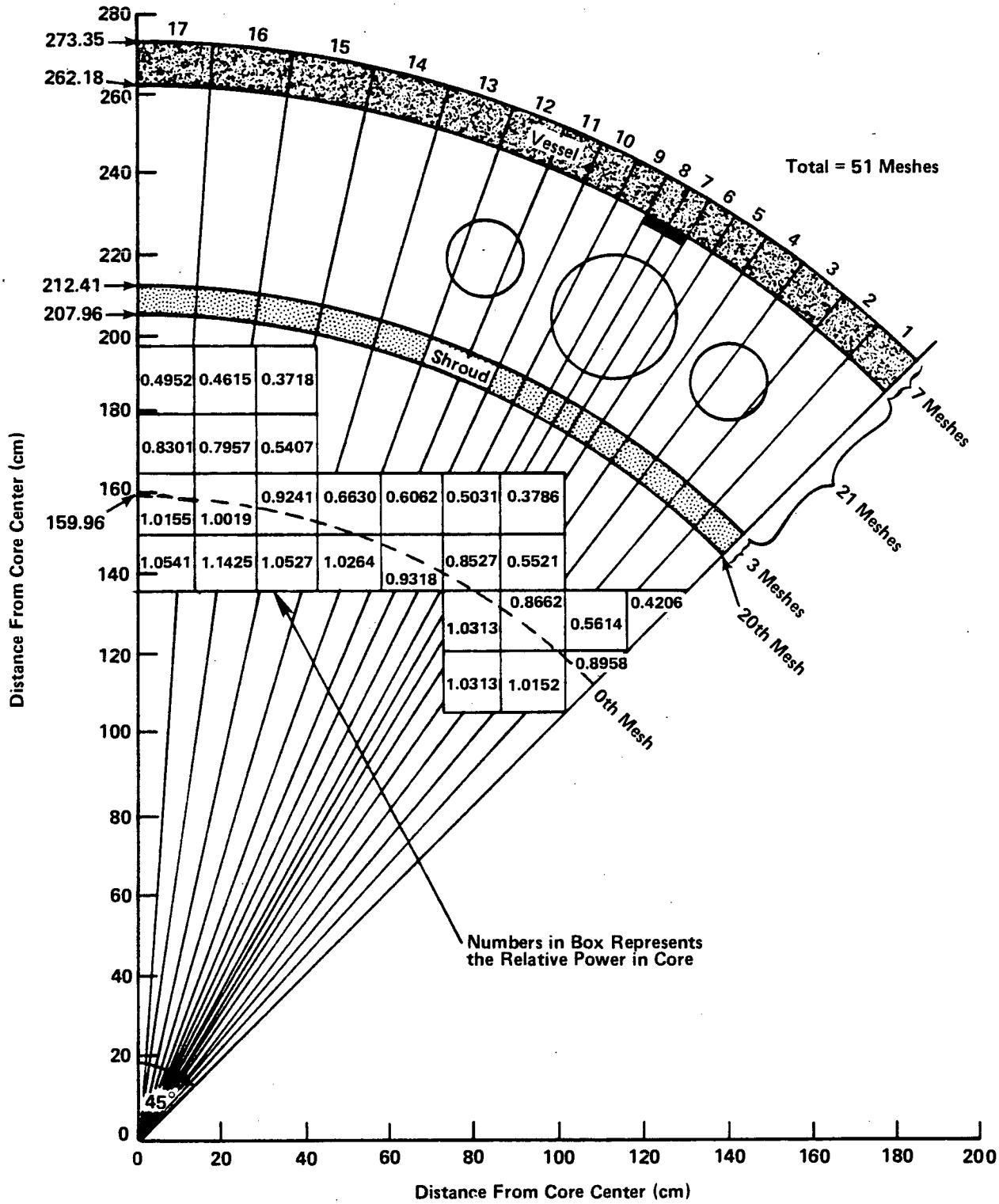

FIGURE 8. MONTICELLO CORE, INTERNAL VESSEL STRUCTURES, AND VESSEL WALL GEOMETRY USED IN THE DOT CALCULATION

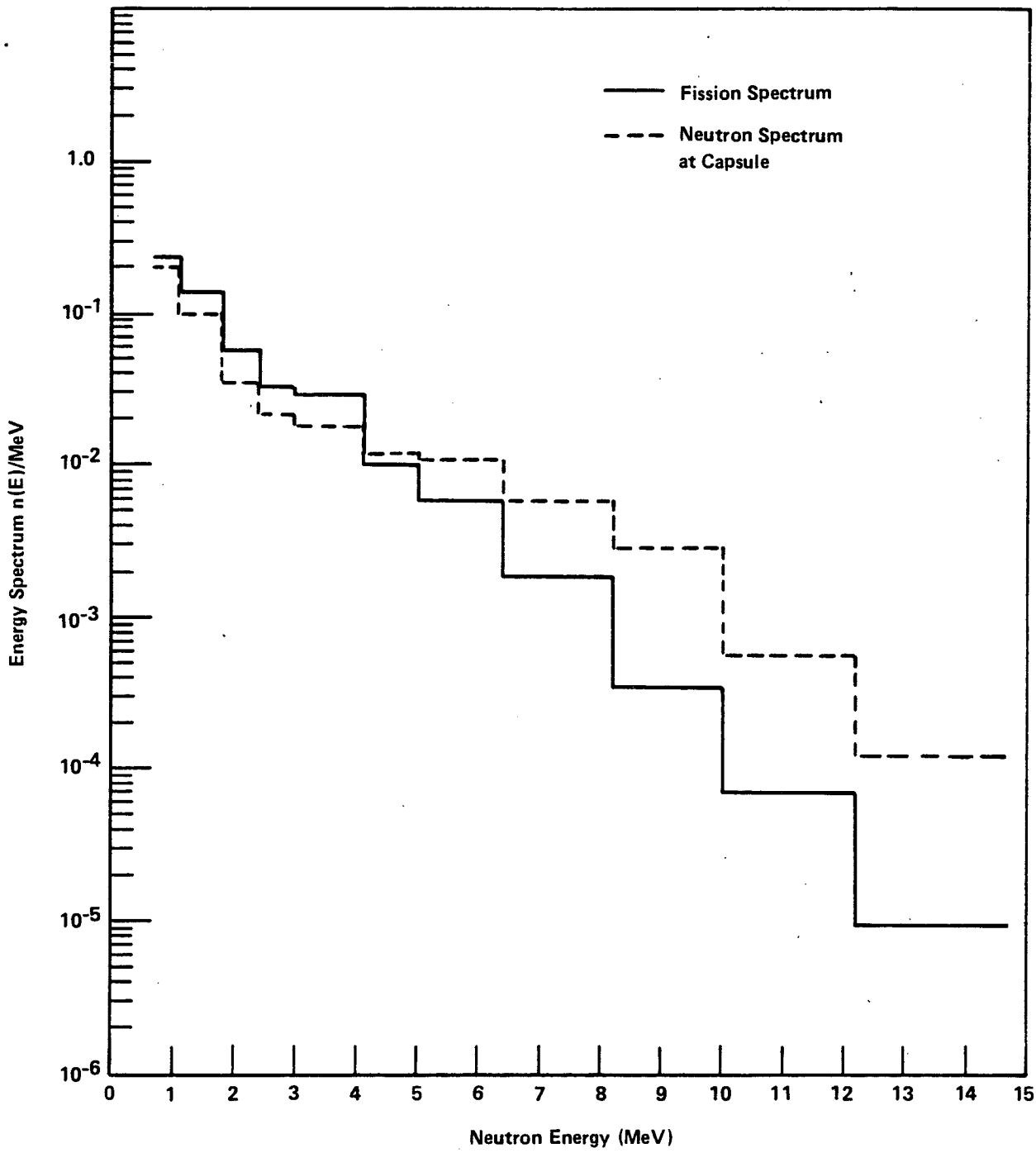

FIGURE 9. COMPARISON OF DOT SPECTRUM WITH FISSION SPECTRUM AT THE SURVEILLANCE CAPSULE

Based upon the fluxes calculated by DOT at r mesh 42 and θ mesh 7 and 8 (the two radial centered meshes used to represent the capsule and the region in which the flux monitors were placed), effective cross sections σ_R (E > 0.1 MeV) and σ_R (E > 1.0 MeV) defined as:

$$\sigma_R (E > E_c) = \frac{\int_0^\infty \sigma(E)\, \phi(E) dE}{\sigma(E_c)\, \phi(E) dE}$$

were calculated for iron and copper in each of the two meshes. The results are shown in Table 3 for σ_R (E > 1.0 MeV) which is of most interest.

Using the results of Table 3 and the geometry shown in Figure 8, the cross section appropriate to each of the monitors can be interpolated. These values and other nuclear constants needed in the third step of the flux-finding procedure are given in Table 4.

In the third step, the full power flux at the capsule location is determined from the radioactivity induced in the monitor foils, the effective cross sections calculated for the monitor elements, and the power history of the reactor during capsule exposure. The fluence at the capsule is then calculated from the integrated power output of the reactor during the exposure interval using the equations outlined in the Experimental Procedures Section of this report.

$$\phi(E > E_c = A/N\, \sigma(E > E_c)\, C$$

This equation was used to find fluxes based on the surveillance capsule activations. The time intervals were taken as one month each and a time integrated relative power value for each month and for each fuel assembly was used for the fractional power level values.

Calculations of the flux and fluence were made with the DECAY code. The reactor power history was supplied in a private communication.[33]

TABLE 3. CROSS-SECTIONS FOR THE IRRADIATED FLUX MONITORS (E>1MeV) IN RADIALLY CENTERED TWO CAPSULE MESHES (MONTICELLO 30 DEGREE SURVEILLANCE CAPSULE)

Material	Energy	Cross-Section (Barns)
Cu	0.1 MeV	1.7558×10^{-3}
	1.0 MeV	3.0214×10^{-3}
Fe	0.1 MeV	1.0896×10^{-1}
	1.0 MeV	1.8749×10^{-1}

TABLE 4. CONSTANTS USED IN DOSIMETRY CALCULATIONS FOR THE MONTICELLO 30 DEGREE SURVEILLANCE CAPSULE

Reaction	Target, percent	Isotopic Abundance, percent	Threshold Energy, MeV	Product Half-Life	Cross-Section, Barns (E>1.0 MeV) (E>0.1 MeV)
$^{54}Fe(n,p)^{54}Mn$	99.865 Fe	5.82	1.5	312.6 days	1.8749×10^{-1}
					1.0896×10^{-1}
$^{63}Cu(n,\alpha)^{60}Co$	99.999 Cu	69.17	5.0	5.27 years	3.0214×10^{-3}
					1.7558×10^{-3}

Dosimetry Results

The Monticello Nuclear Generating Plant surveillance capsule baskets both had the binary code number 19 which corresponds to that number assigned to the Northern States Power Company Monticello Reactor.[7] Both baskets had the capsule number 1. The surveillance capsule was located at the 30 degree azimuthal position at approximately the core midplane position and about 9/16 in. from the inner pressure vessel wall. This capsule was in the reactor for 2786 equivalent full power days or about 7.63 equivalent full power years. The Monticello Nuclear Generating Plant design thermal output is 1670 MW_t.

Four iron (Fe) and four copper (Cu) neutron monitor wires from Charpy packets G-2, G-6, G-7, and G-8 were counted to determine their specific activity. The recommended ASTM procedures[28-32] were followed in determining the specific activity of the Fe and Cu wires. Each dosimeter monitor consisted of an approximately 4-inch length of wire which was rolled into a small coil for counting. The count rate was determined for each wire. The fast flux and fluence calculated using the count rate therefore represented an average over the 4-inch length of that wire. The > 0.1 MeV and > 1.0 MeV full power flux and fluence calculated from initial startup to November 1981 are given in Table 5 for each of the dosimeter wires along with the average of the flux and fluence derived from the Fe, Cu, and Fe plus Cu.

Using the average fluxes (average of Fe and Cu) of 2.0872×10^9 $n/cm^2/sec$ for E > 0.1 MeV and 1.2152×10^9 $n/cm^2/sec$ for E > 1.0 MeV, the fluxes at full power at the inside of the pressure vessel wall, at 1/4 T and at 3/4 T directly behind the capsule (30 degree position) and at the maximum position ($\sim$3 degree position) were calculated. The flux results are tabulated in Table 6. The end of life (EOL) fluences were also calculated and tabulated in Table 6 assuming a reactor pressure vessel lifetime of 40 years and operated at 80 percent full power. The fine mesh and time integrated relative power values[33] shown in Figure 8 for each fuel assembly was used inthe DOT 3.5 code to generate the values in Table 6. A plot of neutron flux (E >1.0 MeV) as a function of azimuthal angle (in degrees) is shown in Figure 10. The fluence values at the maximum position for inner vessel wall,

TABLE 5. FLUX AND FLUENCE VALUES AT THE MONTICELLO SURVEILLANCE CAPSULE (30 DEGREE AZIMUTHAL LOCATION)

Energy	Dosimeter Material	Full Power Flux ($n/cm^2/sec$) x 10^9	Fluence* (n/cm^2) x 10^{17}
>0.1 MeV	Fe (G-6)	2.0659	4.9728
	(G-7)	1.9945	4.8010
	(G-8)	2.1571	5.1924
	(G-2)	1.8471	4.4462
	Average of Fe	2.0162	4.8531 ± 0.2728
	Cu (G-6)	2.1633	5.2073
	(G-7)	2.1310	5.1295
	(G-8)	2.3090	5.5580
	(G-2)	2.0299	4.8862
	Average of Cu	2.1583	5.1953
	Average of Fe and Cu	2.0872 ± 0.1283	5.0242 ± 0.3089
>1.0 MeV	Fe (G-6)	1.2027	2.8950
	(G-7)	1.1612	2.7951
	(G-8)	1.2559	3.0231
	(G-2)	1.0754	2.5886
	Average of Fe	1.1738	2.8255 ± 0.1588
	Cu (G-6)	1.2595	3.0317
	(G-7)	1.2407	2.9865
	(G-8)	1.3443	3.2359
	(G-2)	1.1818	2.8447
	Average of Cu	1.2566	3.0247 ± 0.1401
	Average of Fe and Cu	1.2152 ± 0.0747	2.9251 ± 0.1799

*Fluence based on 2786 equivalent full power days.

TABLE 6. FLUX AND FLUENCE BEHIND THE MONTICELLO SURVEILLANCE CAPSULE AND AT THE MAXIMUM VESSEL WALL POSITION

Energy (MeV)	Location	Full Power Flux in Vessel		Fluence in Vessel			
				Behind Capsule (30°)		Maximum (3°)	
		Behind Capsule ($x10^9$ n/cm^2/sec) (30°)	Maximum ($x10^9$ n/cm^2/sec) (3°)	Nov. 81 (1) ($x10^{17}$ n/cm^2)	EOL (2) ($x10^{18}$ n/cm^2)	Nov. 81 (1) ($x10^{17}$ n/cm^2)	EOL (2) ($x10^{18}$ n/cm^2)
> 0.1	Surface	1.8974	6.9947	4.5672	1.9148	16.837	7.0587
> 0.1	1/4 T	1.7029	6.4296	4.0991	1.7185	15.477	6.4884
> 0.1	3/4 T	0.8654	3.2606	2.0831	0.8733	7.849	3.2904
> 1.0	Surface	0.9788	3.9099	2.3563	0.9878	9.412	3.9457
> 1.0	1/4 T	0.7348	2.9901	1.7687	0.7415	7.197	3.0175
> 1.0	3/4 T	0.2968	1.1874	0.7144	0.2995	2.858	1.1983

(1) Fluence based on 7.633 effective full power years.

(2) Fluence based on 32 effective full power years.

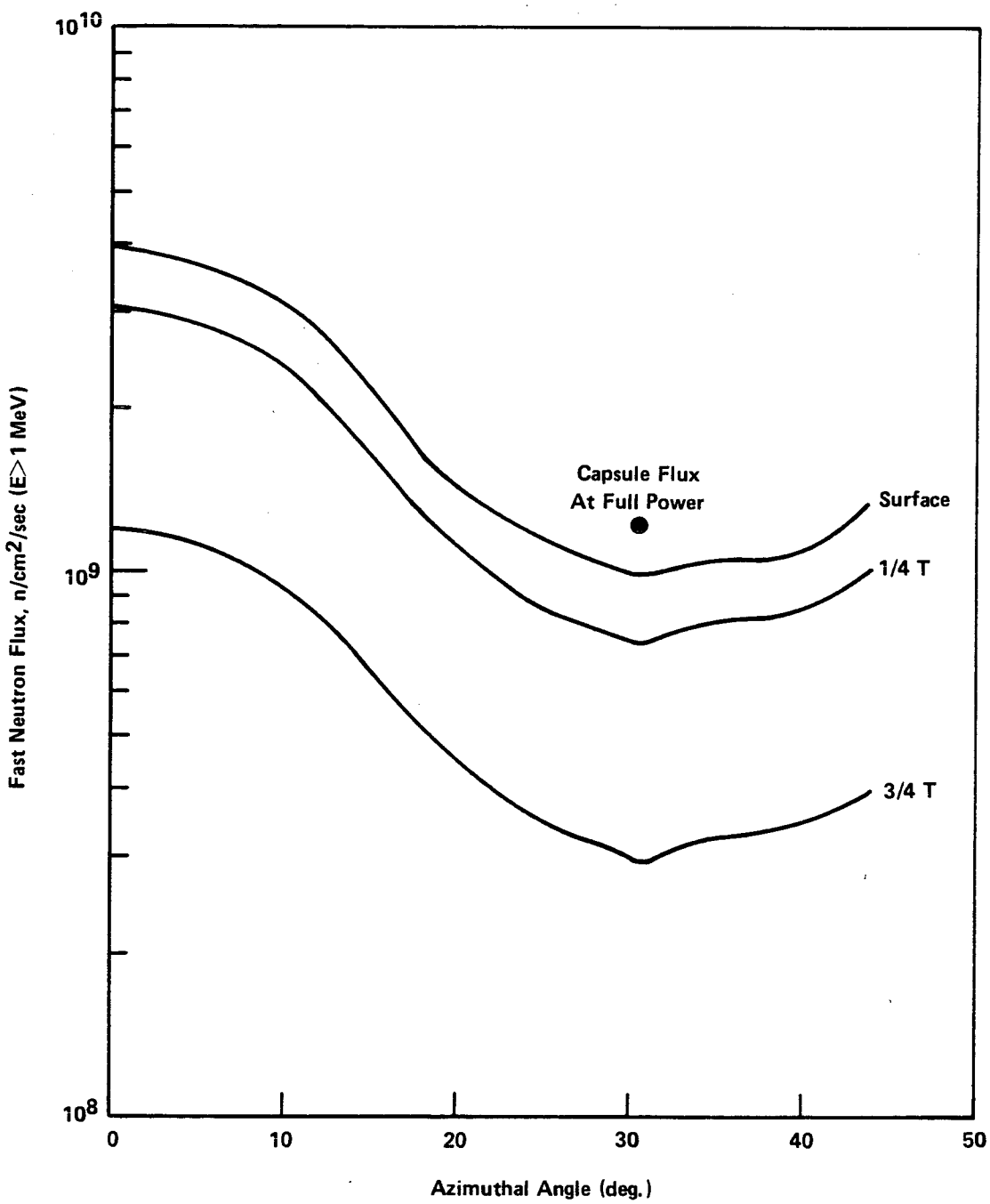

FIGURE 10. CALCULATED FLUX (E > 1MeV) AT THE CAPSULE, INNER WALL, 1/4 THICKNESS, AND 3/4 THICKNESS AS A FUNCTION OF AZIMUTHAL ANGLE

1/4 T and 3/4 T are plotted as a function of time in equivalent full power years (EFPY) for the Monticello vessel in Figure 11. The lead factor, i.e., the ratio of the flux (E > 1.0 MeV) at the surveillance capsule to the largest flux (E > 1.0 MeV) received by the vessel wall at any azimuthal location, is approximately 0.31 ($1.2152 \times 10^9/3.9099 \times 10^9$) at the vessel surface. This result indicates that the flux at the capsule actually lags the flux at certain vessel wall positions. The lead factor at the pressure vessel 1/4 T position was calculated to be 0.41 ($1.2152 \times 10^9/2.9901 \times 10^9$) and 1.05 ($1.2512 \times 10^9/1.1874 \times 10^9$) for the 3/4 T position.

The surveillance capsule end of life (EOL) fluence values (E > 1.0 MeV) predicted[34] by the General Electric Company (GE) at the 1/4 T is 1.2×10^{18} n/cm^2 which is higher than the BCL calculated value of 0.74×10^{18} n/cm^2 (see Table 6). In order to correct for azimuthal variations, GE applied a factor of 1.4 to their calculation and obtained a maximum pressure vessel EOL fluence (E > 1.0 MeV) at the 1/4 T position of 1.68×10^{18} n/cm^2 while BCL calculated 3.02×10^{18} n/cm^2. The GE values have an expected accuracy of $\pm$ 30 percent whereas the BCL values have an expected accuracy of $\pm$ 20 percent. Therefore, the upper bound of the maximum pressure vessel EOL fluence value (E > 1.0 MeV) at the 1/4 T position predicted by GE is 2.2×10^{18} n/cm^2 (1.2×10^{18} n/cm^2 x 1.4 x 1.3) and as calculated by BCL, is 3.6×10^{18} n/cm^2 (3.02×10^{18} n/cm^2 x 1.2). Therefore, since the BCL calculated fluences were derived using the most recent dosimetry data, the power history of the Monticello reactor, and the two dimensional DOT 3.5 and DECAY computer codes, it is concluded that an azimuthal correction factor much larger than 1.4 is required for the Monticello reactor pressure vessel.

When comparing the BCL end of life 1/4 T fluence values for > 1.0 MeV energy range directly behind the surveillance capsule (at 30 degrees azimuthal) and the maximum position fluence value (at between 0 and 5 degrees azimuthal) the azimuthal correction factor is more on the order of 4.0 (see values in Table 6). It is believed that this very high azimuthal correction factor is a result of the small inside diameter of the pressure vessel (about 206.7 in. ID) and the closeness and the relative high power level in the fuel assemblies at the 0 to 15 degrees azimuthal position.

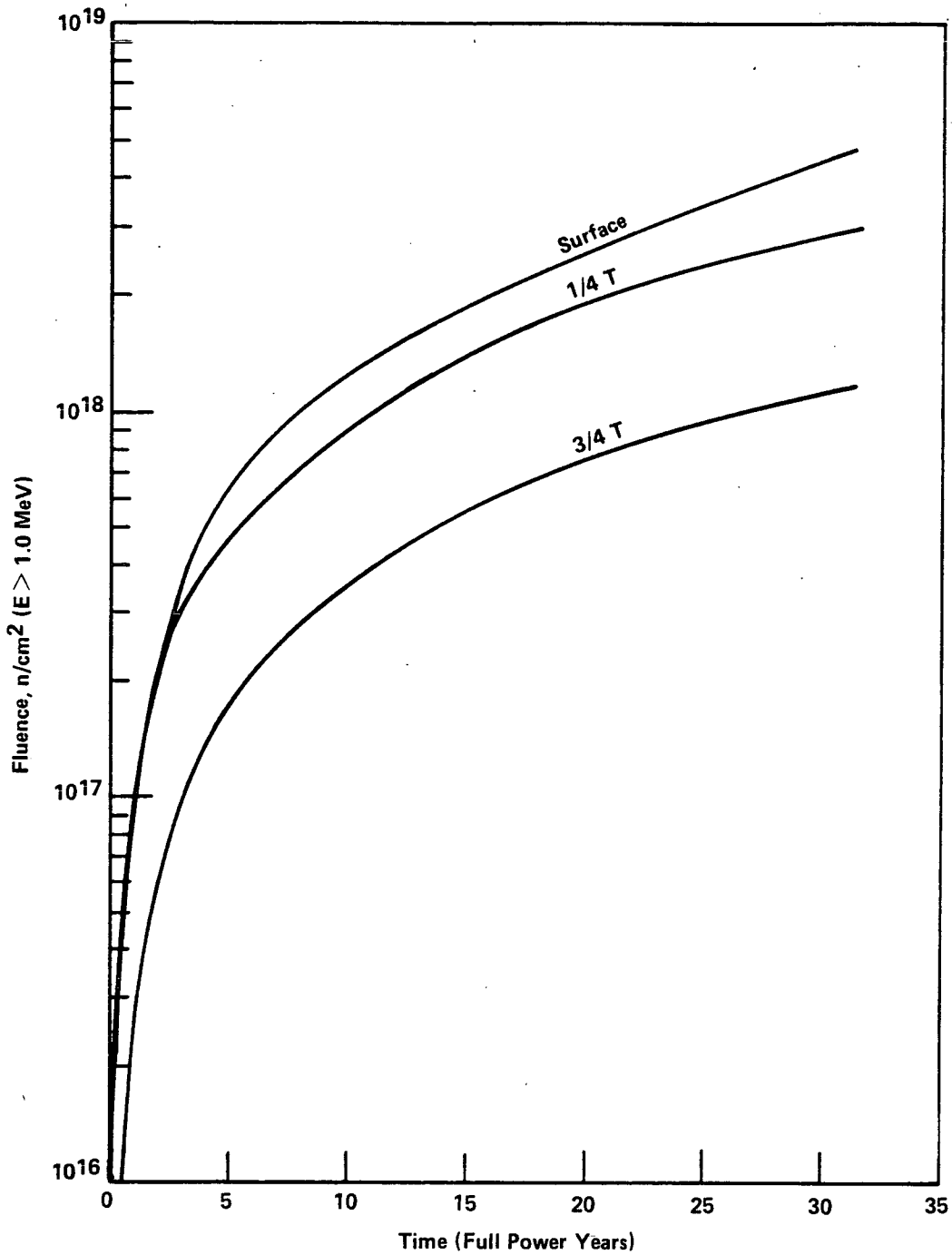

FIGURE 11. FLUENCE AT 14 T AND 3/4 T POSITIONS AS A FUNCTION OF TIME FOR THE MONTICELLO NUCLEAR GENERATING REACTOR VESSEL

Charpy Impact Properties

Introduction

A reactor pressure vessel receives a significant fast neutron exposure during operation and is therefore subject to radiation-induced embrittlement. Charpy V-notch specimens were fabricated and irradiated in a Monticello surveillance capsule at the 30 degree azimuthal position and 0.56 inch from the vessel wall. The specimens were then removed and tested.

Appendix G of the ASME Boiler and Pressure Vessel Code, Section III, Division 1 (Nuclear Power Plant Components) presents a procedure for obtaining allowable loading for ferritic pressure retaining materials to protect against nonductile failure. The procedure is based on the principles of linear elastic fracture mechanics.

Analytical Method

Charpy V-notch tests were conducted over a range of temperatures. The impact energy, lateral expansion, and fracture appearance for the irradiated specimens were determined from the tests.[22] Plots of impact property versus test temperature were plotted for each type of specimen (base metal, weld metal, and HAZ metal) using the hyperbolic tangent fit. From these data, the temperatures at which 30 ft-lb, 50 ft-lb, and 35 mil lateral expansion occurred were determined and the upper shelf energy for each type of specimen was also determined.

Charpy Impact Test Results

Twelve irradiated base metal Charpy V-notch impact specimens, fifteen irradiated weld metal Charpy V-notch impact specimens, and eleven irradiated HAZ metal Charpy V-notch specimens were tested. The results of tests conducted between 0 and 400 F for the base metal specimens are listed in Table 7. The results of tests conducted between -80 and 300 F for the weld metal specimens are listed in Table 8 and the results of tests conducted between -79 and 225 F for the HAZ metal specimens are listed in Table 9. In addition to the total impact energy values, the measured lateral expansion values and the estimated fracture appearance for each specimen are also listed in Tables 7, 8, and 9. The total impact energy is the amount of energy absorbed by the specimen tested at the indicated temperature. Lateral expansion is a measure of the plastic "shear lip" deformation produced by the striking edge of the impact machine hammer when it impacts the specimen. Lateral expansion is determined by the change of specimen thickness directly adjacent to the notch location. Fracture appearance is a visual estimate of the amount of shear (ductile type of fracture) appearing on the specimen fracture surface. Additional data, along with a discussion of test results and of the procedures for conducting instrumented Charpy V-notch impact testing, is given in Appendix A.

Plots of the impact properties (impact energy, lateral expansion, and fracture appearance) versus test temperature are graphically illustrated in Figures 12 through 20. These figures show the change in impact properties as a function of temperature. Note that two weld specimens with a FAB Code designation beginning with D were tested along with the set with the designation beginning with J. The HAZ specimen D72 was not plotted in Figures 18, 19, and 20 because the fracture occurred in the base metal (See note under Table 9). Figures 21, 22, and 23 show the fracture surfaces of the Charpy specimens. A summary of the Monticello surveillance capsule 1 Charpy V-notch impact test data (including the 30 and 50 ft-lb transition temperatures, the 35 mil lateral expansion temperature, and the upper shelf energy) is given in Table 10. The upper shelf is relatively constant at*

*Text continued on page 57.

TABLE 7. CHARPY V-NOTCH IMPACT RESULTS FOR IRRADIATED BASE METAL SPECIMENS FROM THE MONTICELLO 30 DEGREE SURVEILLANCE CAPSULE

Specimen Identification	Test Temperature, F	Impact Energy, ft-lb	Lateral Expansion, mils	Fracture Appearance, Percent Shear
JE3	0	7.0	11.6	10
JDU	40	24.8	22.6	25
JDJ	60	30.5	30.0	25
JE1	76	44.1	35.8	30
JDY	100	55.4	43.6	35
JD1	110	58.7	45.8	40
JE5	120	43.3	40.6	40
JCP	160	75.5	57.6	55
JE4	200	91.0	74.4	100
JDA	300	110.0	69.8	100
JD5	350	103.0	73.8	100
JD4	400	105.0	71.2	100

(a) Instrumented results are contained in Appendix A, Table A-1.

TABLE 8. CHARPY V-NOTCH IMPACT RESULTS FOR IRRADIATED WELD METAL SPECIMENS FROM THE MONTICELLO 30 DEGREE SURVEILLANCE CAPSULE

Specimen Identification	Test Temperature, F	Impact Energy, ft-lb	Lateral Expansion, mils	Fracture Appearance, Percent Shear
JEK	-80	24.5	20.9	25
JEL	-60	22.5	20.6	20
JJE	-40	68.7	54.0	40
JJP	-35	22.0	24.6	30
D6B	-30	22.9	32.0	30
JKA	-30	71.3	54.0	50
JEM	-20	39.5	34.4	35
D57	-15	78.5	70.2	65
JJM	0	36.3	30.8	35
JEP	0	65.2	51.2	55
JEY	20	75.8	58.8	50
JJT	76	96.0	81.4	90
JJ7	160	118.5	90.2	100
JEU	225	127.8	86.8	100
JK5	300	113.0	82.0	100

(a) Instrumented results are contained in Appendix A, Table A-2.

TABLE 9. CHARPY V-NOTCH IMPACT RESULTS FOR IRRADIATED HAZ METAL SPECIMENS FROM THE MONTICELLO 30 DEGREE SURVEILLANCE CAPSULE

Specimen Identification	Test Temperature, F	Impact Energy, ft-lb	Lateral Expansion, mils	Fracture Appearance, Percent Shear
JKD	-79	19.5	32.6	15
JLE	-60	28.5	25.4	20
JKK	-40	65.0	49.4	35
JLC	-20	40.0	33.6	50
JKT	-10	33.0	27.6	40
JLB	-10	50.1	38.6	50
JL2	0	57.9	43.0	50
JKM	76	110.2	84.4	100
JLM	159	103.0	78.0	100
JLK	225	123.3	94.8	100
D72*	40	21.3	23.0	

(a) Instrumented results are contained in Appendix Table A, Table A-3.

* The notch was located approximately 1/8 inches from the fusion line as determined by posttest etching. ASTM E185 specifies the notch to be less than 1/32 inches from the fusion line. Therefore, these test results were not plotted in Figures 18, 19, and 20.

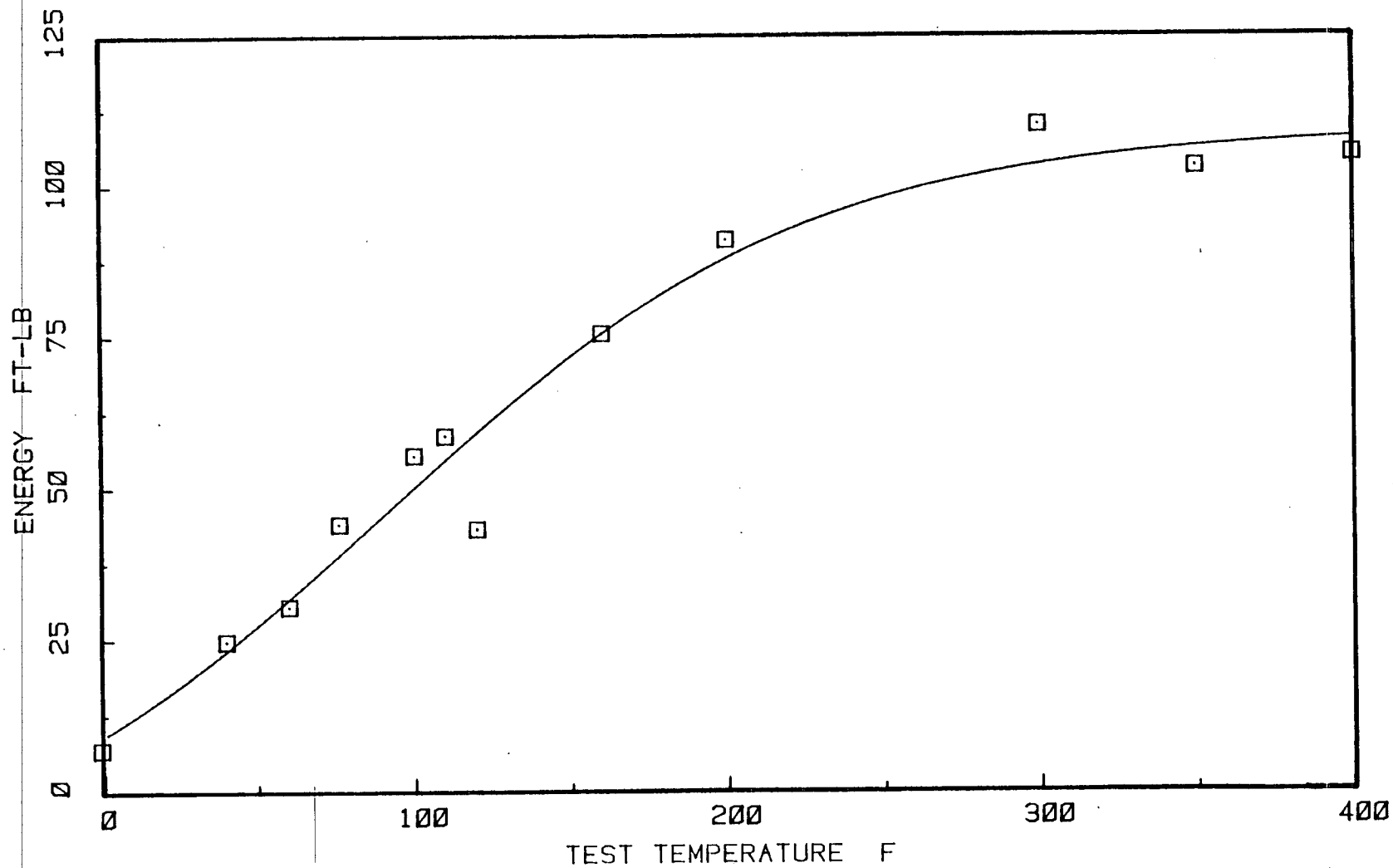

FIGURE 12. CHARPY V-NOTCH IMPACT ENERGY VERSUS TEST TEMPERATURE FOR THE IRRADIATED BASE METAL SPECIMENS FROM THE MONTICELLO 30 DEGREE SURVEILLANCE CAPSULE

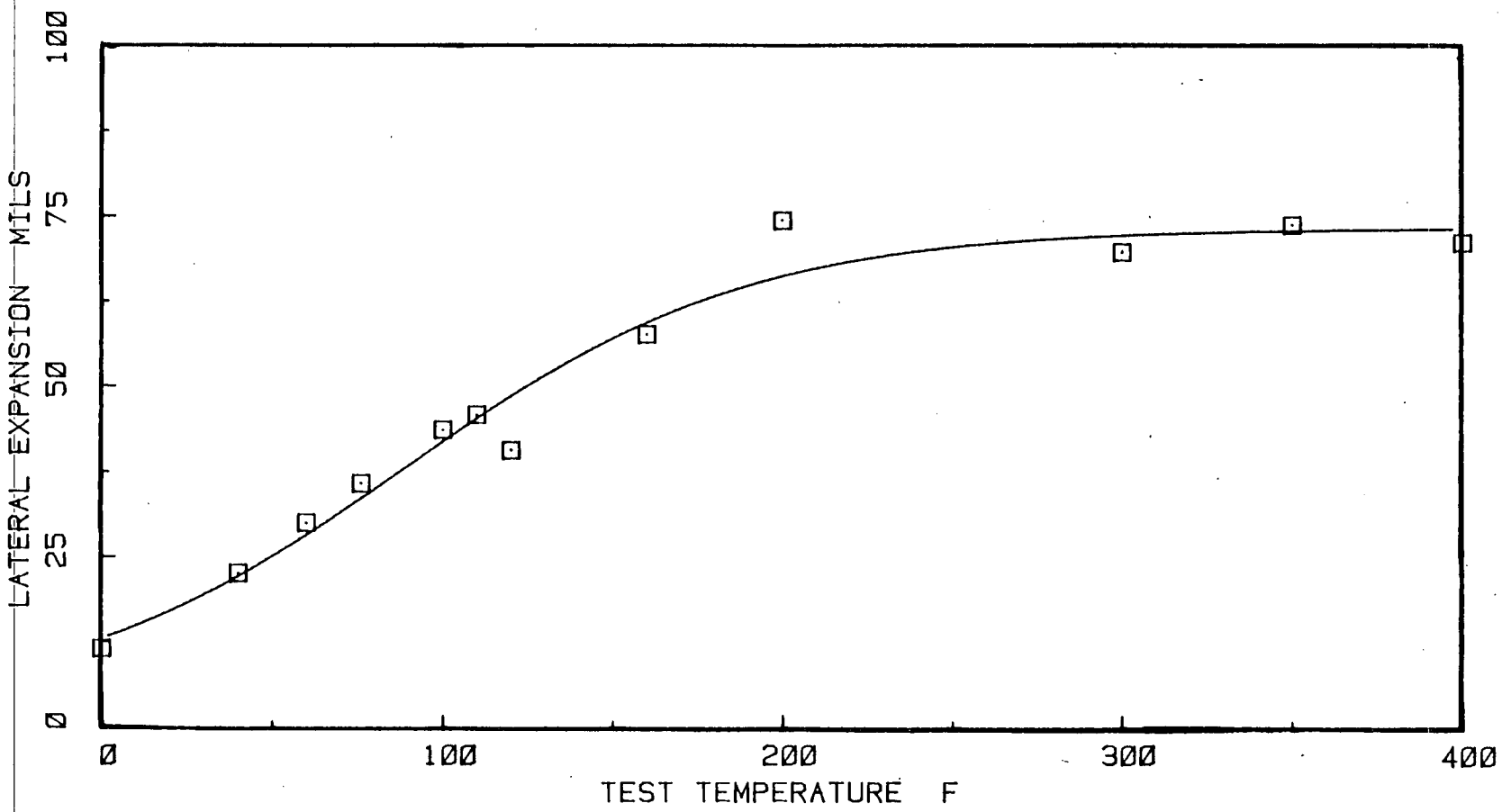

FIGURE 13. CHARPY V-NOTCH LATERAL EXPANSION VERSUS TEST TEMPERATURE FOR THE IRRADIATED BASE METAL SPECIMENS FROM THE MONTICELLO 30 DEGREE SURVEILLANCE CAPSULE

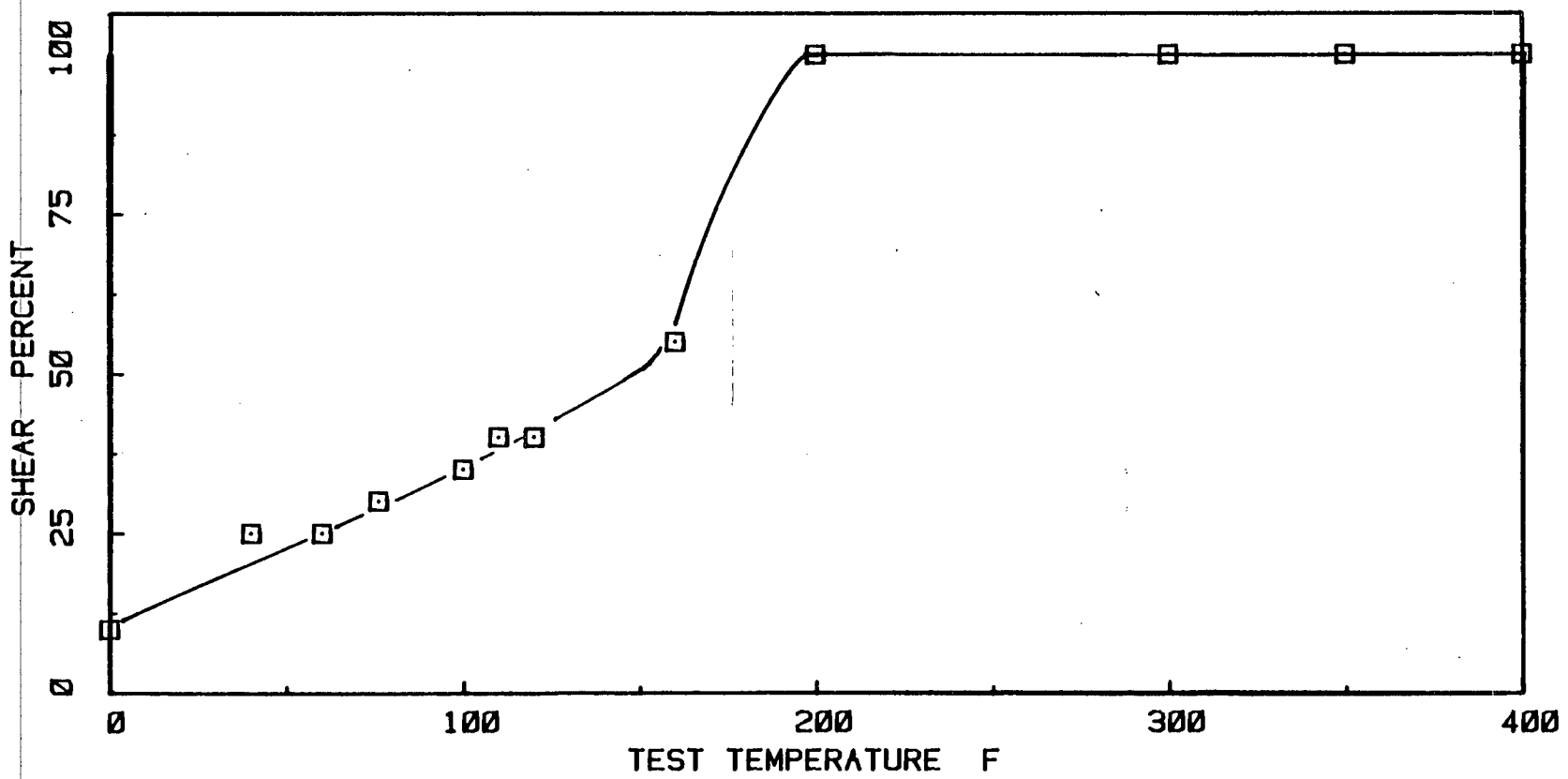

FIGURE 14. CHARPY V-NOTCH PERCENT DUCTILE SHEAR VERSUS TEST TEMPERATURE FOR THE IRRADIATED BASE METAL SPECIMENS FROM THE MONTICELLO 30 DEGREE SURVEILLANCE CAPSULE

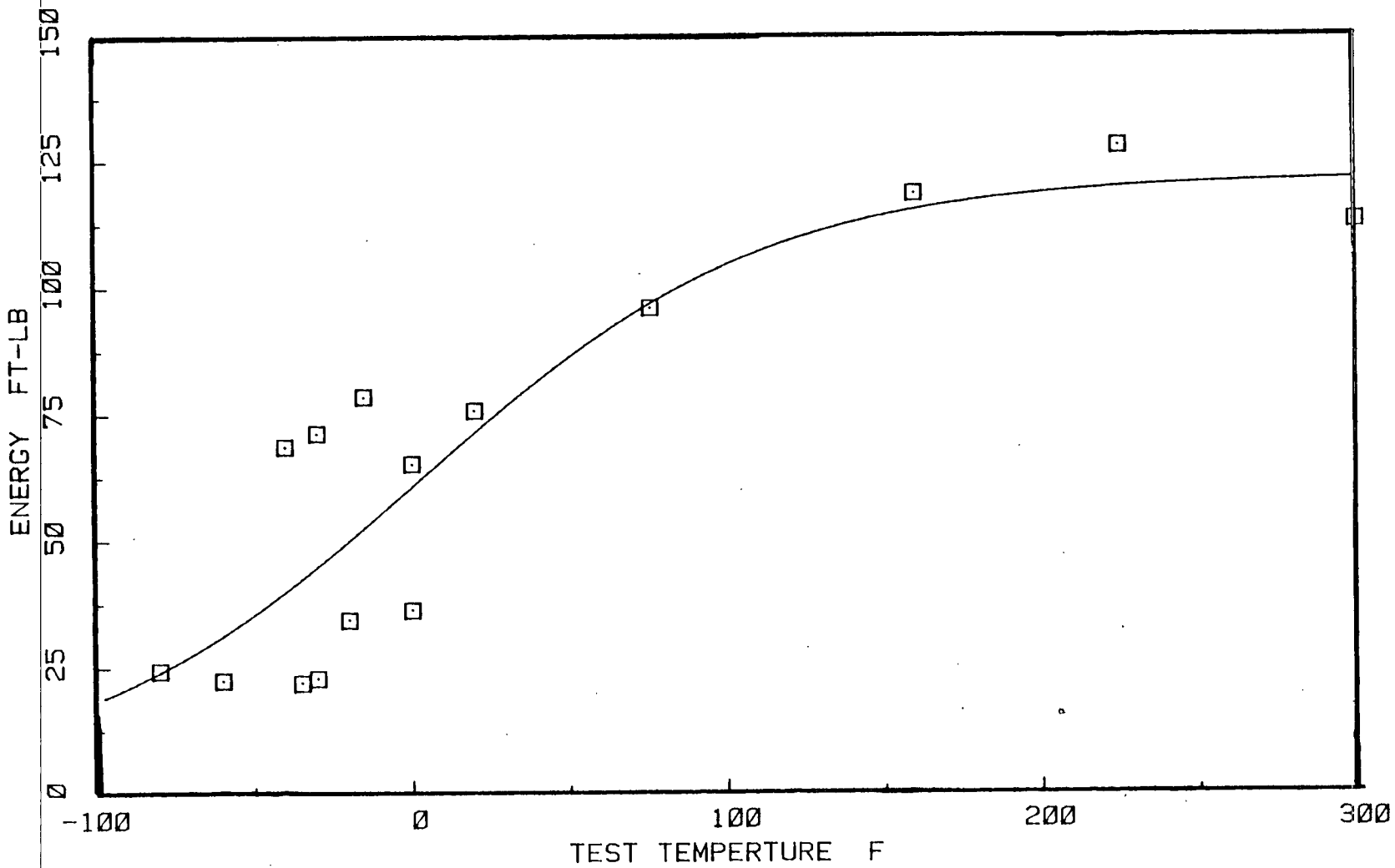

FIGURE 15. CHARPY V-NOTCH IMPACT ENERGY VERSUS TEST TEMPERATURE FOR THE IRRADIATED WELD METAL SPECIMENS FROM THE MONTICELLO 30 DEGREE SURVEILLANCE CAPSULE

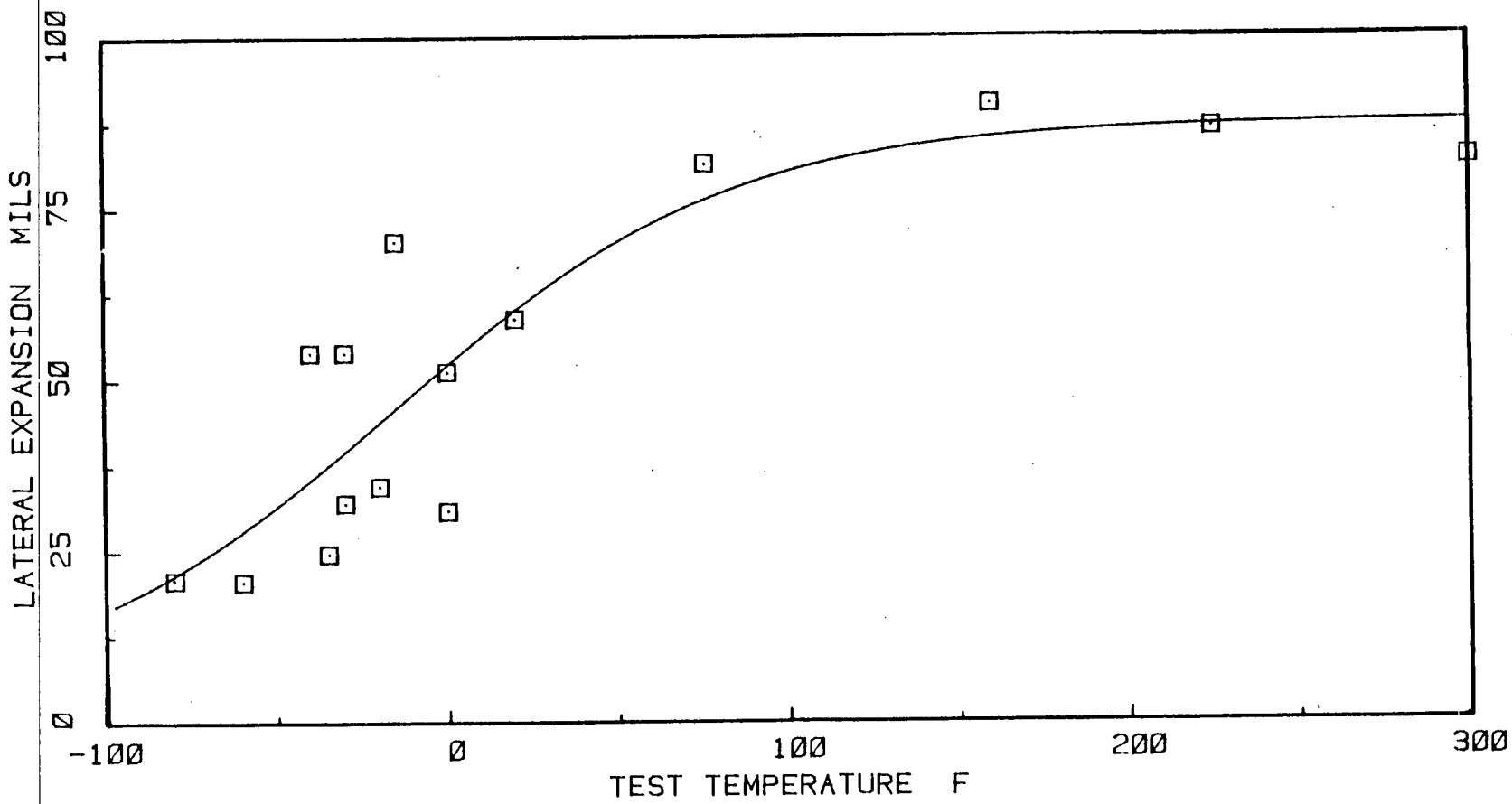

FIGURE 16. CHARPY V-NOTCH LATERAL EXPANSION VERSUS TEST TEMPERATURE FOR THE IRRADIATED WELD METAL SPECIMENS FROM THE MONTICELLO 30 DEGREE SURVEILLANCE CAPSULE

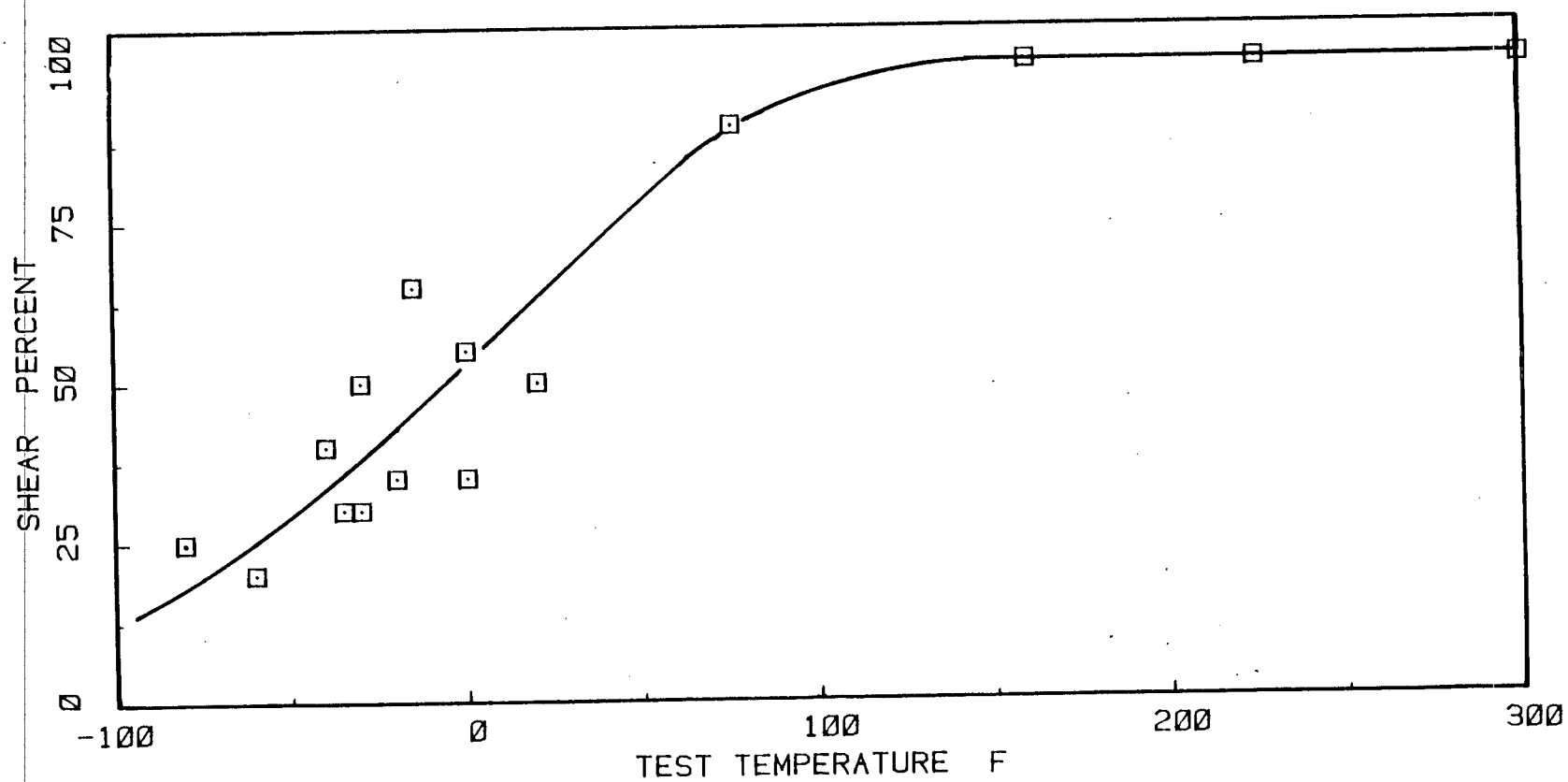

FIGURE 17. CHARPY V-NOTCH PERCENT DUCTILE SHEAR VERSUS TEST TEMPERATURE FOR THE IRRADIATED WELD METAL SPECIMENS FROM THE MONTICELLO 30 DEGREE SURVEILLANCE CAPSULE

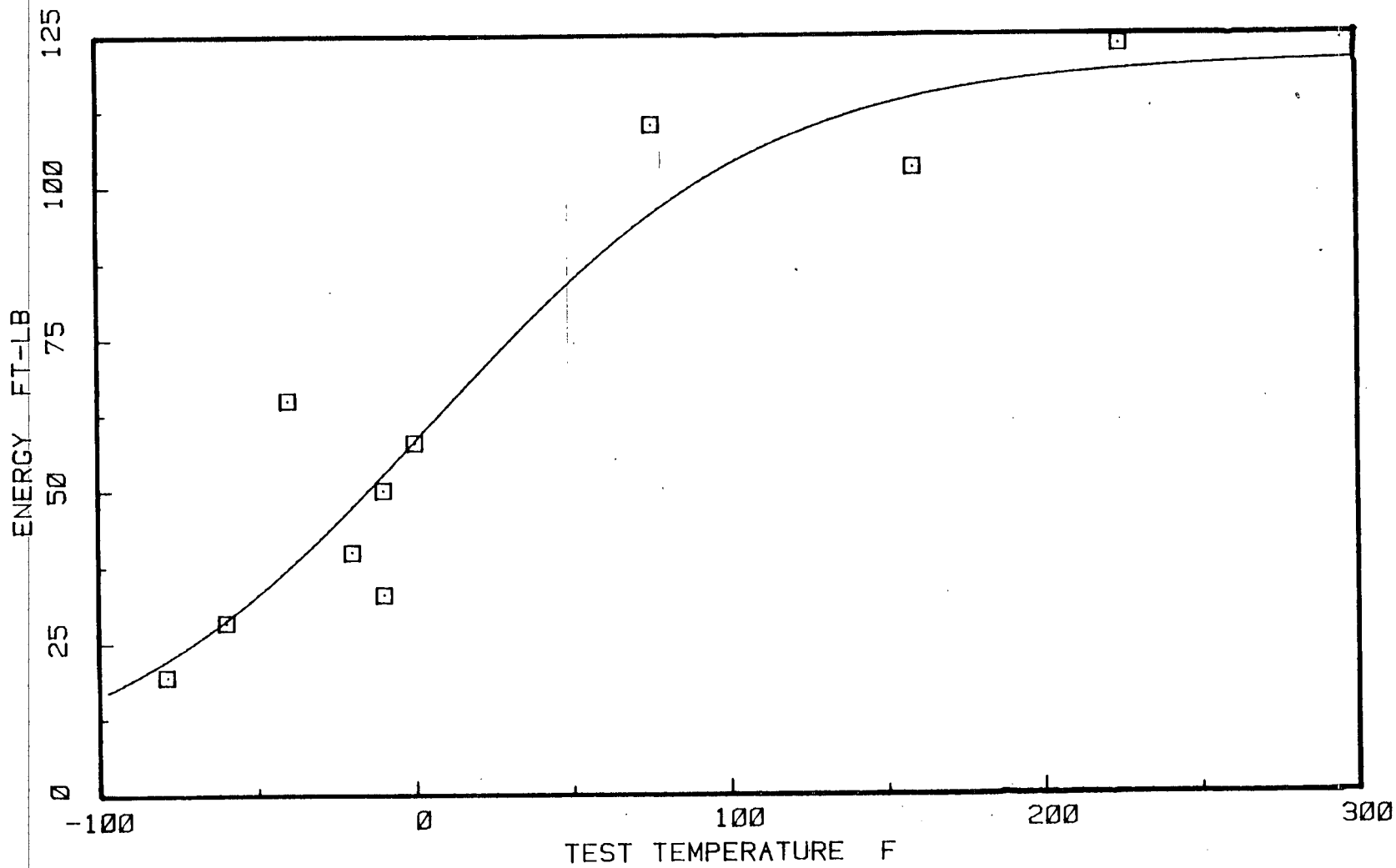

FIGURE 18. CHARPY V-NOTCH IMPACT ENERGY VERSUS TEST TEMPERATURE FOR THE IRRADIATED HAZ METAL SPECIMENS FROM THE MONTICELLO 30 DEGREE SURVEILLANCE CAPSULE

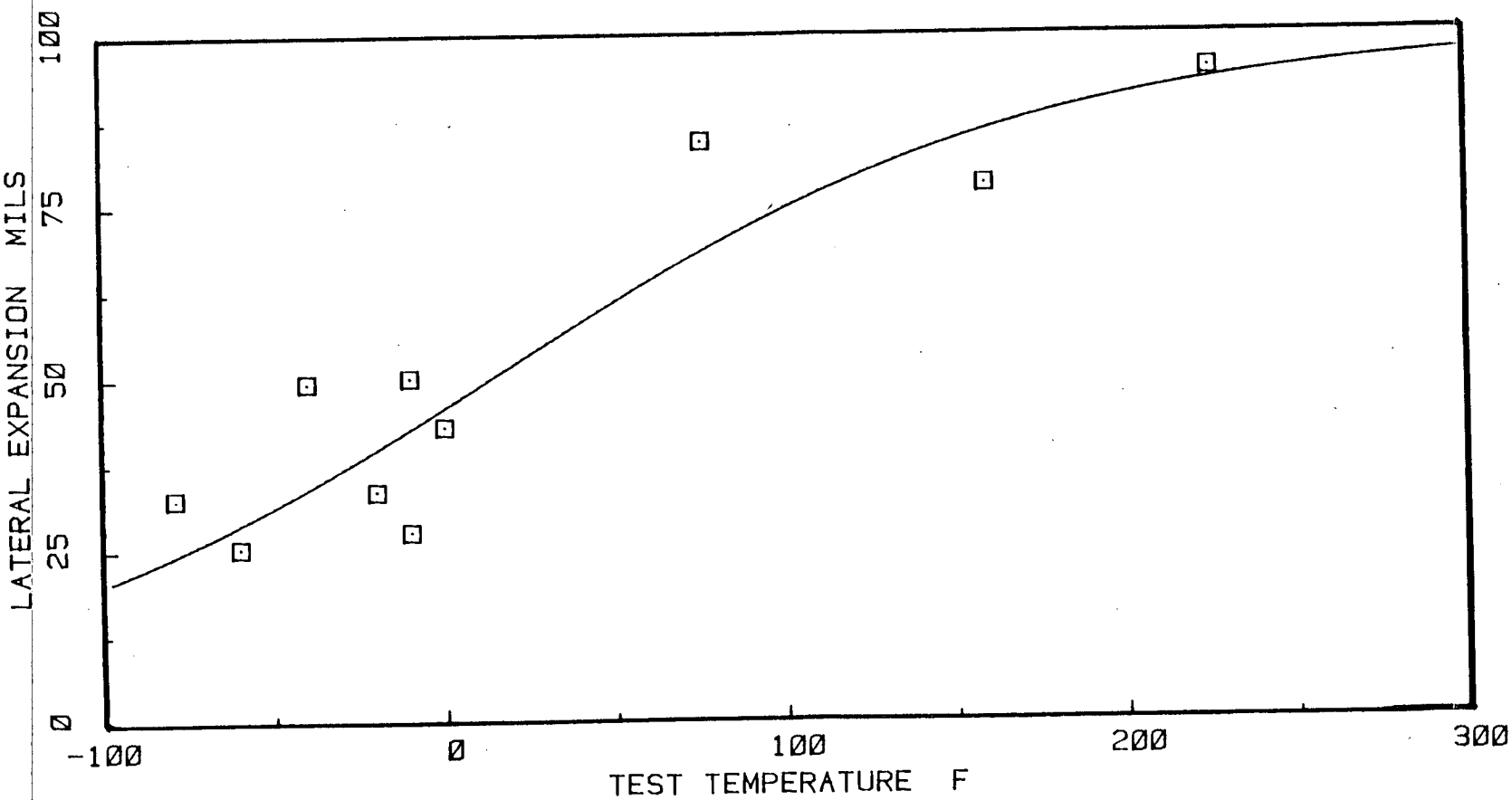

FIGURE 19. CHARPY V-NOTCH LATERAL EXPANSION VERSUS TEST TEMPERATURE FOR THE IRRADIATED HAZ METAL SPECIMENS FROM THE MONTICELLO 30 DEGREE SURVEILLANCE CAPSULE

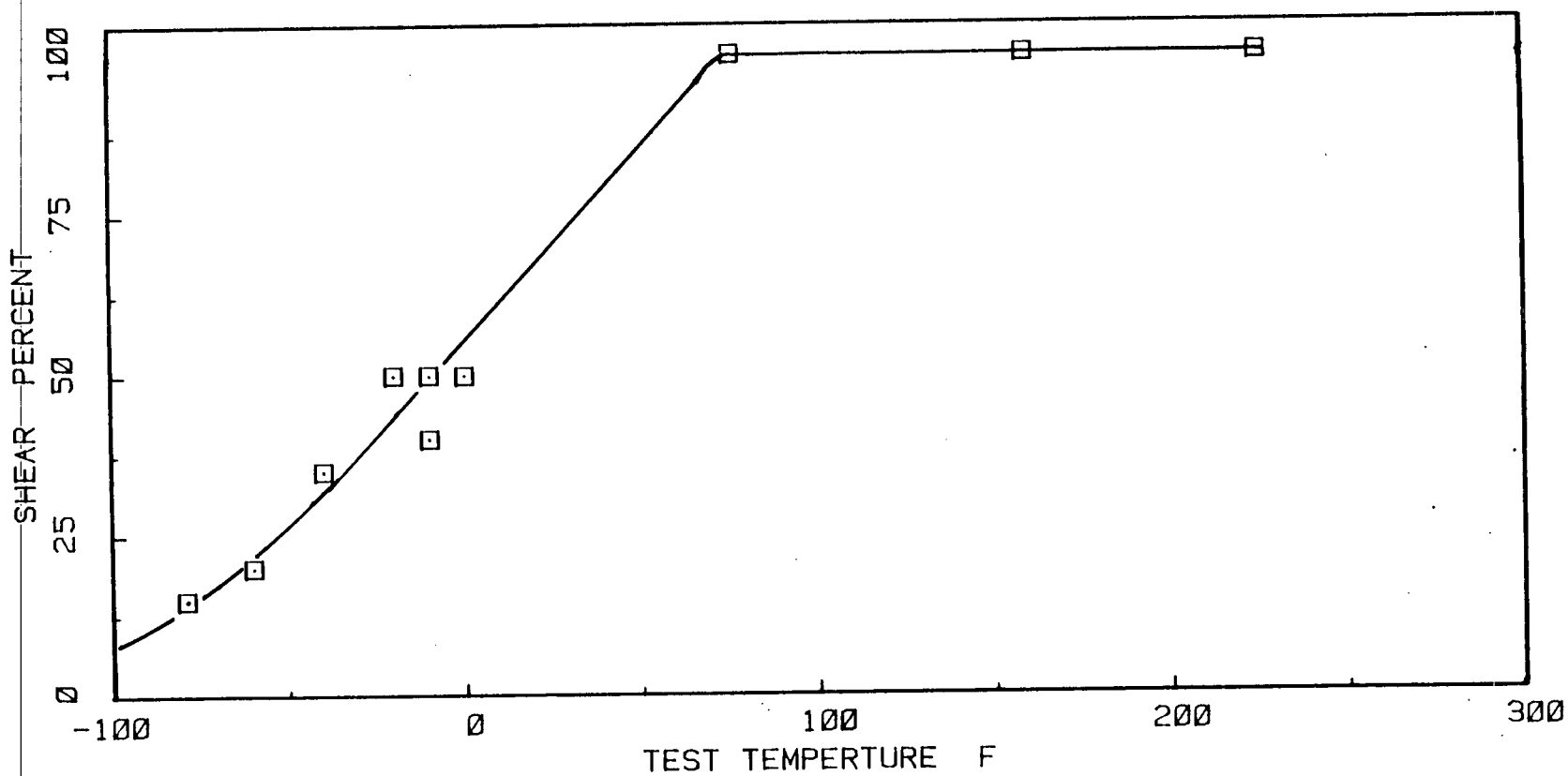

FIGURE 20. CHARPY V-NOTCH PERCENT DUCTILE SHEAR VERSUS TEST TEMPERATURE FOR THE IRRADIATED HAZ METAL SPECIMENS FROM THE MONTICELLO 30 DEGREE SURVEILLANCE CAPSULE

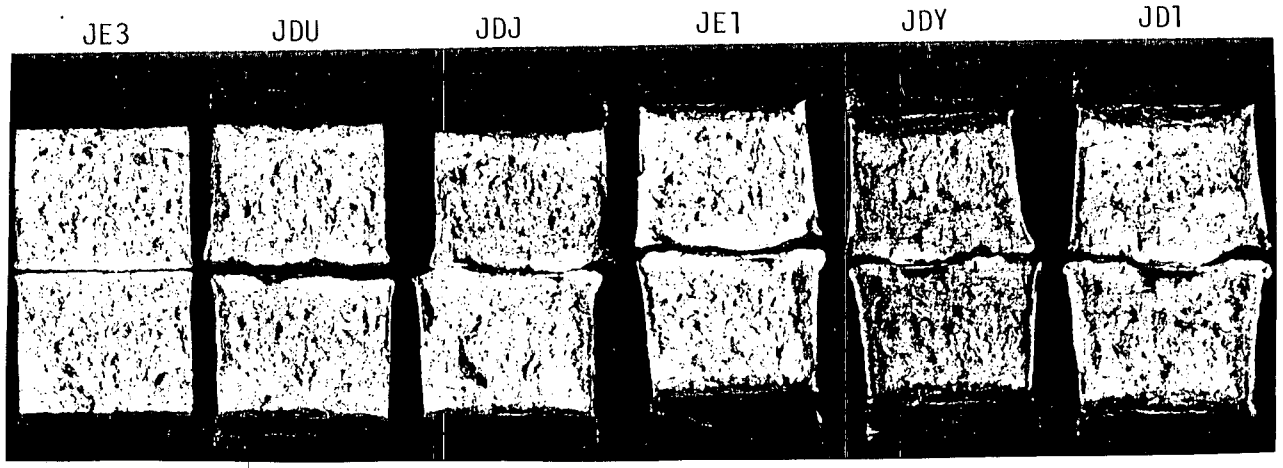

2X

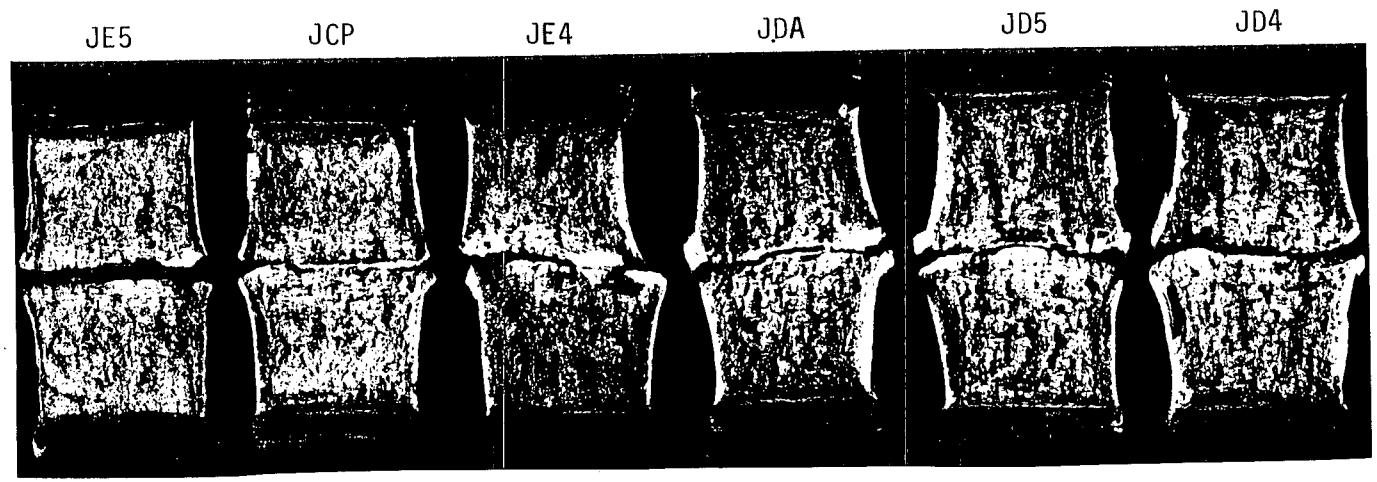

2X

FIGURE 21. CHARPY IMPACT SPECIMEN FRACTURE SURFACES FOR THE IRRADIATED BASE METAL SPECIMENS FROM THE MONTICELLO 30 DEGREE SURVEILLANCE CAPSULE

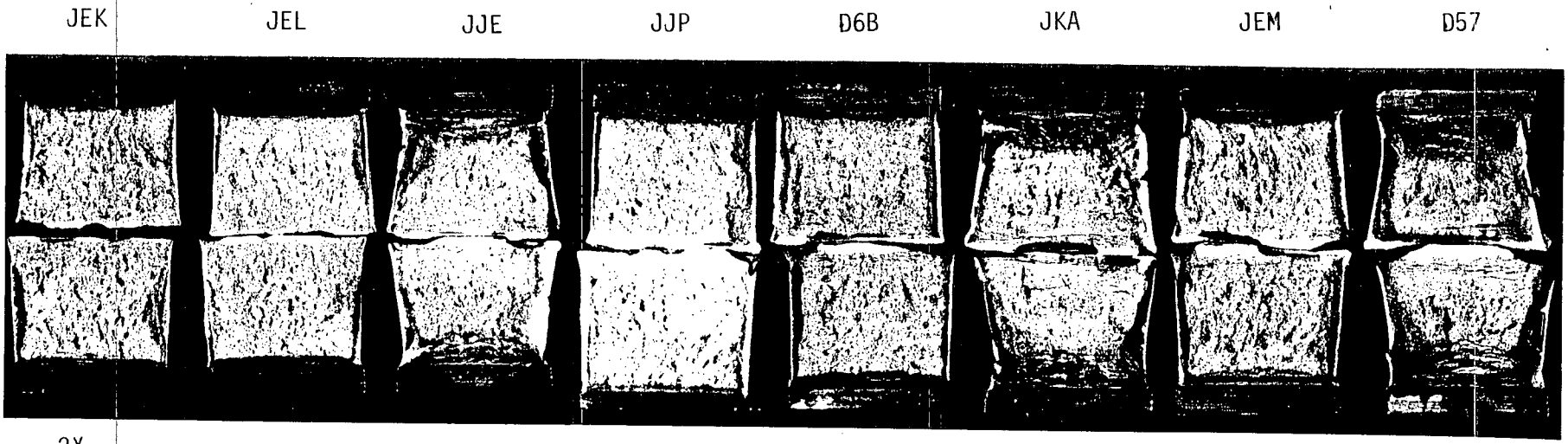

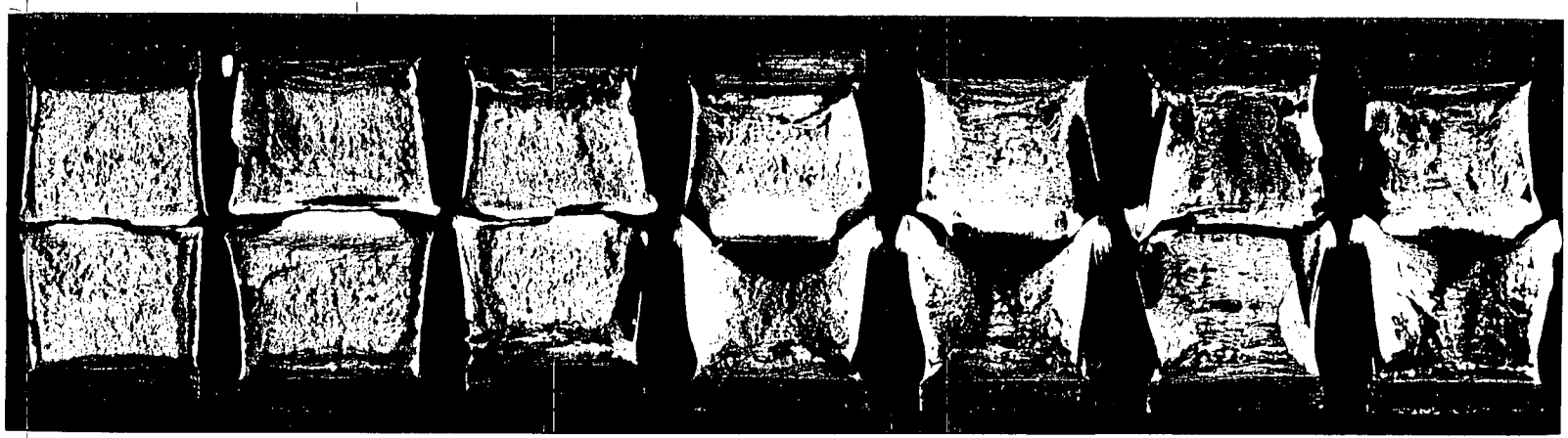

FIGURE 22. CHARPY IMPACE SPECIMEN FRACTURE SURFACES FOR THE IRRADIATED WELD METAL SPECIMENS FROM THE MONTICELLO 30 DEGREE SURVEILLANCE CAPSULE

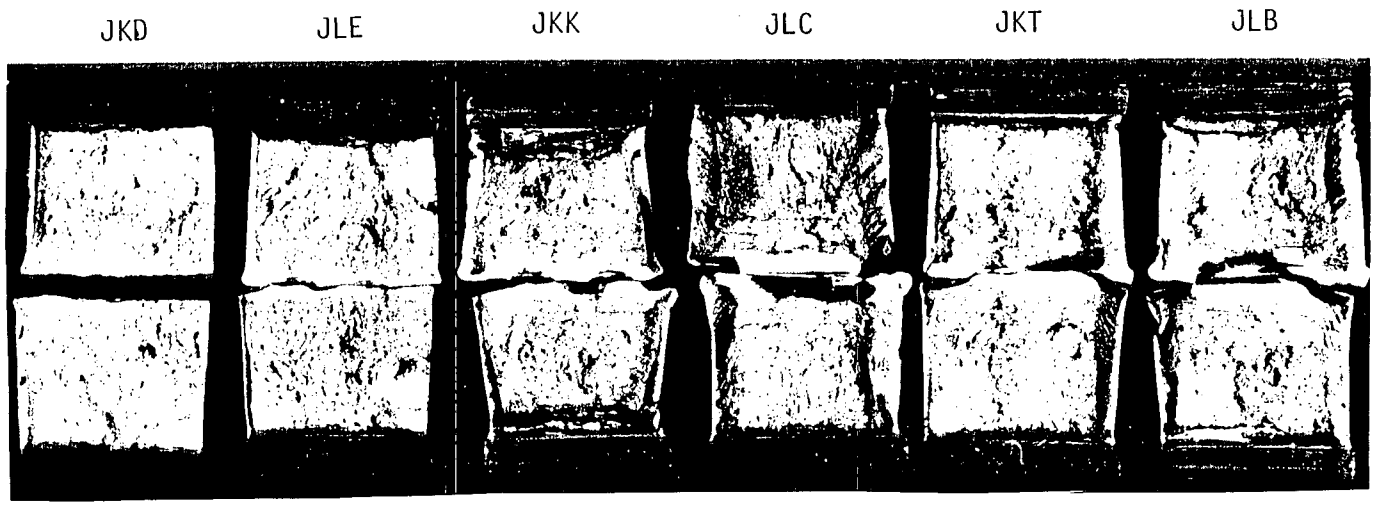

FIGURE 23. CHARPY IMPACT SPECIMEN FRACTURE SURFACES FOR THE IRRADIATED HAZ METAL SPECIMENS FROM THE MONTICELLO 30 DEGREE SURVEILLANCE CAPSULE

TABLE 10. SUMMARY OF CHARPY IMPACT PROPERTIES FOR IRRADIATED MATERIALS FROM THE MONTICELLO 30 DEGREE SURVEILLANCE CAPSULE

Material	E>1.0 MeV Fluence, n/cm^2	30 ft-lb Transition Temperature, F	50 ft-lb Transition Temperature, F	35-Mil Lateral Expansion Temperature, F	Upper Shelf Energy, ft-lb
Base	2.98×10^{17}	56	100	85	109
Weld	2.98×10^{17}	-65	-25	-40	122
HAZ	2.98×10^{17}	-57	-15	-36	121

109 ft-lb for the base metal, 122 ft-lb for the weld metal, and 121 ft-lb for the HAZ metal. These valuse are well above this minimum allowable upper shelf energy of 50 ft-lb.

The unirradiated drop weight and Charpy V-notch impact data[16] are shown below.

Plate	Drop Weight T_{NDT} (F)	Test Temperature (F)	Charpy V-notch (ft-lb)
C2220-1 (1-14)	0	10	60
C2220-1 (1-14)	0	10	93
C2220-1 (1-14)	0	10	81
C2220-2 (1-15)	0	10	81
C2220-2 (1-15)	0	10	33
C2220-2 (1-15)	0	10	61

Tensile Properties

Introduction

The tensile specimens were irradiated in the Monticello surveillance capsule which was located at the 30 degree azimuthal position and 0.56 inch from the vessel wall. The tensile specimens were tested and the yield strength, ultimate tensile strength, uniform elongation, total elongation, and reduction-in-area of the irradiated materials were determined.

Analytical Method

Prior to testing, each tensile specimen diameter was measured using a blade micrometer and an initial cross-sectional area was calculated for each specimen. Load-elongation data were recorded on a strip chart for each test. The 0.2 percent offset yield load, maximum tensile load, uniform elongation, and total elongation data were taken directly from the strip chart. The percent elongation was calculated for a 1 inch gage section and was verified by posttest measurements of the increase in distance between the tensile specimen punch marks (originally positioned 1 inch apart). The yield load and ultimate load divided by the initial cross-sectional area provided the yield and ultimate tensile strengths, respectively. The percent reduction-in-area was calculated by subtracting the posttest cross-sectional area from the initial cross-sectional area, dividing by the initial cross-sectional area, and multiplying by 100. The fracture strength was calculated by dividing the failure load by the pretest cross-sectional area and the fracture stress was calculated by dividing the failure load by the posttest cross-sectional area.

Tensile Test Results

The tensile test parameters and irradiated specimen tensile properties are listed in Table 11 and plotted in Figures 24 and 25. This table lists the specimen number, material, and test temperature. Also listed are the 0.2 percent offset yield strength, ultimate tensile strength, fracture strength, fracture stress, reduction in area, uniform elongation, and total elongation for each specimen tested. Photographs of the tested tensile specimen (longitudinal and end-on) are shown in Figures 26, 27, and 28. As can be seen, the necking occurred between the initial 1 inch punch marks for all nine tensile specimens and all failures were in a ductile cup-and-cone mode. A typical tensile test curve is shown in Figure 29.*

*Text continued on page 66.

TABLE 11. TENSILE PROPERTIES OF THE IRRADIATED MATERIALS FROM THE MONTICELLO 30 DEGREE CAPSULE

Specimen No.	Material Type	Test Temp.(1) (F)	Strength, psi			Fracture Stress (psi)	Reduction in Area (percent)	Elongation, percent(2)	
			Yield	Ultimate	Fracture			Uniform	Total
JB2	Base	RT	71,590	85,340	50,920	192,310	73.5	13.9	27.4(20.7)
JB6	Base	200	64,140	77,580	46,060	176,740	73.9	10.3	22.6(16.5)
DC2	Base	550	62,630	90,120	63,140	162,300	61.1	9.6	19.6(14.6)
JC1	Weld	RT	67,240	91,730	62,240	183,730	66.1	14.4	28.0
JC2	Weld	200	63,650	85,740	58,550	177,020	66.9	12.1	24.5
JBM	Weld	550	58,300	87,650	64,780	160,000	59.5	12.6	22.1
JC6	Haz	RT	67,450	87,650	55,100	188,810	70.8	11.2	24.7
JCK	Haz	200	64,080	82,140	51,020	181,160	71.8	8.5	20.8
JCM	Haz	550	62,880	87,830	57,810	165,700	65.1	11.2	22.5

(1) RT if room temperature - 75°F.

(2) The elongation is for a 1-inch gauge length and the values in parentheses are for a 2-inch gauge length.

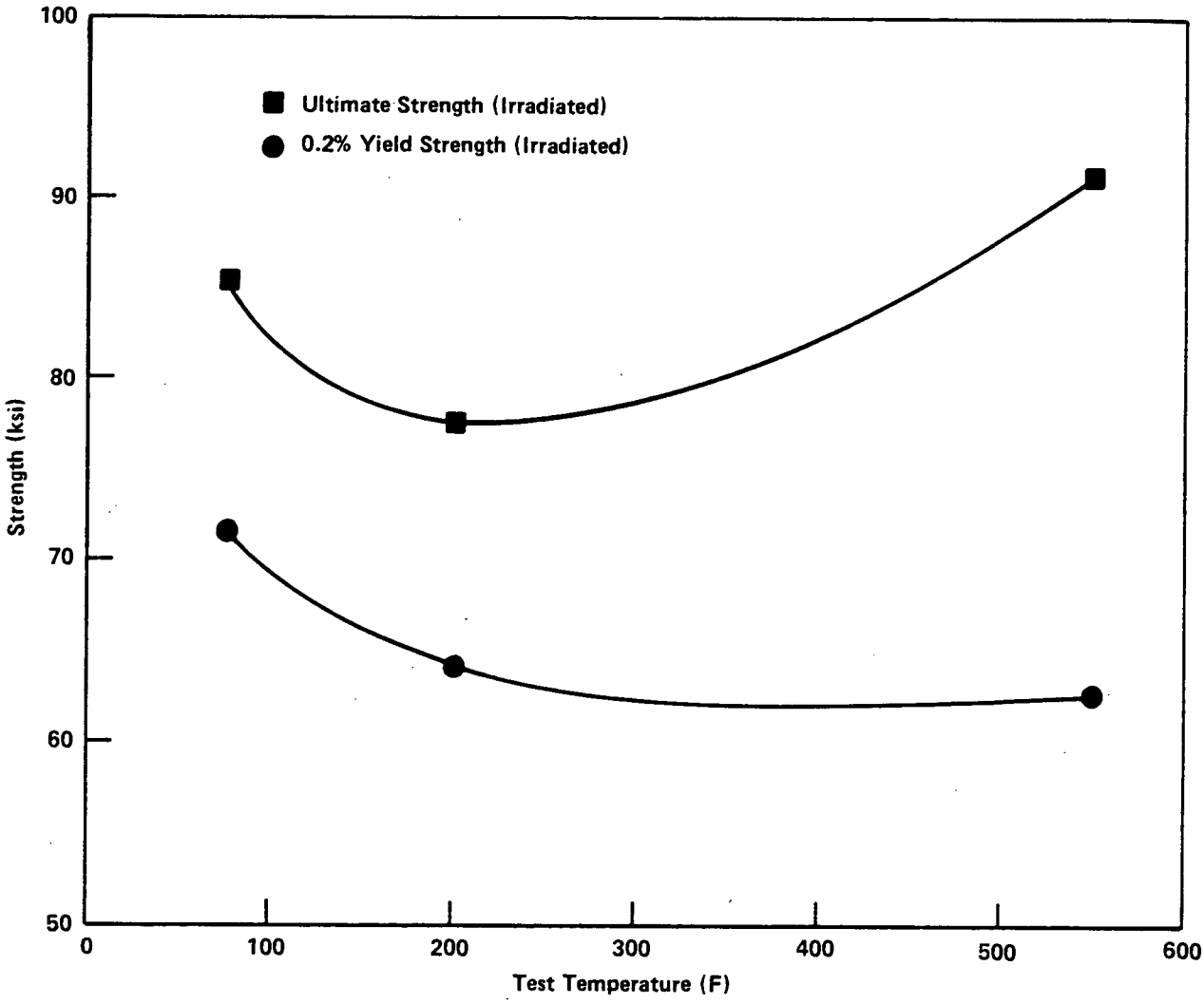

FIGURE 24. BASE METAL YIELD AND ULTIMATE TENSILE STRENGTHS VERSUS TEST TEMPERATURE FOR THE IRRADIATED TENSILE SPECIMENS FROM THE MONTICELLO 30 DEGREE SURVEILLANCE CAPSULE

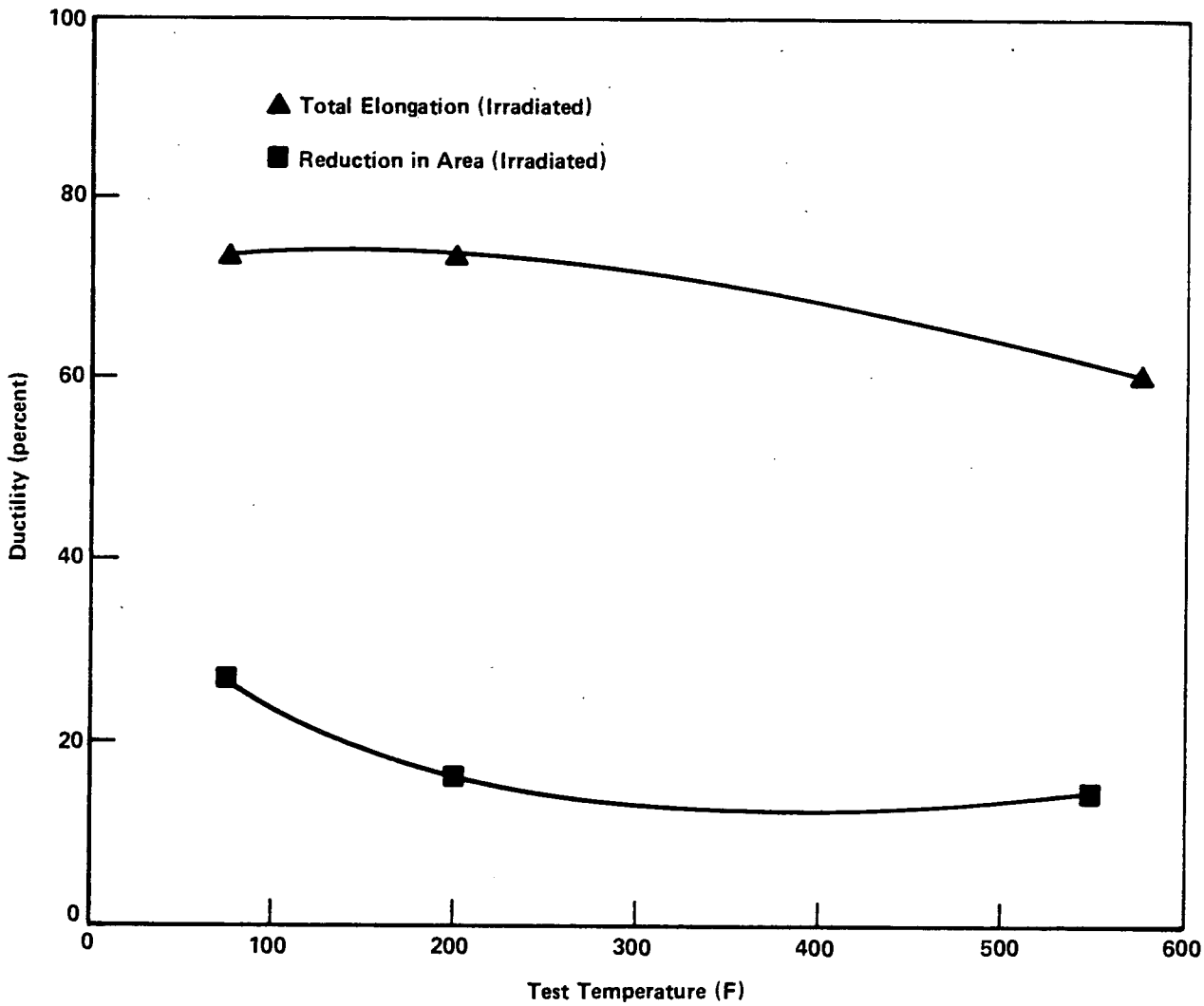

FIGURE 25. BASE METAL TOTAL ELONGATION AND REDUCTION IN AREA VERSUS TEST TEMPERATURE FOR THE IRRADIATED TENSILE SPECIMENS FROM THE MONTICELLO 30 DEGREE SURVEILLANCE CAPSULE

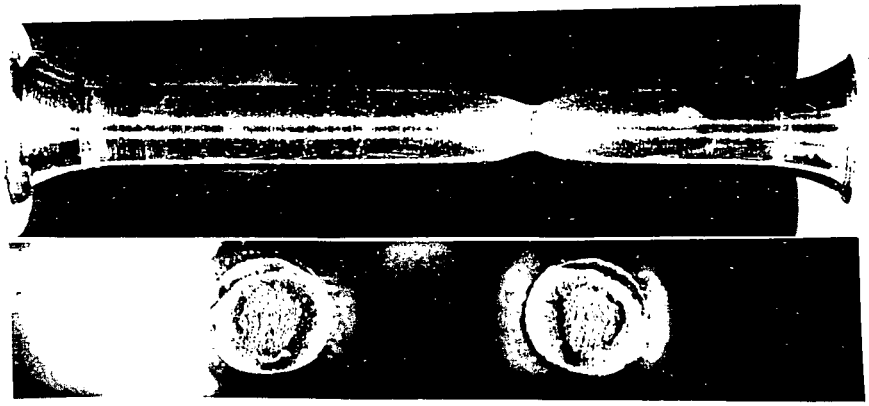

2X JB2 C-9895 & -9896

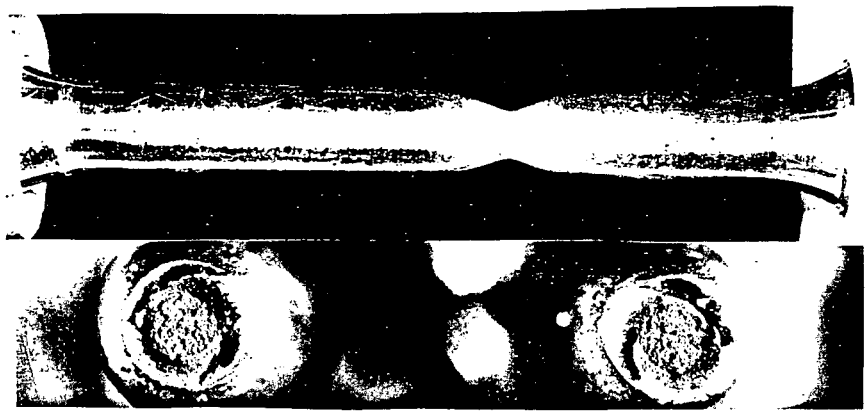

2X JB6 C-9885 & -9891

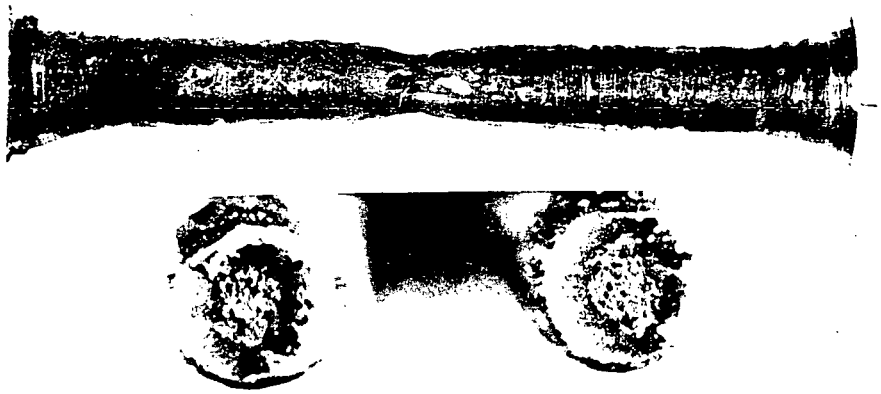

2X DC2 C-9875 & -9889

FIGURE 26. POSTTEST PHOTOGRAPHS OF THE IRRADIATED BASE METAL TENSILE SPECIMENS SHOWING BOTH THE REDUCED AREAS AND FRACTURE SURFACES (MONTICELLO 30 DEGREE SURVEILLANCE CAPSULE)

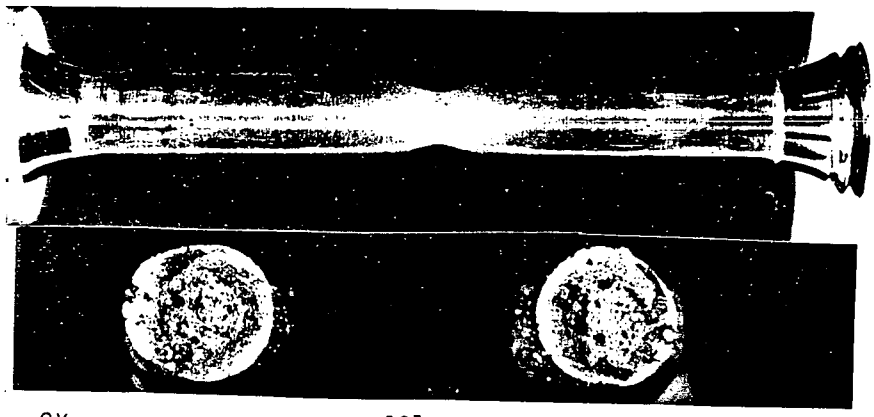

2X JC1 C-9894 & -9898

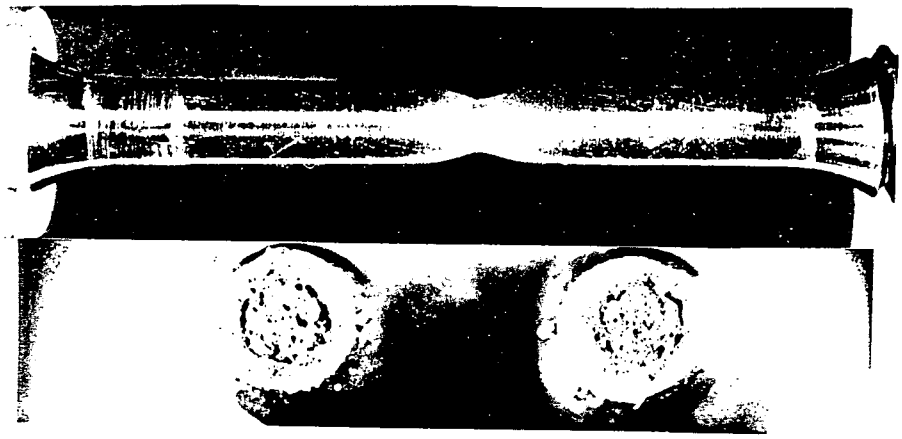

2X JC2 C-9887 & -9890

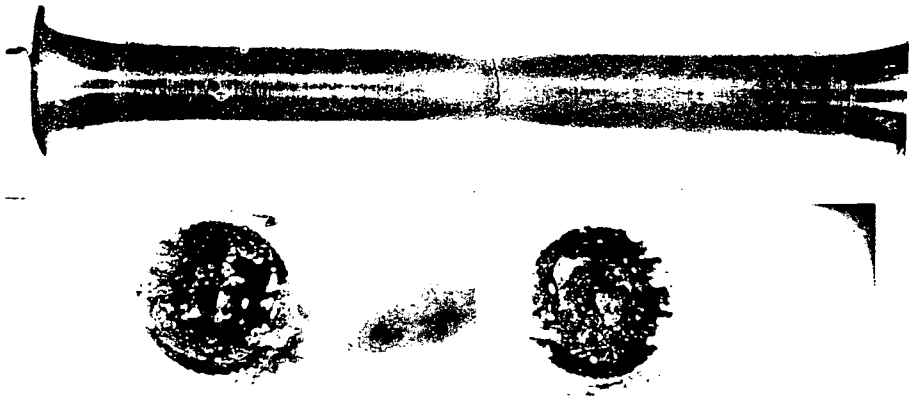

2X JBM C-9873 & -9888

FIGURE 27. POSTTEST PHOTOGRAPHS OF THE IRRADIATED WELD METAL TENSILE SPECIMENS SHOWING BOTH THE REDUCED AREAS AND FRACTURE SURFACES (MONTICELLO 30 DEGREE SURVEILLANCE CAPSULE)

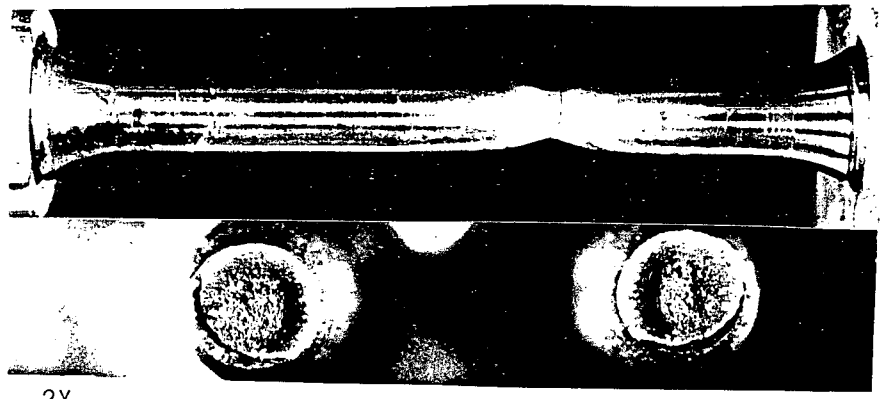

2X JC6 C-9893 & -9897

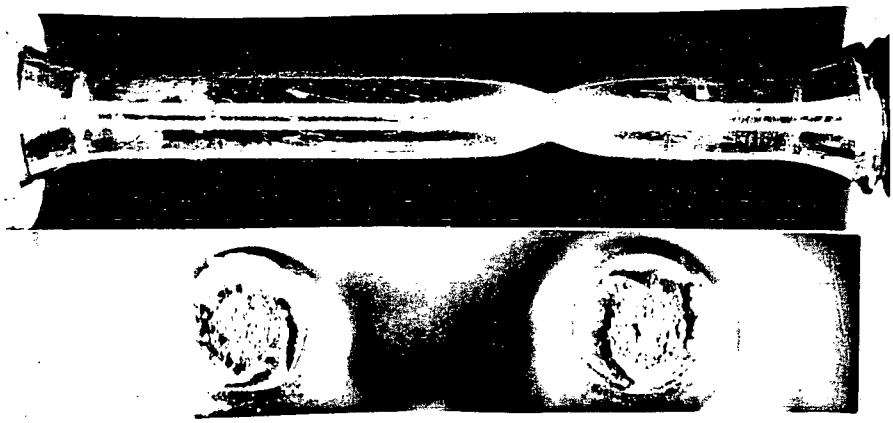

2X JCK C-9886 & -9892

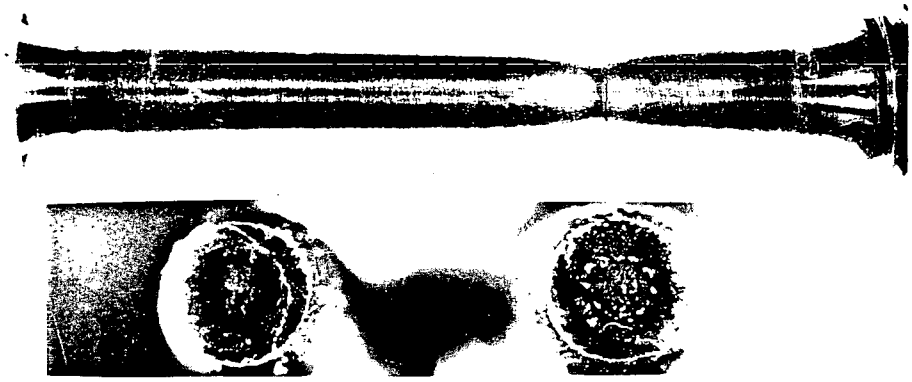

2X JCM C-9874 & -9877

FIGURE 28. POSTTEST PHOTOGRAPHS OF THE IRRADIATED HAZ METAL TENSILE SPECIMENS SHOWING BOTH THE REDUCED AREAS AND FRACTURE SURFACES (MONTICELLO 30 DEGREE SURVEILLANCE CAPSULE)

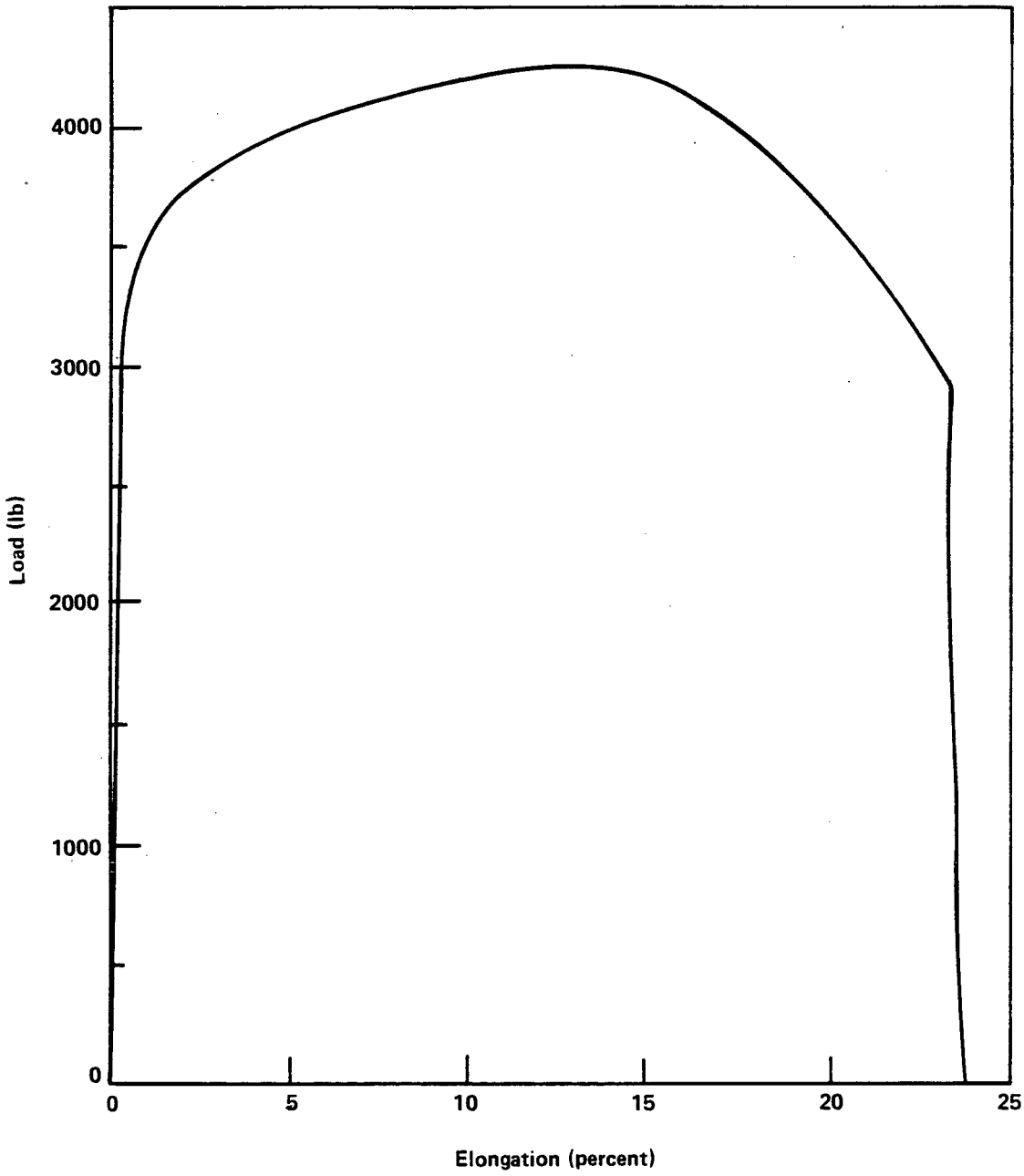

FIGURE 29. TYPICAL TENSILE LOAD-ELONGATION CURVE

Tensile tests were conducted at room temperature (75 F), 200 F, and 550 F. All three materials, base metal, weld metal, and HAZ metal exhibited decreases in yield strength, ultimate strength, and fracture strength when the test temperature was increased from room temperature to 200 F. These tensile properties appear, however, to recover partially (and in some cases totally) at the test temperature of 550 F when compared with the room temperature test results. The 0.2 percent offset yield strength and fracture stress exhibited a monotonic decrease with increasing test temperature between room temperature and 550 F for all three material types. The percent reduction in area for the three materials was relatively constant at test temperatures of 75 F (room temperature) and 200 F but decreased slightly (6 to 13 percent) at a test temperature of 550 F. Within experimental standard deviation, the base metal and weld metal tensile elongations (uniform and total) generally decreased with increased test temperature. However, both the uniform elongation and total elongation appear to decrease when the test temperature was increased from 75 to 200 F and appears to recover at the test temperature of 550 F.

It should be noted that the base metal specimen tested at 550 F bore the FAB Code designation D whereas the two tested at room temperature and 200 F had the FAB designation J. A recent record search has revealed that the specimens designated with a J may be from a different plate than those specimens designated with a D. This may be the reason the room temperature and 550 F ultimate strengths are nearly the same. Therefore, until furhter information is obtained or additional testing performed, no conclusions or comparisons can be made.

Chemical Analysis

Introduction

It had been known for some time that the chemical composition of a pressure vessel steel affected the extent to which material properties such as

fracture and crack propagation were changed during irradiation. The Nuclear Regulatory Commission (NRC) Regulatory Guide 1.99 was issued as a guide for estimating the effect of copper and phosphorus on the reference nil-ductility (transition) temperature (RT_{NDT}) as a function of fluence. In order to use this guide or to establish the copper and phosphorus content, a chemical analysis must be performed. It was originally believed that the weld metal was the only Monticello core beltline surveillance material for which no adequate traceability could be found in existing chemical and physical properties reports.[16] Therefore, base metal chemistry was not determined. A chemical analysis was performed to establish the weld metal constituents including copper (Cu), phosphorus (P), nickel (Ni), molybdenum (Mo), chromium (Cr), manganese (Mn), vanadium (V), silicon (Si), sulfur (S), and carbon (C).

Analytical Method

Each sample (one half of a broken weld metal Charpy V-notch specimen) was ground and polished through 600 grit grinding paper, masked-down, and bombarded with primary X-rays to produce measurable characteristic or secondary X-rays. Qualification and calibration was achieved by comparing the accumulated intensities and wavelengths of the secondary X-rays to those emitted by NBS standards. The standards possess a known concentration range for each element. Counts on the major X-ray and at off-line background X-ray positions were accumulated for up to 200 seconds at least twice for each sample to improve counting statistics. Electronic pulse height analysis (PHA) was used for phosphorus, vanadium, silicon, and sulfur count evaluation to eliminate excessive background due to the radioactivity of the sample. The chemical analysis for Cu, Ni, Mo, Cr, and Mn content was obtained using standard curves of characteristic X-ray intensities as a function of the percent of each element in the NBS standards. The chemical analysis for P, V, Si, and S content was obtained by ratioing the net intensities of the characteristic X-rays for each element emitted by the weld metal sample to the net intensities obtained for each NBS standard. The NBS comparison standards

were chosen so that the elemental composition (percent of each element) was as close as possible to the percent of each element expected in the Monticello Charpy V-notch weld metal samples.

Each weld metal Charpy V-notch specimen was first drilled. Chips from the weld metal drilling were analyzed for carbon content using the combustion gravimetric method outlined in ASTM E350-82 Sections 169 to 174.

Chemical Analysis Results

Three broken weld metal Charpy V-notch specimen halves were analyzed for elemental constituents including Cu, P, Ni, Mo, Cr, Mn, V, Si, S, and C. The analytical results for the three irradiated weld metal samples are listed in Table 12.

TABLE 12. CHEMICAL ANALYSES RESULTS FOR IRRADIATED MONTICELLO WELD METAL SPECIMENS FROM THE SURVEILLANCE CAPSULE

Specimen	Elements, Weight Percent									
	Cu	P	Ni	Mo	Cr	Mn	V	Si	S	C
JKA	0.06	0.01	0.92	0.46	0.05	1.04	0.010	0.20	0.01	0.077
JEL	0.03	0.01	0.95	0.51	0.03	0.97	0.010	0.32	0.01	0.067
JEP	0.04	0.01	0.90	0.44	0.04	1.02	0.010	0.10	0.01	0.068
Calculated Accuracy ± %	15.0	---	6.0	6.0	---	2.0	---	4.5	---	5.0
Estimated Detection Limit, wt. %	0.02	0.01	0.01	0.02	0.01	0.02	0.01	0.02	0.01	0.005

It can be seen from Table 12 that the irradiated weld metal elements (Cu, P, and Ni) which have been identified as the major contributors to irradiated pressure vessel steel embrittlement are less than 0.1 weight percent for Cu, 0.01 weight percent or less for P, and 0.92 $\pm$ 0.02 weight percent for Ni. This copper content is consistent with that assumed by the Nuclear Regulatory Commission for the Monticello manual shielded-metal-arc-welded reactor pressure vessel shell.[35]

CONCLUSIONS

Evaluation of the fast neutron dosimetry, chemical analysis, and mechanical property test (Charpy V-notch and tensile) results for specimens from the Monticello Nuclear Generating Plant surveillance Capsule 1 led to the following conclusions:

Neutron Dosimetry

- The Monticello capsule and surveillance specimens at the 30 degree azimuthal location received a fast neutron fluence ($E > 0.1$ MeV) of 2.93×10^{17} n/cm^2 as a result of operation from initial startup to November 1981 (7.633 EFPY).
- The Monticello pressure vessel azimuthal fluence (or flux) varied by as much as a factor of 4. The maximum fast neutron exposure occurred at about the 3 degree azimuthal position and the lead factor was only 0.31 for the pressure vessel inside surface, 0.41 for the 1/4T, and 1.05 for the 3/4T positions.
- The maximum fast neutron fluence ($E > 1.0$ MeV) at the pressure vessel 1/4T position was 7.20×10^{17} n/cm^2 as a result of operation from initial startup to November 1981 (7.633 EFPY).
- Extrapolating the present data to the end of life (EOL) of 32 equivalent full power years (EFPY), the maximum calculated EOL fast neutron fluence ($E > 1.0$ MeV) at the pressure vessel 1/4T position would be 3.02×10^{18} n/cm^2. If a 20 percent accuracy is assumed, the upper bound of the maximum EOL fast neutron fluence ($E > 1.0$ MeV) at the pressure vessel 1/4T position would be 3.6×10^{18} n/cm^2.
- The EOL projected maximum fast neutron fluence ($E > 1.0$ MeV) of 3.6×10^{18} n/cm^2 at the pressure vessel 1/4T position is about 60 percent higher than the value of 2.2×10^{18} n/cm^2 predicted by the reactor vendor.

Charpy

- After a fast neutron fluence (E > 1.0 MeV) of 2.93×10^{17} n/cm^2, the irradiated Charpy V-notch specimens from the Monticello 30 degree surveillance capsule indicate a base metal upper shelf energy of 109 ft-lb, a weld metal upper shelf energy of 122 ft-lb, and a HAZ metal upper shelf energy of 121 ft-lb. These values are well above the minimum allowable upper shelf energy of 50 ft-lb.

Tensile

- All tensile test specimens exhibited ductile failures as evidenced by the cup-and-cone type fracture shape.

Chemistry

- The weld metal specimens JKA, JEL, and JEP contained a maximum of 0.1 weight percent copper, a maximum of 0.01 weight percent phorphorus, and approximately 1.0 weight percent nickel.

REFERENCES

1. Reuther, T. C. and Swilsky, K. M., "The Effects of Neutron Irradiation on the Toughness and Ductility of Steels", in Proceedings of Toward Improved Ductility and Toughness Symposium, published by Iron and Steel Institute of Japan (October, 1971), pp 289-319.

2. Steele, L. E., "Major Factors Affecting Neutron Irradiation Embrittlement of Pressure-Vessel Steels and Weldments", NRL Report 7176 (October 30, 1970).

3. Berggren, R. G., "Critical Factors in the Interpretation of Radiation Effects on the Mechanical Properties of Structural Metals", Welding Research Council Bulletin, 87, 1 (1963).

4. Hawthorne, J. R., "Radiation Effects Information Generated on the ASTM Reference Correlation-Monitor Steels", American Society for Testing and Materials Data Series Publication DS54 (1974).

5. Steele, L. E. and Serpan, C. Z., "Neutron Embrittlement of Pressure Vessel Steels - A Brief Review", Analysis of Reactor Vessel Radiation Effects Surveillance Programs, American Society for Testing and Materials Special Technical Publication 481 (1969(, pp 47-102.

6. Integrity of Reactor Vessels for Light-Water Power Reactors, Report by the USAEC Advisory Committee on Reactor Safeguards (January, 1974).

7. Higgins, J. P. and Brandt, F. A., "Mechanical Property Surveillance of General Electric BWR Vessels", General Electric Report NEDO-10115 (July, 1969).

8. "Standard Practice for Conducting Surveillance Tests for Light-Water Cooled Nuclear Power Reactor Vessels", ASTM Designation E185-82, Annual Book of ASTM Standards, Part 45 (1982), pp 888-896.

9. Perrin, J. S., "Nuclear Reactor Pressure Vessel Surveillance Capsule Examinations: Application of American Society for Testing and Materials Standards", paper presented at the October, 1977, International Atomic Energy International Symposium on Application of Reliability Technology to Nuclear Power Plants (Reliability Problems of Reactor Pressure Components) in Vienna, Austria, and published in the Proceedings of that Conference.

10. Proposed Research Program (Proposal No. 585-K-4189) on "Examination and Evaluation of Irradiated Surveillance Specimens from the Monticello Nuclear Generating Plant" to Northern States Power Company from Battelle Columbus Laboratories, January 16, 1981.

11. "Standard Methods and Definitions for Mechanical Testing of Steel Products", ASTM Designation A370-77, Annual Book of ASTM Standards, Part 10 (1982), pp 28-83.

12. ASME Boiler and Pressure Vessel Code, Section III, Appendix G for Nuclear Power Plant Components, Division 1, "Protection Against Nonductile Failure", 1980 Edition, pp 543-552.

13. Code of Federal Regulation, Title 10, Part 50, Appendix G, "Fracture Toughness Requirements", 1982, pp 424-427.

14. ASME Boiler and Pressure Vessel Code, Section III, Subsection NB (Class 1 Components) for Nuclear Power Plant Components, Division 1, NB-2330 and 2331, "Test Requirements and Acceptance Standards", 1980 Edition, p 15.

15. "Standard Method for Conducting Drop-Weight Test to Determine Nil-Ductility Transition Temperature of Ferritic Steels", ASTM Designation E208-81, Annual Book of ASTM Standards, Part 10 (1982), pp 420-439.

16. "Monticello Nuclear Generating Plant Information on Reactor Vessel Material Surveillance Program", General Electric Report NEDO-24197, Revision 1, October 1979.

17. Private Communications, D. J. Brosche of Northern States Power Company to L. M. Lowry of Battelle's Columbus Laboratory, November 4, 1982.

18. Evaluated Reference Cross Section Library by R. L. Simons and W. N. McElroy, BNWL-1312, May, 1970, Battelle Memorial Institute, Pacific Northwest Laboratories, Richland, Washington 99352.

19. "Reference Cross Section Library for SAND II", A Computer-Automated Interactive Method for Neutron Flux Spectra Determination by Foil Activation, AGWL-TR-67-41, Vol. III, Air Force Weapons Laboratory, Kirtland AFB, New Mexico, August, 1965.

20. RSIC Computer Code Collection, DOT 3.5-Two Dimensional Discrete Ordinates Radiation Transport Code, Radiation Shielding Information Center, Oak Ridge National Laboratory, Oak Ridge, Tennessee, November 17, 1975.

21. CASK, 40 Group Coupled Neutron and Gamma-Ray Cross Section Data, RSIC Library DLC-23/CASK, September, 1974.

22. Standard Methods for "Notched Bar Impact Testing of Metallic Materials", ASTM Designation E23-82, Book of ASTM Standards, Part 10 (1982), pp 277-300.

23. Perrin, J. S., Fromm, E. O., and Lowry, L. M., "Remote Disassembly and Examination of Nuclear Pressure Vessel Surveillance Capsules", Proceedings of the 25th Conference on Remote Systems Technology, American Nuclear Society (1977).

24. "Standard Methods of Tension Testing of Metallic Materials", ASTM Designation E8-81, Annual Book of ASTM Standards, Part 10 (1982), pp 197-217.

25. "Standard Recommended Practice for Elevated Temperature Tension Tests of Metallic Materials", ASTM Designation E21-79, Annual ASTM Book of Standards, Part 10 (1982), pp 267-276.

26. "Standard Methods for Chemical Analysis of Carbon Steel, Low Alloy Steel, Silicon Electrical Steel, Ingot Iron, and Wrought Iron", ASTM Designation E350-82 (Sections 169 to 179 Entitled "Carbon, total, by the Combustion Gravimetric Method"), Annual Book of ASTM Standards, Part 12 (1982), pp 561-563.

27. The relative power data for the Monticello core were supplied in a letter from R. O. Anderson and Laura McCarten of Northern States Power Company to Dr. Richard Jung of Battelle's Columbus Laboratory, dated April 20, 1982.

28. "Standard Method for Measuring Neutron Flux, Fluence, and Spectra by Radioactivation Techniques", ASTM Designation E261-77, Annual Book of ASTM Standards, Part 45 (1982), pp 930-941.

29. "Standard Method for Determining Fast-Neutron Flux Density by Radioactivation of Iron", ASTM Designation E263-82, Annual Book of ASTM Standards, Part 45 91982), pp 951-956.

30. "Standard Guide for Application of Neutron Transport Methods for Reactor Vessel Surveillance", ASTM Designation E482-82, Annual Book of ASTM Standards, Part 45 (1982), pp 1088-1092.

31. "Standard Method for Calibration of Germanium Detectors for Measurement of Gamma-Ray Emission of Radionuclides", ASTM Designation E522-78, Annual Book of ASTM Standards, Part 45 (1982), pp 1139-1144.

32. "Standard Method for Determining Fast-Neutron Flux Density by Radioactivation of Copper", ASTM Designation E523-82, Annual Book of ASTM Standards, Part 45 (1982), pp 1145-1152.

33. Private communication, R. Streng of Northern States Power Company to A. M. Walters of Battelle's Columbus Laboratory, November 20, 1982.

34. Private communication with G. H. Scott, Service Supervisor of General Electric Company to D. Musolf of Northern States Power Company, dated September 20, 1979.

35. Letter from T. A. Ippolito of the NRC Operating Reactors Branch #2, Division of Licensing to L. O. Mayer, Nuclear Support Services Manager of Northern States Power Company, Docket No. 50-263, dated July 16, 1981.

36. Kass, J. N., Giannuzzi, A. J., Hughes, D. A., Jones, R. D., and Hayes, T. R., "Radiation Effects in Boiling Water Reactor Pressure Vessel Steels", A Licensing Topical Report, NEDO-21708 (77NED168 Class I), October 1977.

APPENDIX A

INSTRUMENTED CHARPY EXAMINATION

APPENDIX A

INSTRUMENTED CHARPY EXAMINATION

INTRODUCTION

The radiation-induced embrittlement of the pressure vessel of a commercial nuclear reactor is monitored by evaluation of Charpy V-notch impact specimens in surveillance capsules. In a conventional Charpy V-notch impact test, the information obtained for each specimen includes the absorbed energy, the lateral expansion, and the fracture appearance. Curves of energy versus temperature and lateral expansion versus temperature can be drawn for a series of specimens of a given irradiated material tested over a range of temperature. These curves, when compared to similar curves for the unirradiated material, show the shift in behavior due to irradiation.

Information in addition to the energy absorbed can be determined from a Charpy V-notch impact test by instrumenting the equipment used to perform the test. The loads during impact are obtained by instrumenting the Charpy striker or tup with strain gages, so that the striker is essentially a load cell. The details of this technique have been reported previously(1,2,3).

The additional information obtained from the instrumented Charpy test includes the general yield load, P_{GY} (plastic yielding across the entire cross section of the Charpy specimen), the maximum load, P_{max}, and the crack arrest load. In addition, if brittle fracture occurs, the brittle fracture load, P_F, and the time to brittle fracture can be obtained (see Figure A-1). The area under the load-time curve corresponds to the total energy absorbed, which is the only data obtained in a normal uninstrumented Charpy test. The instrumented test, however, allows separation of the energy abosrbed into (1) the energy required for crack initiation (approximated by the premaximum load energy), (2) the energy required for ductile tearing (postmaximum load

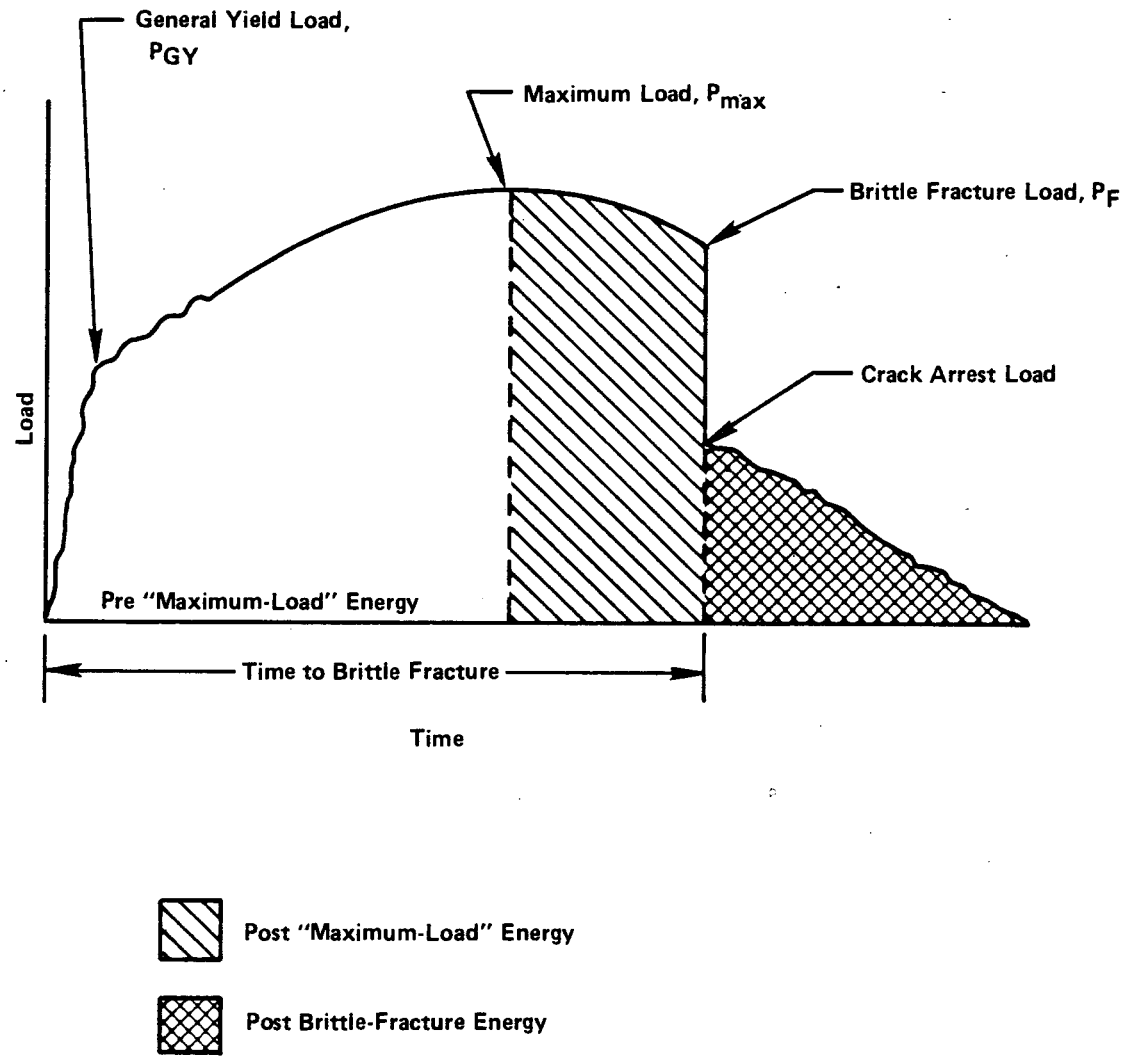

FIGURE A-1. AN IDEALIZED LOAD-TIME HISTORY FOR A CHARPY IMPACT TEST

energy), and (3) the energy associated with shear lip formation (postbrittle fracture energy), as shown in Figure A-1. Material properties, such as the yield strength and flow strength, appropriate to the loading rate of the Charpy impact test, may be subsequently calculated from the load information obtained by instrumenting the Charpy test[4]. This information enhances the value of the relatively small Charpy specimens to reactor vessel surveillance programs. These procedures have received the endorsement of the technical community[5].

The instrumented Charpy test also gives the information shown in Figure A-1 as a function of temperature, as shown by the example in Figure A-2. Various investigators[5-8] have developed theories that permit a detailed analysis of the load-temperature diagram. This diagram can be divided into four regions of fracture behavior, as shown in Figure A-2. In each region, different fracture parameters are involved[1]. The temperature corresponding to the intersection of the maximum or failure load curve and that of the general yield load in Figure A-2 is the temperature at which fracture occurs upon general yielding. Extended discussions of these fracture parameters can be found in the references indicated above.

EXPERIMENTAL PROCEDURES

The general procedures for the instrumented Charpy test are the same as those for the conventional impact test, and are described in the main text of this report. The additional data are obtained through a fairly simple electronic configuration, as shown in the schematic diagram of Figure A-3.

The striker of the impact machine is modified to make it a dynamic load sensor. The modification consists of a four-arm resistance strain gage bridge positioned on the striker to detect the compression loading of the striker during the impact loading of the specimen. The compressive elastic strain signal resulting from the striker contacting the specimen is conditioned by a high-gain dynamic amplifier and the output is fed into a digital oscilloscope. The load-time information is digitized and displayed on the

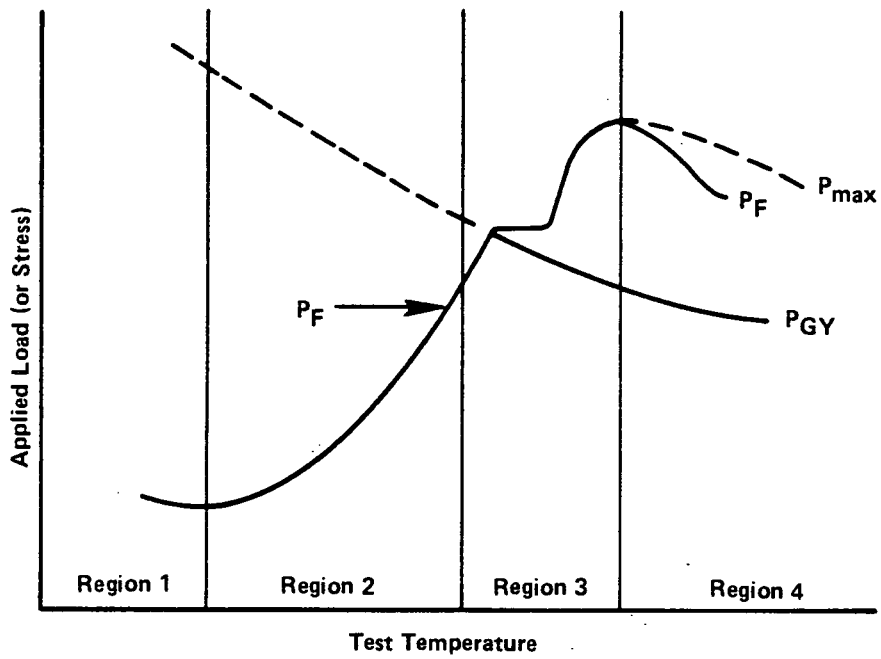

FIGURE A-2. GRAPHICAL ANALYSIS OF CHARPY IMPACT DATA

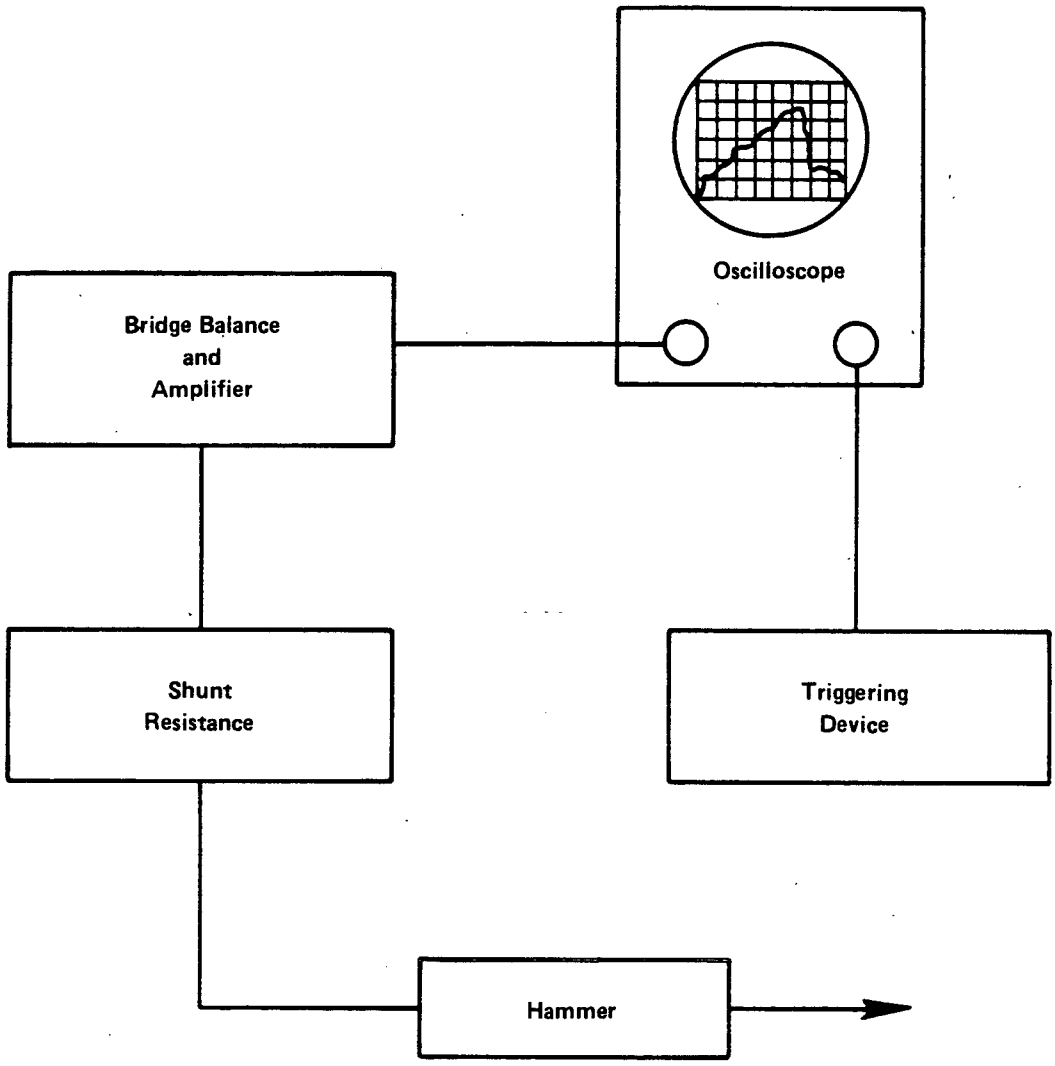

FIGURE A-3. DIAGRAM OF INSTRUMENTATION ASSOCIATED WITH INSTRUMENTED CHARPY EXAMINATION

screen of the digital oscilloscope. It is subsequently plotted on an X-Y recorder. The load-time history as a function of test temperature forms the basis for further data analysis. The digital oscilloscope is triggered by a light beam device at the correct time to capture the amplifier output signal[3,4].

RESULTS AND DISCUSSIONS

Specimens of three materials were tested. These materials are base metal (longitudinal orientation), weld metal, and heat-affected zone (HAZ) material. The instrumented Charpy results are presented in Tables A-1 through A-3. The tables list the specimen number, test temperature, impact energy, general yield load, maximum load, brittle fracture load, and crack arrest load. The load time curves are presented in Figures A-4 through A-6. It can readily be observed that the features of the load-time curves change as a function of temperature. The energy values listed in the table are those obtained from the impact machine dial. Each curve falls into one of the six distinctive notch-bar bending classifications shown in Figure A-7. The pertinent data used in the analysis of each record are the general yield load (P_{GY}), the maximum load (P_{max}), the fast (brittle) fracture load (P_F), and the arrest load. The load-temperature curves obtained for the three materials are shown in Figures A-8 through A-10.

TABLE A-1. INSTRUMENTED CHARPY IMPACT RESULTS FOR THE IRRADIATED BASE METAL SPECIMENS FROM THE MONTICELLO 30 DEGREE SURVEILLANCE CAPSULE

(The energy values listed are obtained from the impact machine dial.)

Specimen Identification	Test Temperature, F	Impact Energy ft-lb	General Yield, Load P_{GY}, lb	Maximum Load, P_{max}, lb	Fast Fracture, Load, lb	Arrest Load, lb
JE3	0	7.0	3299	3299	3246	23
JDU	40	24.8	3140	4026	4010	256
JDJ	60	30.5	3033	4034	4034	594
JE1	76	44.1	2988	4020	4020	734
JDY	100	55.4	3061	4274	4211	1544
JD1	110	58.7	2848	4306	4278	1757
JE5	120	43.3	2821	4077	4077	1138
JCP	160	75.5	2777	4200	4101	2442
JE4	200	91.0	2639	4026	N/A	N/A
JDA	300	110.0	2497	3947	N/A	N/A
JD5	350	103.0	2454	3813	N/A	N/A
JD4	400	105.0	2383	3699	N/A	N/A

TABLE A-2. INSTRUMENTED CHARPY IMPACT RESULTS FOR THE IRRADIATED WELD METAL SPECIMENS FROM THE MONTICELLO 30 DEGREE SURVEILLANCE CAPSULE

(The energy values listed are obtained from the impact machine dial.)

Specimen Identification	Test Temperature, F	Impact Energy ft-lb	General Yield, Load P_{GY}, lb	Maximum Load, P_{max}, lb	Fast Fracture, Load, lb	Arrest Load, lb
JEK	-80	24.5	3538	4290	4290	460
JEL	-60	22.5	3368	4038	4034	185
JJE	-40	68.7	3494	4487	3569	1327
JJP	-35	22.0	3380	3892	3880	819
D6B	-30	22.9	3451	4093	4093	488
JKA	-30	71.3	3482	4668	4227	1847
JEM	-20	39.5	3274	4290	4259	1118
D57	-15	78.5	3475	4318	3605	1438
JJM	0	36.2	3222	4180	4176	721
JEP	0	65.2	3382	4377	4265	1987
JEY	20	75.8	3116	4184	3861	1875
JJT	76	96.0	2955	4014	3175	2100
JJ7	160	118.5	2777	4033	N/A	N/A
JEV	225	127.5	2761	3892	N/A	N/A
JK5	300	113.0	2529	3636	N/A	N/A

TABLE A-3. INSTRUMENTED CHARPY IMPACT RESULTS FOR THE IRRADIATED HAZ METAL SPECIMENS FROM THE MONTICELLO 30 DEGREE SURVEILLANCE CAPSULE

(The energy values listed are obtained from the impact machine dial.)

Specimen Identification	Test Temperature, F	Impact Energy ft-lb	General Yield, Load P_{GY}, lb	Maximum Load, P_{max}, lb	Fast Fracture, Load, lb	Arrest Load, lb
JKD	-79	19.5	3573	4144	4129	114
JLE	-60	28.5	3490	4400	4393	122
JKK	-40	65.0	3408	4464	4272	1217
JLC	-20	40.0	3486	4160	4160	2352
JKT	-10	33.0	3522	4129	4125	1343
JLB	-10	50.1	3408	4345	4298	2186
JL2	0	57.5	3211	4408	4389	1970
JKM	76	110.2	2909	4031	N/A	N/A
JLM	159	103.0	2775	3893	N/A	N/A
JLK	225	123.3	2785	4054	N/A	N/A
D72[a]	40	21.3	3104	3786	3786	673

(a) The notch was located approximately 1/8 inches from the fusion line as determined by past-test etching. ASTM E185 specifies the notch be less than 1/32 inches from the fusion line.

SPECIMEN NO. :	JE3
TEST TEMPERATURE (F) :	0
DIAL ENERGY, (FT-LBS) :	7
GENERAL YIELD LOAD (LB) :	3299
MAXIMUM LOAD (LB) :	3299
FAST FRACTURE LOAD (LB) :	3246
ARREST LOAD (LB) :	23

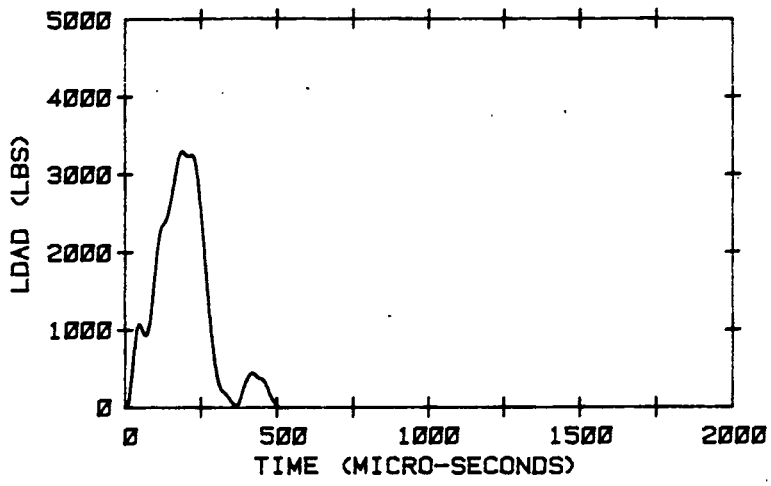

SPECIMEN NO. :	JOU
TEST TEMPERATURE (F) :	40
DIAL ENERGY, (FT-LBS) :	24.8
GENERAL YIELD LOAD (LB) :	3140
MAXIMUM LOAD (LB) :	4026
FAST FRACTURE LOAD (LB) :	4010
ARREST LOAD (LB) :	256

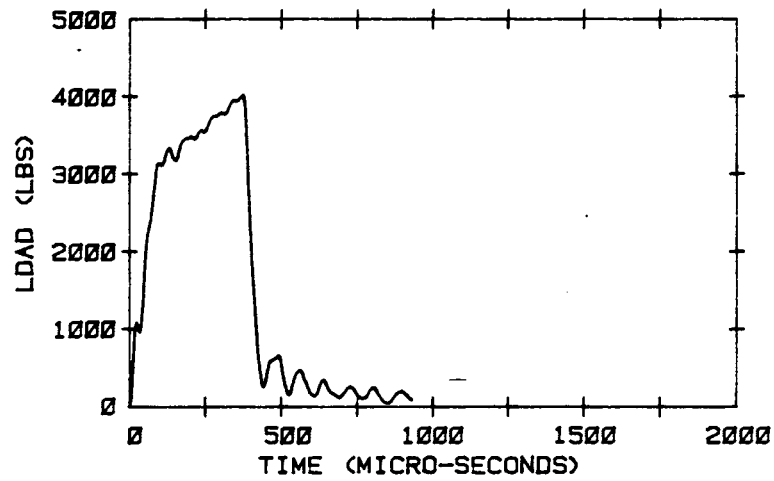

SPECIMEN NO. :	JDJ
TEST TEMPERATURE (F) :	60
DIAL ENERGY, (FT-LBS) :	30.5
GENERAL YIELD LOAD (LB) :	3033
MAXIMUM LOAD (LB) :	4034
FAST FRACTURE LOAD (LB) :	4034
ARREST LOAD (LB) :	594

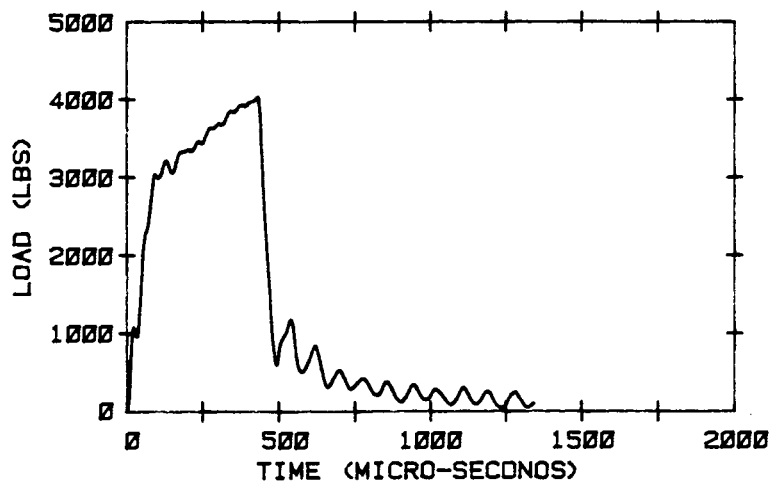

FIGURE A-4. INSTRUMENTED CHARPY IMPACT DATA FOR IRRADIATED BASE METAL SPECIMENS FROM THE MONTICELLO 30 DEGREE SURVEILLANCE CAPSULE

SPECIMEN NO. : JE1
TEST TEMPERATURE (F) : 76
DIAL ENERGY, (FT-LBS) : 44.1
GENERAL YIELD LOAD (LB) : 2988
MAXIMUM LOAD (LB) : 4020
FAST FRACTURE LOAD (LB) : 4020
ARREST LOAD (LB) : 734

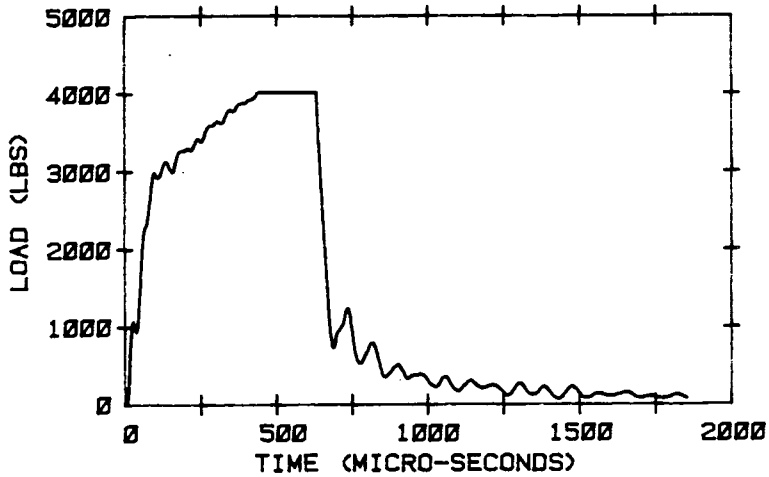

SPECIMEN NO. : JOY
TEST TEMPERATURE (F) : 100
DIAL ENERGY, (FT-LBS) : 55.4
GENERAL YIELD LOAD (LB) : 3061
MAXIMUM LOAD (LB) : 4274
FAST FRACTURE LOAD (LB) : 4211
ARREST LOAD (LB) : 1544

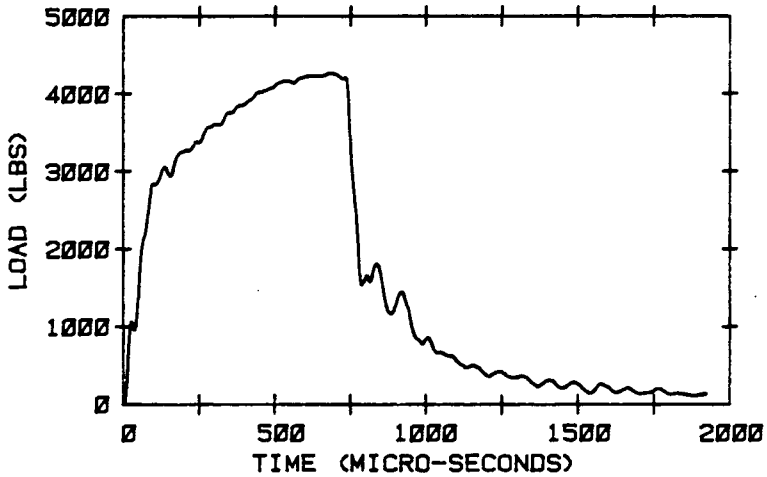

SPECIMEN NO. : J01
TEST TEMPERATURE (F) : 110
DIAL ENERGY, (FT-LBS) : 58.7
GENERAL YIELD LOAD (LB) : 2848
MAXIMUM LOAD (LB) : 4306
FAST FRACTURE LOAD (LB) : 4278
ARREST LOAD (LB) : 1757

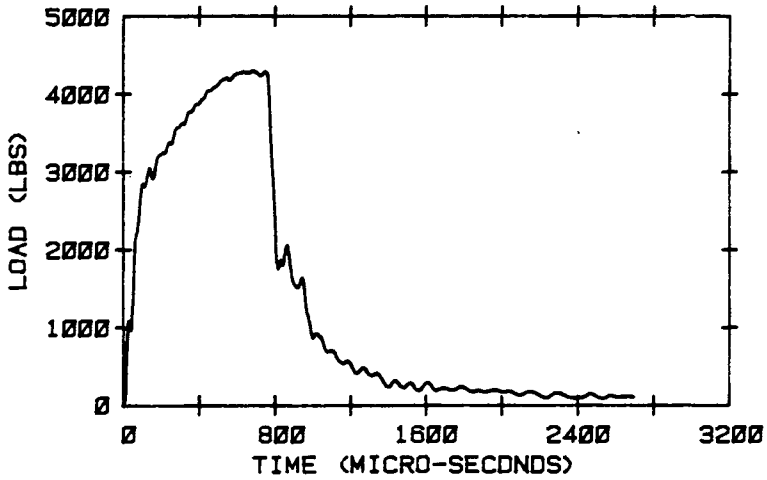

FIGURE A-4. (Continued)

SPECIMEN NO. : JE5
TEST TEMPERATURE (F) : 120
DIAL ENERGY, (FT-LBS) : 43.3
GENERAL YIELD LOAD (LB) : 2821
MAXIMUM LOAD (LB) : 4077
FAST FRACTURE LOAD (LB) : 4077
ARREST LOAD (LB) : 1138

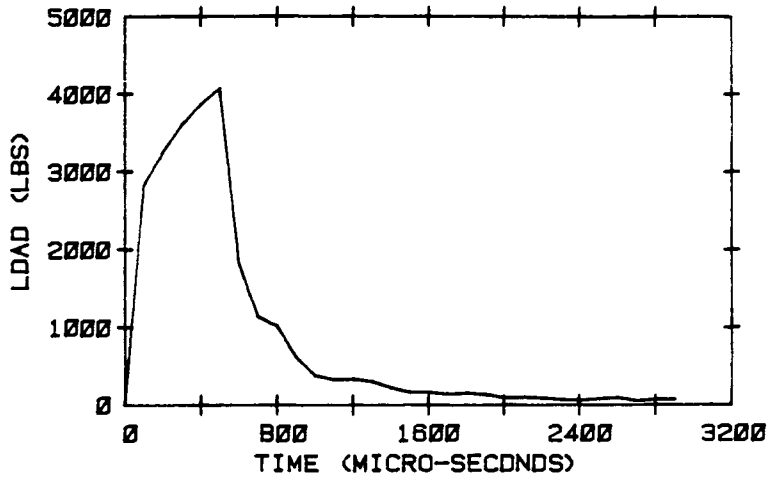

SPECIMEN NO. : JCP
TEST TEMPERATURE (F) : 160
DIAL ENERGY, (FT-LBS) : 75.5
GENERAL YIELD LOAD (LB) : 2777
MAXIMUM LOAD (LB) : 4200
FAST FRACTURE LOAD (LB) : 4101
ARREST LOAD (LB) : 2442

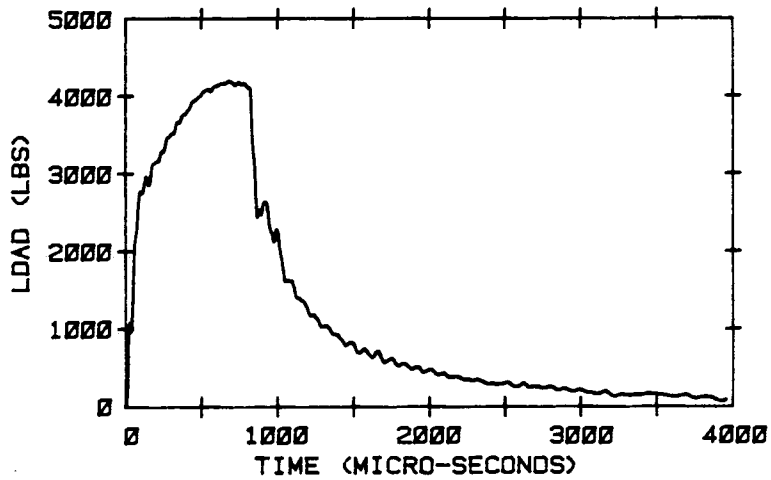

SPECIMEN NO. : JE4
TEST TEMPERATURE (F) : 200
DIAL ENERGY, (FT-LBS) : 91
GENERAL YIELD LOAD (LB) : 2639
MAXIMUM LOAD (LB) : 4026
FAST FRACTURE LOAD (LB) : N/A
ARREST LOAD (LB) : N/A

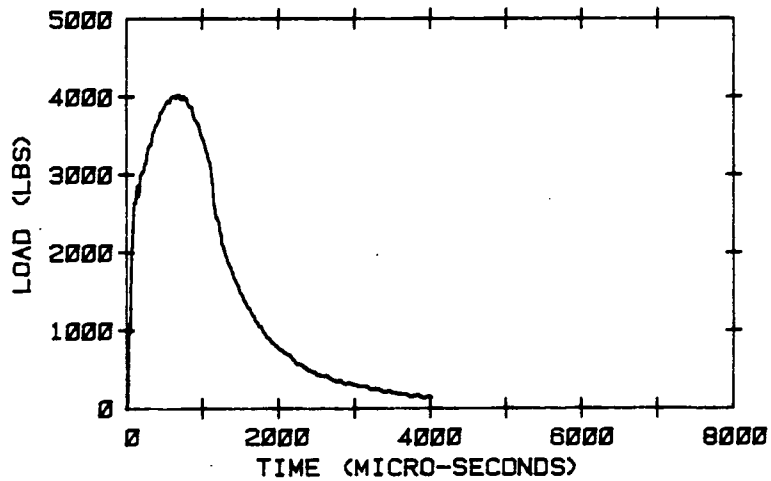

FIGURE A-4. (Continued)

SPECIMEN NO. : JDA
TEST TEMPERATURE (F) : 300
DIAL ENERGY, (FT-LBS) : 110
GENERAL YIELD LOAD (LB) : 2497
MAXIMUM LOAD (LB) : 3947
FAST FRACTURE LOAD (LB) : N/A
ARREST LOAD (LB) : N/A

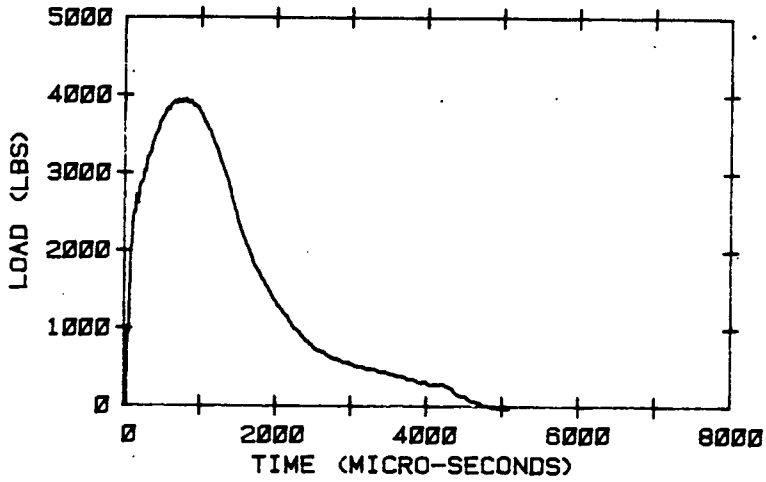

SPECIMEN NO. : J05
TEST TEMPERATURE (F) : 350
DIAL ENERGY, (FT-LBS) : 103
GENERAL YIELD LOAD (LB) : 2454
MAXIMUM LOAD (LB) : 3813
FAST FRACTURE LOAD (LB) : N/A
ARREST LOAD (LB) : N/A

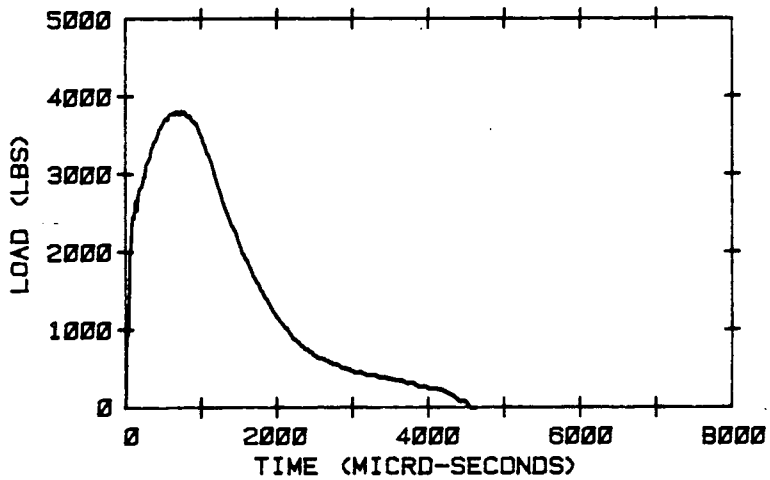

SPECIMEN NO. : J04
TEST TEMPERATURE (F) : 400
DIAL ENERGY, (FT-LBS) : 105
GENERAL YIELD LOAD (LB) : 2383
MAXIMUM LOAD (LB) : 3699
FAST FRACTURE LOAD (LB) : N/A
ARREST LOAD (LB) : N/A

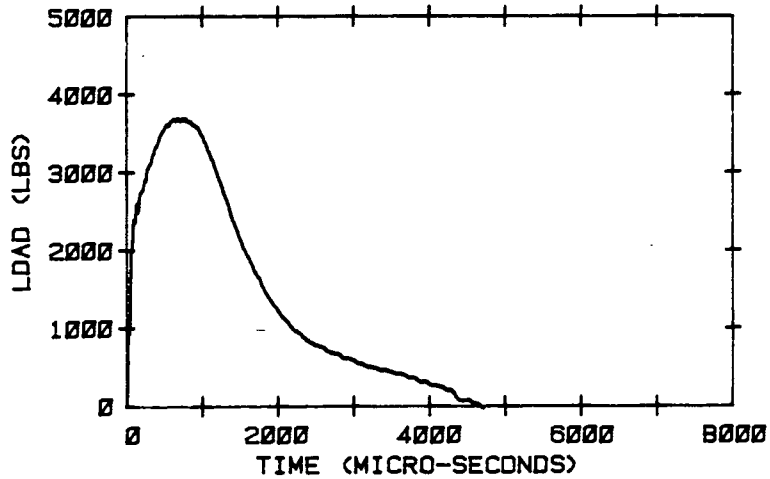

FIGURE A-4. (Concluded)

SPECIMEN NO. : JEK
TEST TEMPERATURE (F) : -80
DIAL ENERGY, (FT-LBS) : 24.5
GENERAL YIELD LOAD (LB) : 3538
MAXIMUM LOAD (LB) : 4290
FAST FRACTURE LOAD (LB) : 4290
ARREST LOAD (LB) : 460

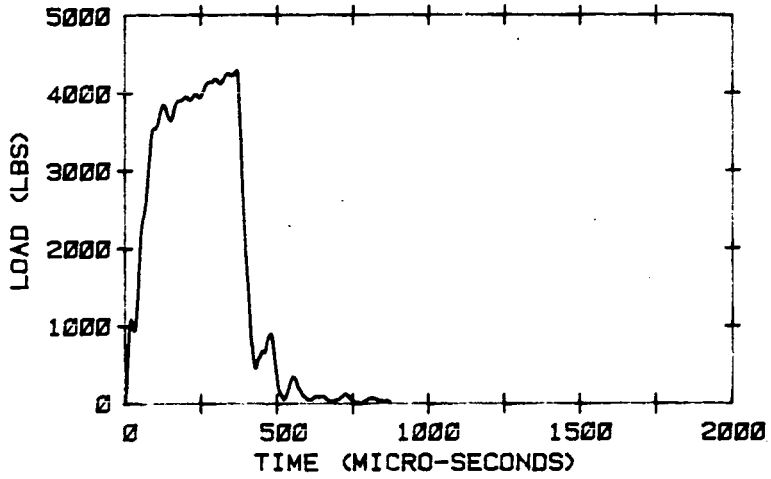

SPECIMEN NO. : JEL
TEST TEMPERATURE (F) : -60
DIAL ENERGY, (FT-LBS) : 22.5
GENERAL YIELD LOAD (LB) : 3368
MAXIMUM LOAD (LB) : 4038
FAST FRACTURE LOAD (LB) : 4034
ARREST LOAD (LB) : 185

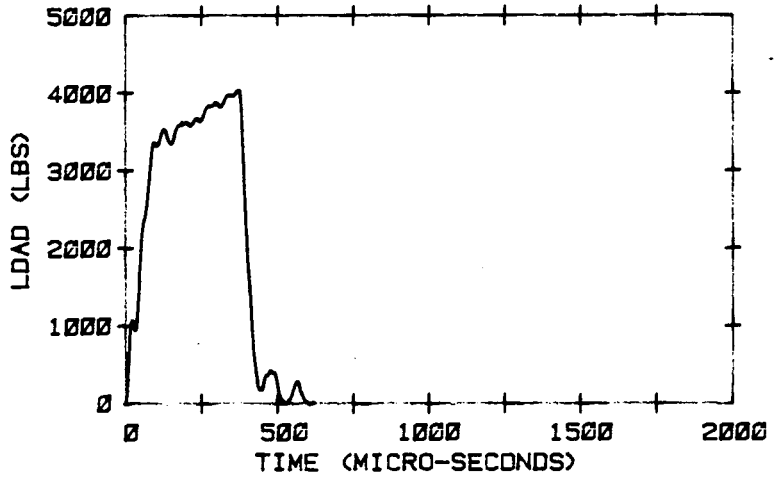

SPECIMEN NO. : JJE
TEST TEMPERATURE (F) : -40
DIAL ENERGY, (FT-LBS) : 68.7
GENERAL YIELD LOAD (LB) : 3494
MAXIMUM LOAD (LB) : 4487
FAST FRACTURE LOAD (LB) : 3569
ARREST LOAD (LB) : 1327

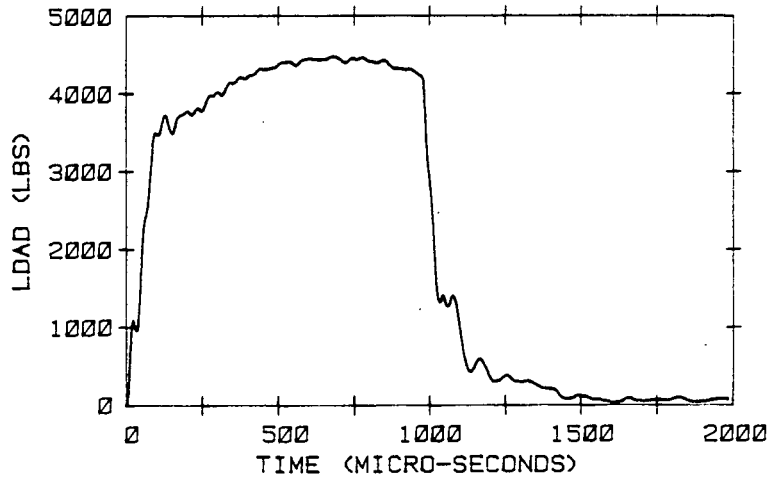

FIGURE A-5. INSTRUMENTED CHARPY IMPACT DATA FOR IRRADIATED WELD METAL SPECIMENS FROM THE MONTICELLO 30 DEGREE SURVEILLANCE CAPSULE

SPECIMEN NO. : JJP
TEST TEMPERATURE (F) : -35
DIAL ENERGY, (FT-LBS) : 22
GENERAL YIELD LOAD (LB) : 3380
MAXIMUM LOAD (LB) : 3892
FAST FRACTURE LOAD (LB) : 3880
ARREST LOAD (LB) : 819

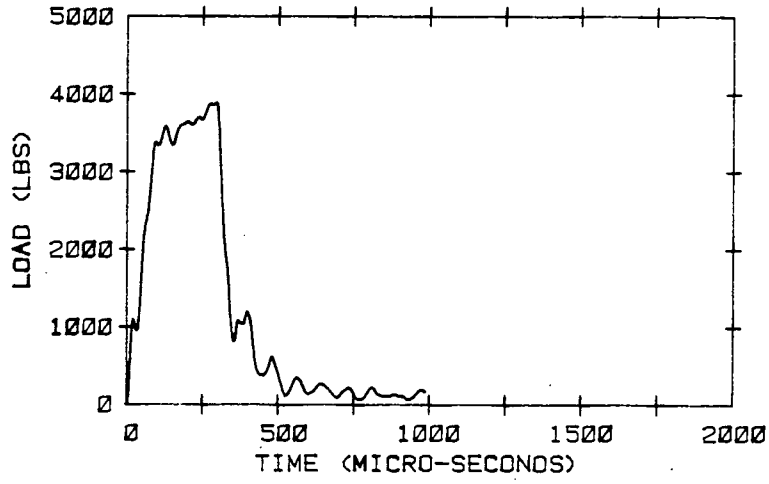

SPECIMEN NO. : JKA
TEST TEMPERATURE (F) : -30
DIAL ENERGY, (FT-LBS) : 71.3
GENERAL YIELD LOAD (LB) : 3482
MAXIMUM LOAD (LB) : 4668
FAST FRACTURE LOAD (LB) : 4227
ARREST LOAD (LB) : 1847

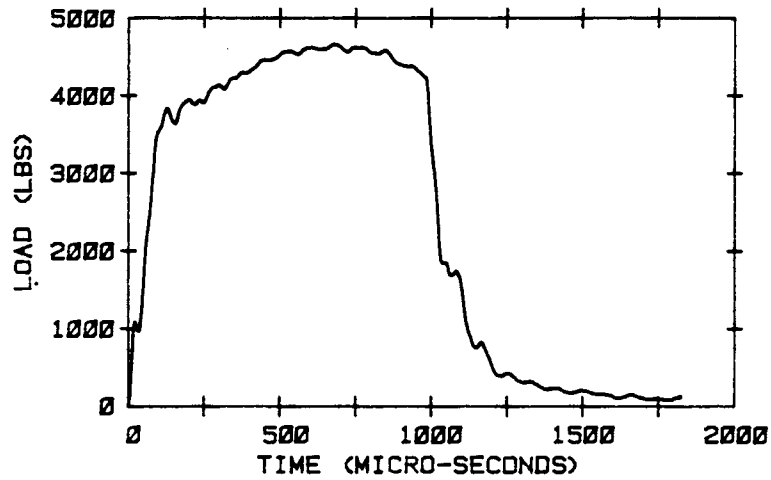

SPECIMEN NO. : 057
TEST TEMPERATURE (F) : -15
DIAL ENERGY, (FT-LBS) : 78.5
GENERAL YIELD LOAD (LB) : 3475
MAXIMUM LOAD (LB) : 4318
FAST FRACTURE LOAD (LB) : 3605
ARREST LOAD (LB) : 1438

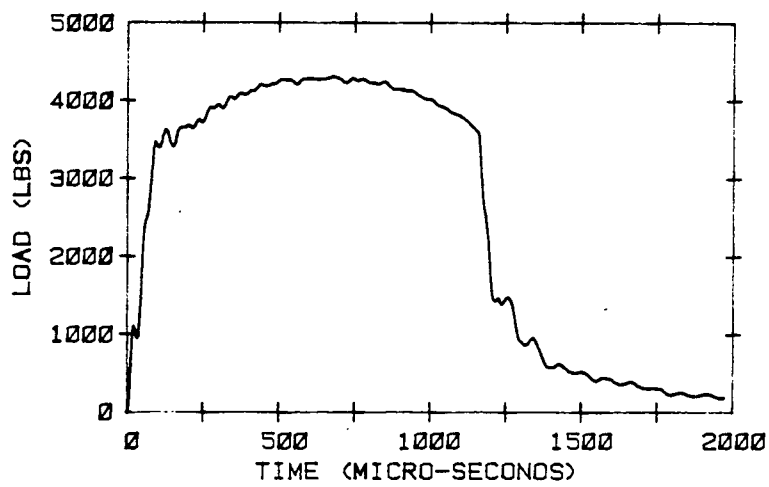

FIGURE A-5. (Continued)

SPECIMEN NO. : JEM
TEST TEMPERATURE (F) : -20
DIAL ENERGY, (FT-LBS) : 39.5
GENERAL YIELD LOAD (LB) : 3274
MAXIMUM LOAD (LB) : 4290
FAST FRACTURE LOAD (LB) : 4259
ARREST LOAD (LB) : 1118

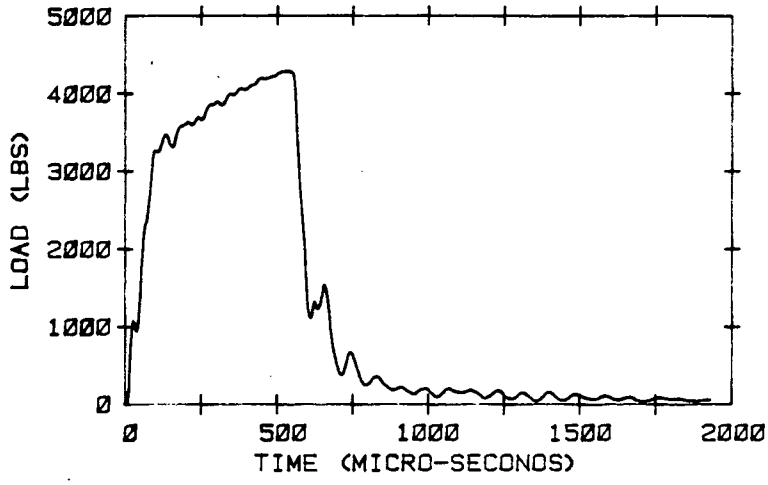

SPECIMEN NO. : D6B
TEST TEMPERATURE (F) : -30
DIAL ENERGY, (FT-LBS) : 22.9
GENERAL YIELD LOAD (LB) : 3451
MAXIMUM LOAD (LB) : 4093
FAST FRACTURE LOAD (LB) : 4093
ARREST LOAD (LB) : 488

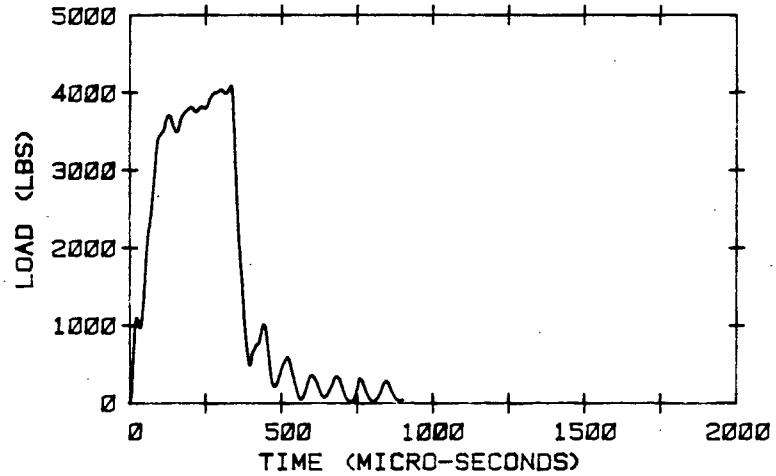

SPECIMEN NO. : JJM
TEST TEMPERATURE (F) : 0
DIAL ENERGY, (FT-LBS) : 36.2
GENERAL YIELD LOAD (LB) : 3222
MAXIMUM LOAD (LB) : 4180
FAST FRACTURE LOAD (LB) : 4176
ARREST LOAD (LB) : 721

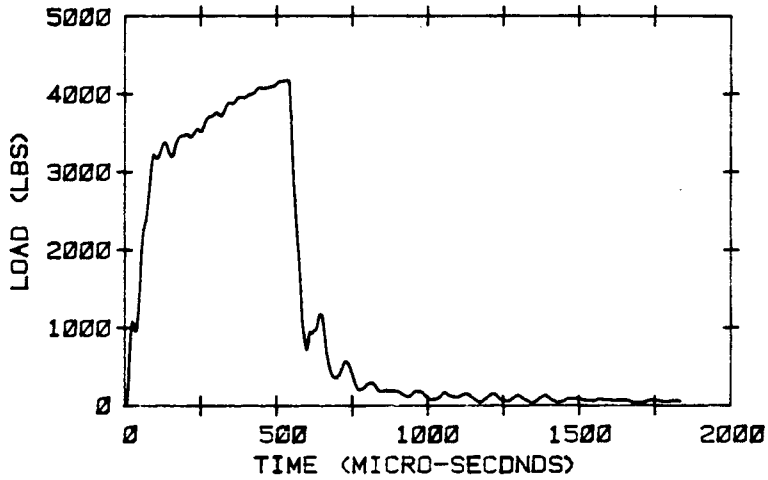

FIGURE A-5. (Continued)

SPECIMEN NO. : JEP
TEST TEMPERATURE (F) : 0
DIAL ENERGY, (FT-LBS) : 65.2
GENERAL YIELD LOAD (LB) : 3382
MAXIMUM LOAD (LB) : 4377
FAST FRACTURE LOAD (LB) : 4265
ARREST LOAD (LB) : 1987

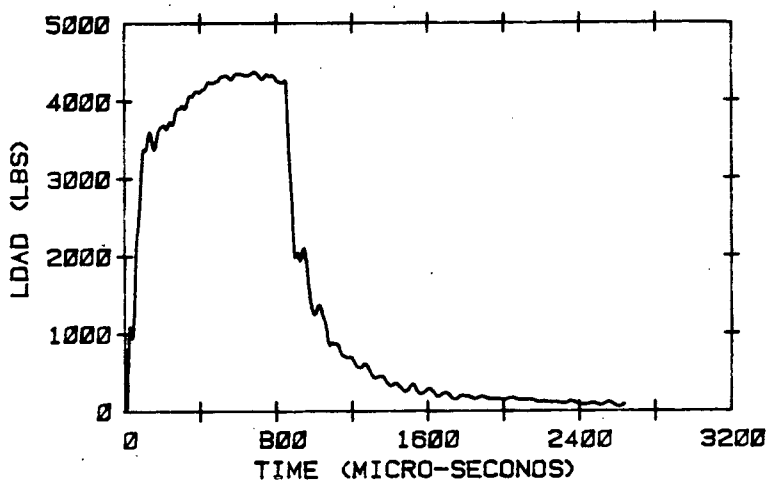

SPECIMEN NO. : JEY
TEST TEMPERATURE (F) : 20
DIAL ENERGY, (FT-LBS) : 75.8
GENERAL YIELD LOAD (LB) : 3116
MAXIMUM LOAD (LB) : 4184
FAST FRACTURE LOAD (LB) : 3861
ARREST LOAD (LB) : 1875

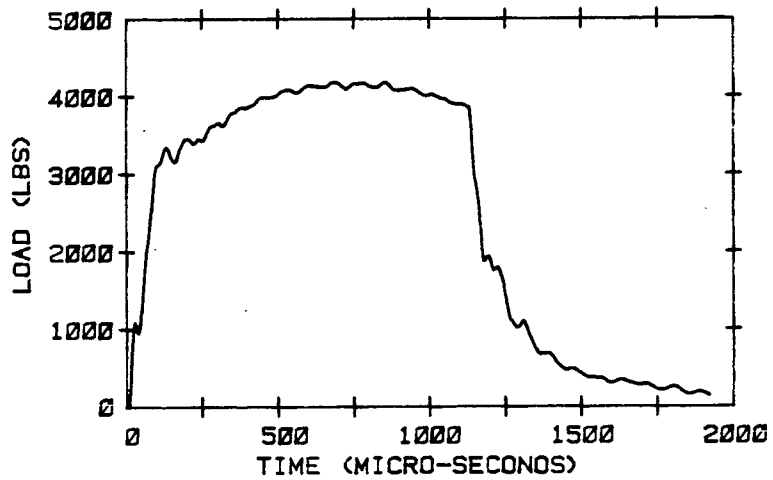

SPECIMEN NO. : JJT
TEST TEMPERATURE (F) : 76
DIAL ENERGY, (FT-LBS) : 96
GENERAL YIELD LOAD (LB) : 2955
MAXIMUM LOAD (LB) : 4014
FAST FRACTURE LOAD (LB) : 3175
ARREST LOAD (LB) : 2100

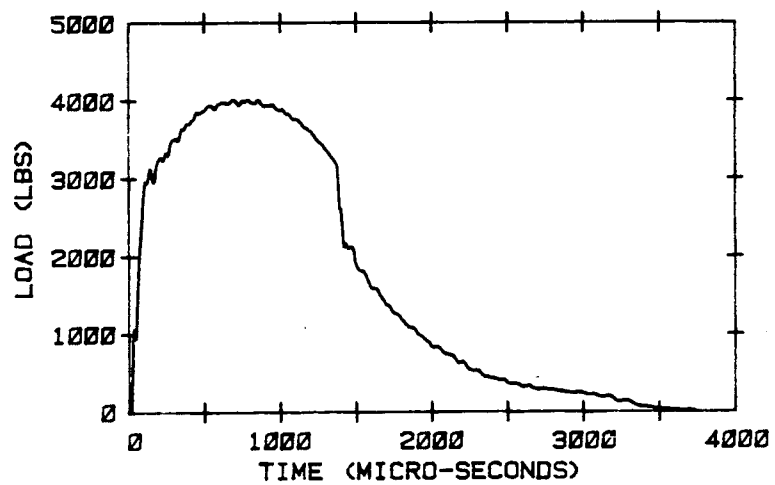

FIGURE A-5. (Continued)

SPECIMEN NO. : JJ7
TEST TEMPERATURE (F) : 160
DIAL ENERGY, (FT-LBS) : 118.5
GENERAL YIELD LOAD (LB) : 2777
MAXIMUM LOAD (LB) : 4003
FAST FRACTURE LOAD (LB) : N/A
ARREST LOAD (LB) : N/A

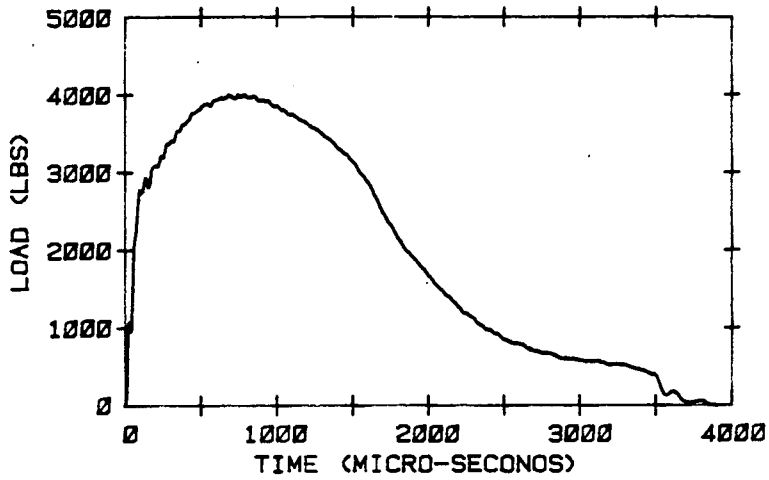

SPECIMEN NO. : JEV
TEST TEMPERATURE (F) : 225
DIAL ENERGY, (FT-LBS) : 127.5
GENERAL YIELD LOAD (LB) : 2761
MAXIMUM LOAD (LB) : 3892
FAST FRACTURE LOAD (LB) : N/A
ARREST LOAD (LB) : N/A

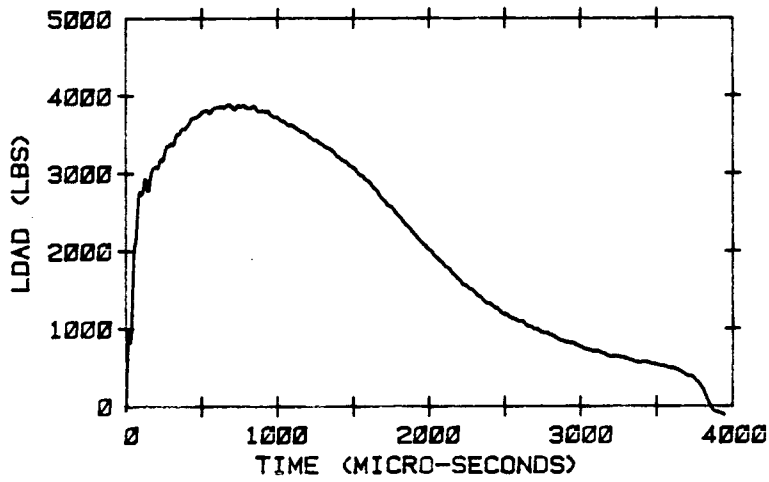

SPECIMEN NO. : JK5
TEST TEMPERATURE (F) : 300
DIAL ENERGY, (FT-LBS) : 113
GENERAL YIELD LOAD (LB) : 2529
MAXIMUM LOAD (LB) : 3936
FAST FRACTURE LOAD (LB) : N/A
ARREST LOAD (LB) : N/A

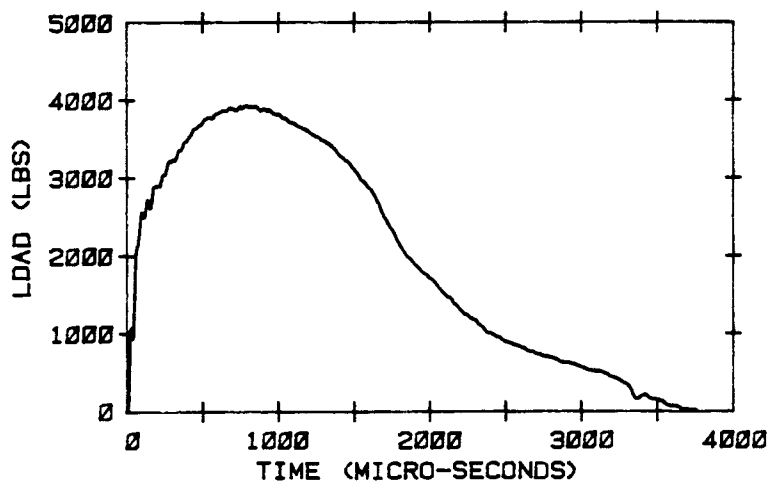

FIGURE A-5. (Concluded)

SPECIMEN NO. : JKD
TEST TEMPERATURE (F) : -79
DIAL ENERGY, (FT-LBS) : 19.5
GENERAL YIELD LOAD (LB) : 3573
MAXIMUM LOAD (LB) : 4144
FAST FRACTURE LOAD (LB) : 4129
ARREST LOAD (LB) : 114

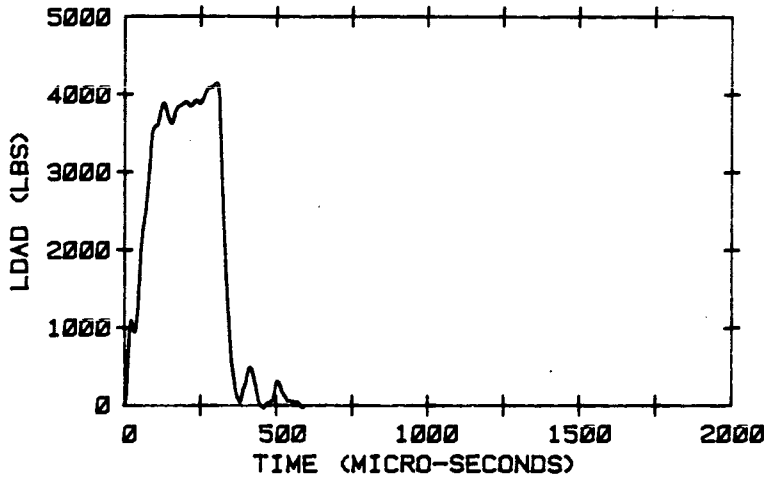

SPECIMEN NO. : JLE
TEST TEMPERATURE (F) : -60
DIAL ENERGY, (FT-LBS) : 28.5
GENERAL YIELD LOAD (LB) : 3490
MAXIMUM LOAD (LB) : 4400
FAST FRACTURE LOAD (LB) : 4393
ARREST LOAD (LB) : 122

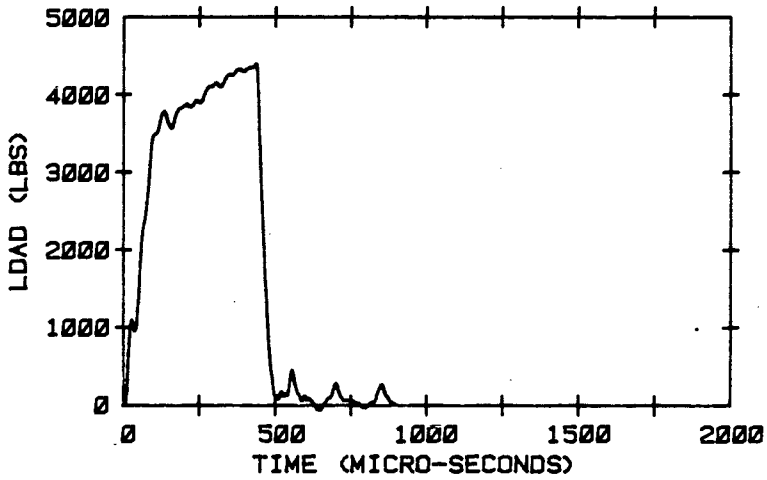

SPECIMEN NO. : JKK
TEST TEMPERATURE (F) : -40
DIAL ENERGY, (FT-LBS) : 65
GENERAL YIELD LOAD (LB) : 3408
MAXIMUM LOAD (LB) : 4464
FAST FRACTURE LOAD (LB) : 4274
ARREST LOAD (LB) : 1217

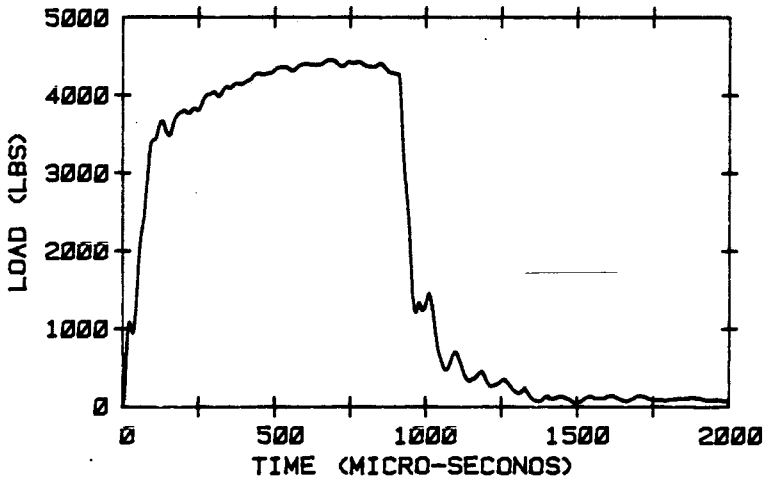

FIGURE A-6. INSTRUMENTED CHARPY IMPACT DATA FOR IRRADIATED HAZ METAL SPECIMENS FROM MONTICELLO 30 DEGREE SURVEILLANCE CAPSULE

SPECIMEN NO. : JLC
TEST TEMPERATURE (F) : -20
DIAL ENERGY, (FT-LBS) : 40
GENERAL YIELD LOAD (LB) : 3486
MAXIMUM LOAD (LB) : 4160
FAST FRACTURE LOAD (LB) : 4160
ARREST LOAD (LB) : 2352

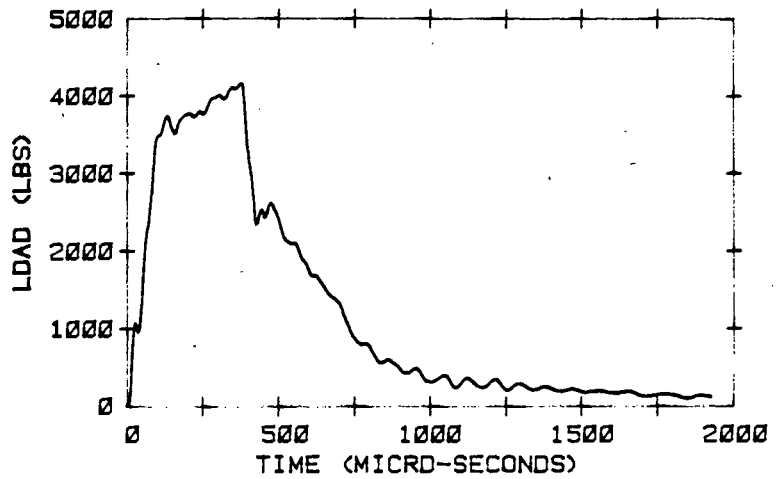

SPECIMEN NO. : JKT
TEST TEMPERATURE (F) : -10
DIAL ENERGY, (FT-LBS) : 33
GENERAL YIELD LOAD (LB) : 3522
MAXIMUM LOAD (LB) : 4129
FAST FRACTURE LOAD (LB) : 4125
ARREST LOAD (LB) : 1343

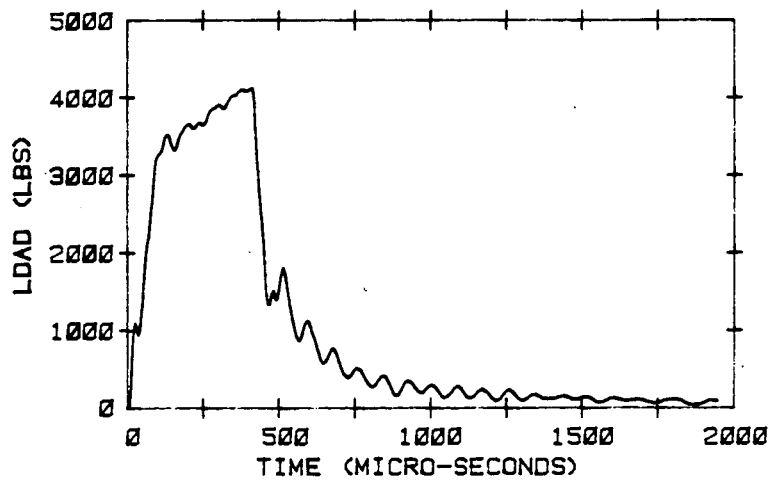

SPECIMEN NO. : JLB
TEST TEMPERATURE (F) : -10
DIAL ENERGY, (FT-LBS) : 50.1
GENERAL YIELD LOAD (LB) : 3408
MAXIMUM LOAD (LB) : 4345
FAST FRACTURE LOAD (LB) : 4298
ARREST LOAD (LB) : 2186

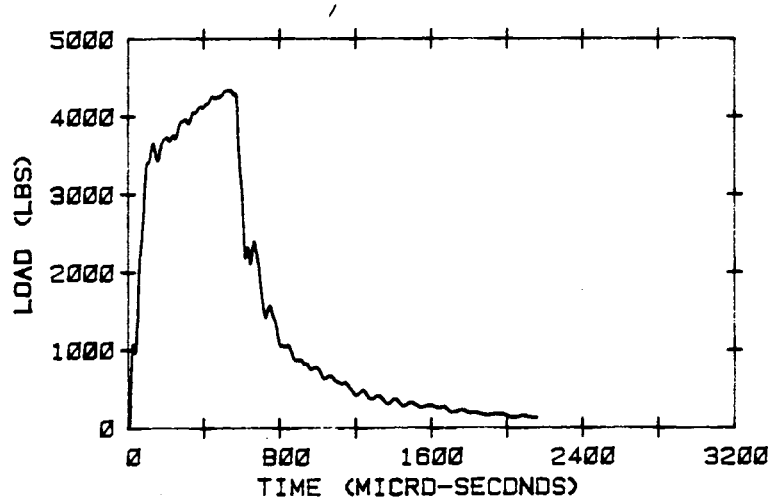

FIGURE A-6. (Continued)

SPECIMEN NO. : JL2
TEST TEMPERATURE (F) : 0
DIAL ENERGY, (FT-LBS) : 57.5
GENERAL YIELD LOAD (LB) : 3211
MAXIMUM LOAD (LB) : 4408
FAST FRACTURE LOAD (LB) : 4389
ARREST LOAD (LB) : 1970

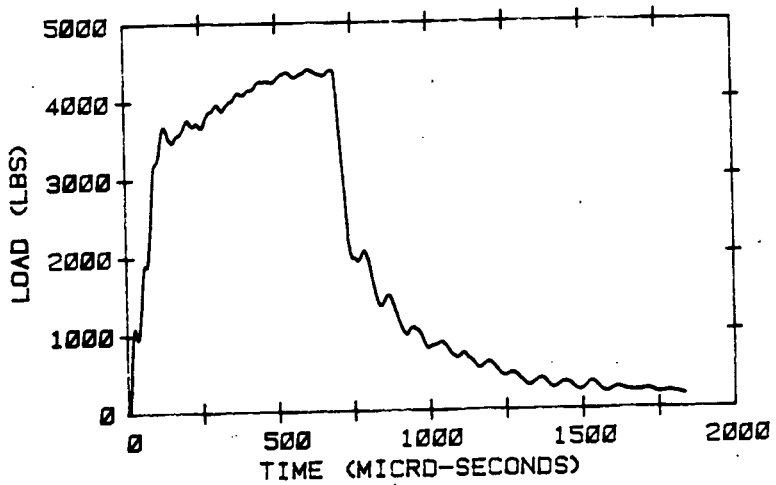

SPECIMEN NO. : JKM
TEST TEMPERATURE (F) : 76
DIAL ENERGY, (FT-LBS) : 110.2
GENERAL YIELD LOAD (LB) : 2909
MAXIMUM LOAD (LB) : 4031
FAST FRACTURE LOAD (LB) : N/A
ARREST LOAD (LB) : N/A

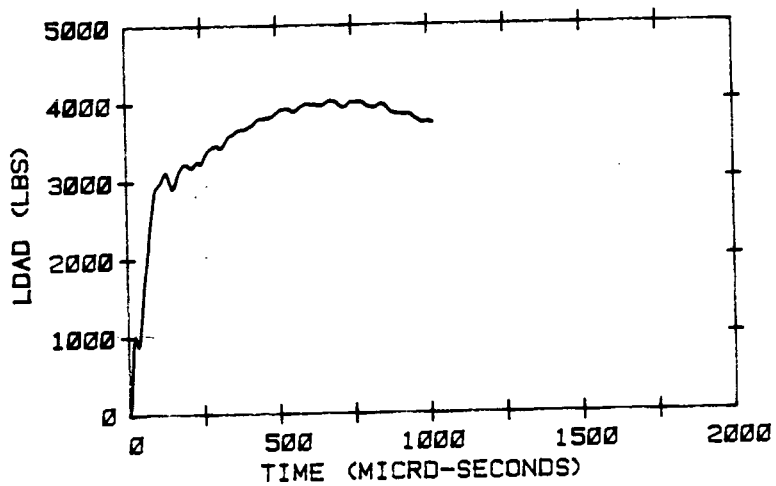

SPECIMEN NO. : JLM
TEST TEMPERATURE (F) : 159
DIAL ENERGY, (FT-LBS) : 103
GENERAL YIELD LOAD (LB) : 2775
MAXIMUM LOAD (LB) : 3893
FAST FRACTURE LOAD (LB) : N/A
ARREST LOAD (LB) : N/A

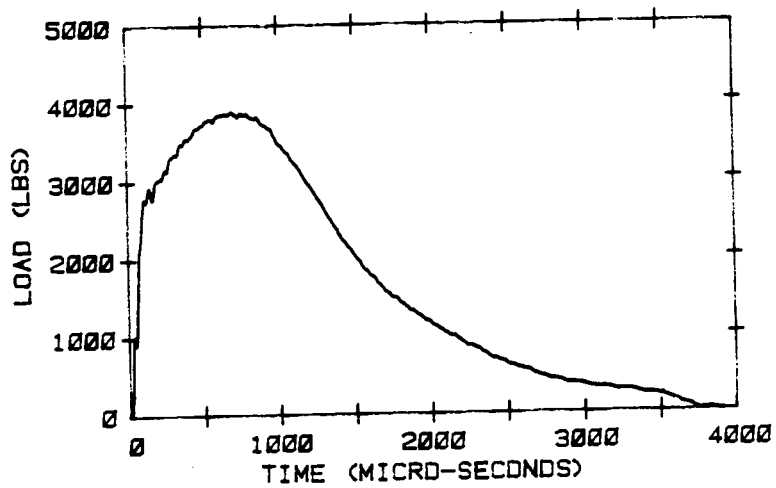

FIGURE A-6. (Continued)

SPECIMEN NO. : JLK
TEST TEMPERATURE (F) : 225
DIAL ENERGY, (FT-LBS) : 123.3
GENERAL YIELD LOAD (LB) : 2785
MAXIMUM LOAD (LB) : 4054
FAST FRACTURE LOAD (LB) : N/A
ARREST LOAD (LB) : N/A

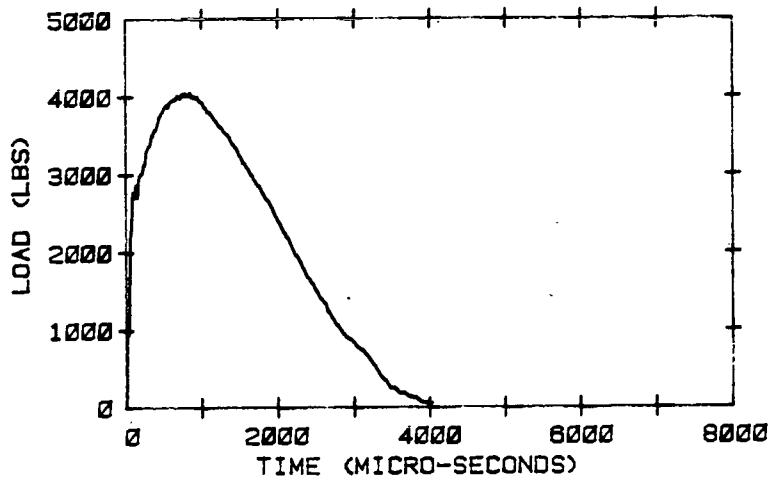

SPECIMEN NO. : D72
TEST TEMPERATURE (F) : 40
DIAL ENERGY, (FT-LBS) : 21.3
GENERAL YIELD LOAD (LB) : 3104
MAXIMUM LOAD (LB) : 3786
FAST FRACTURE LOAD (LB) : 3786
ARREST LOAD (LB) : 673

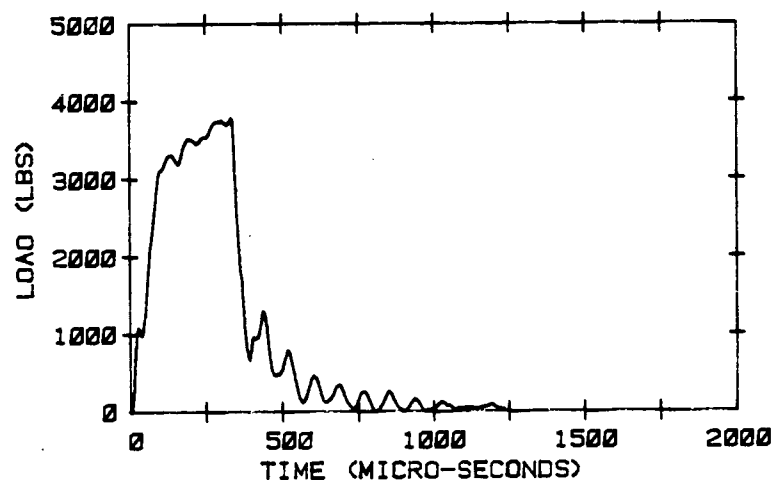

FIGURE A-6. (Concluded)

Fracture Type	Load-Displacement Curves	Raw Data	Remarks
I	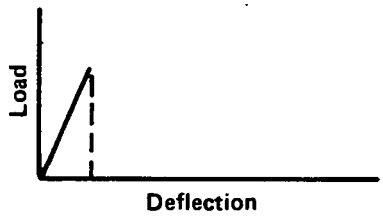	P_F	Brittle fracture
II	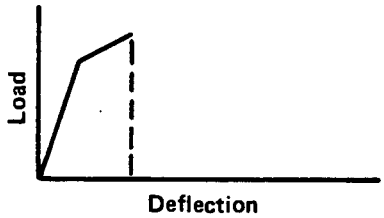	P_{GY}	Brittle fracture
III	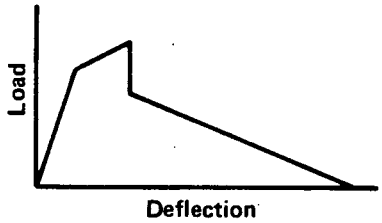	P_{GY}	Brittle fracture followed by fracture indicative of shear lip formation
IV	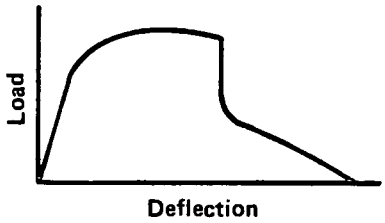	P_{GY}, P_{max}	Stable crack propagation followed by unstable brittle fracture and fracture indicative of shear lip formation
V	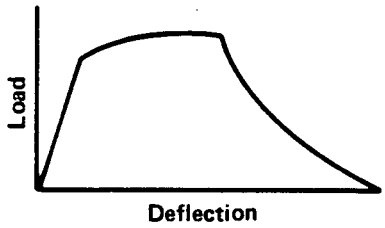	P_{GY}, P_{max}	Stable crack propagation followed by fracture indicative of shear lip formation
VI	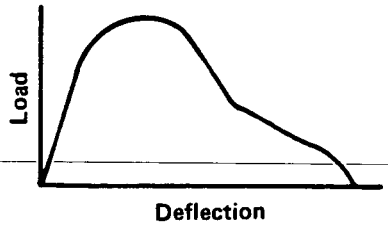	P_{GY}, P_{max}	Stable crack propagation followed by gross deformation

FIGURE A-7. THE SIX TYPES OF FRACTURES FOR NOTCHED BAR BENDING

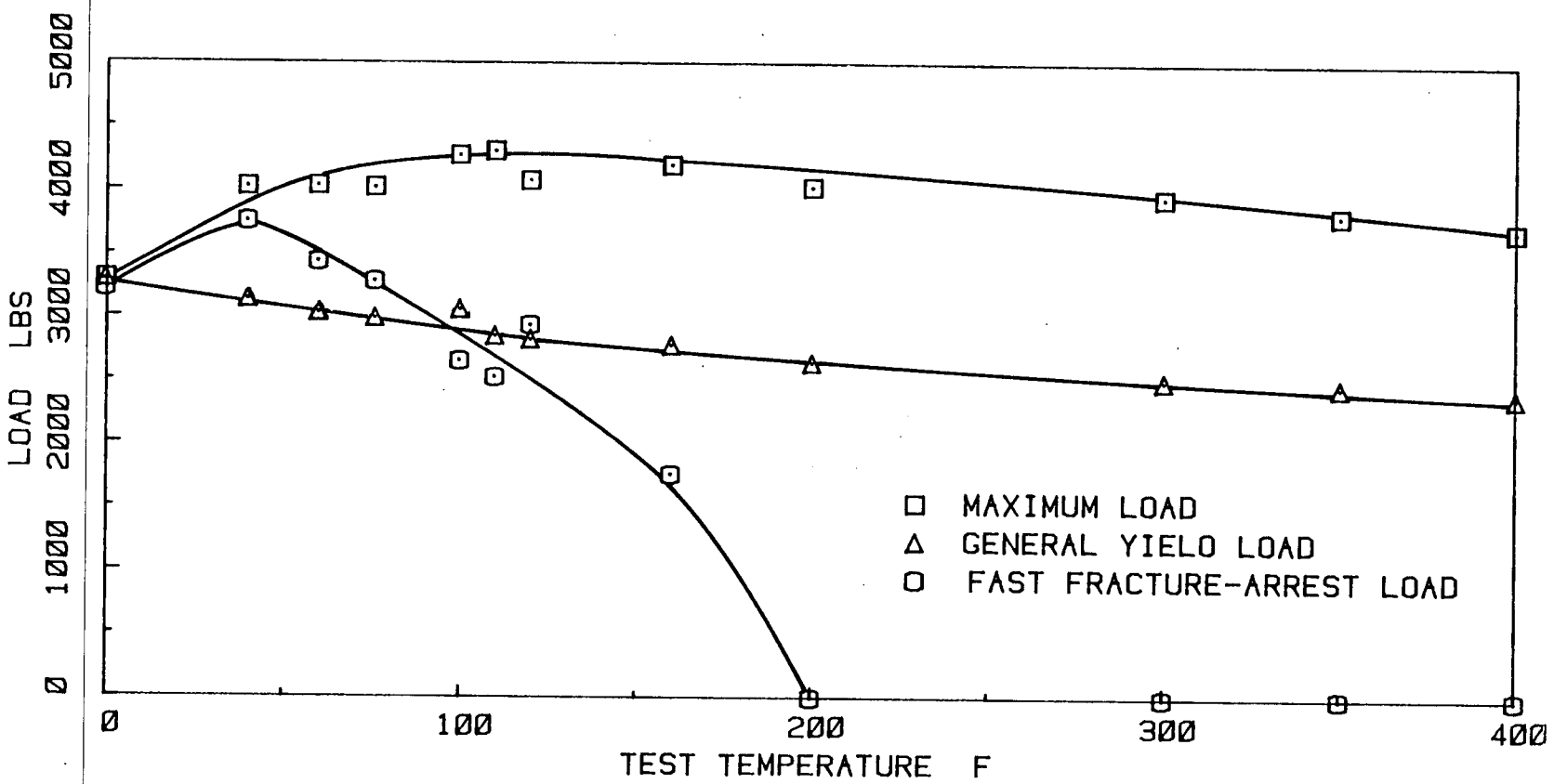

FIGURE A-8. INSTRUMENTED CHARPY LOAD VERSUS TEST TEMPERATURE FOR IRRADIATED BASE METAL SPECIMENS FROM THE MONTICELLO 30 DEGREE SURVEILLANCE CAPSULE

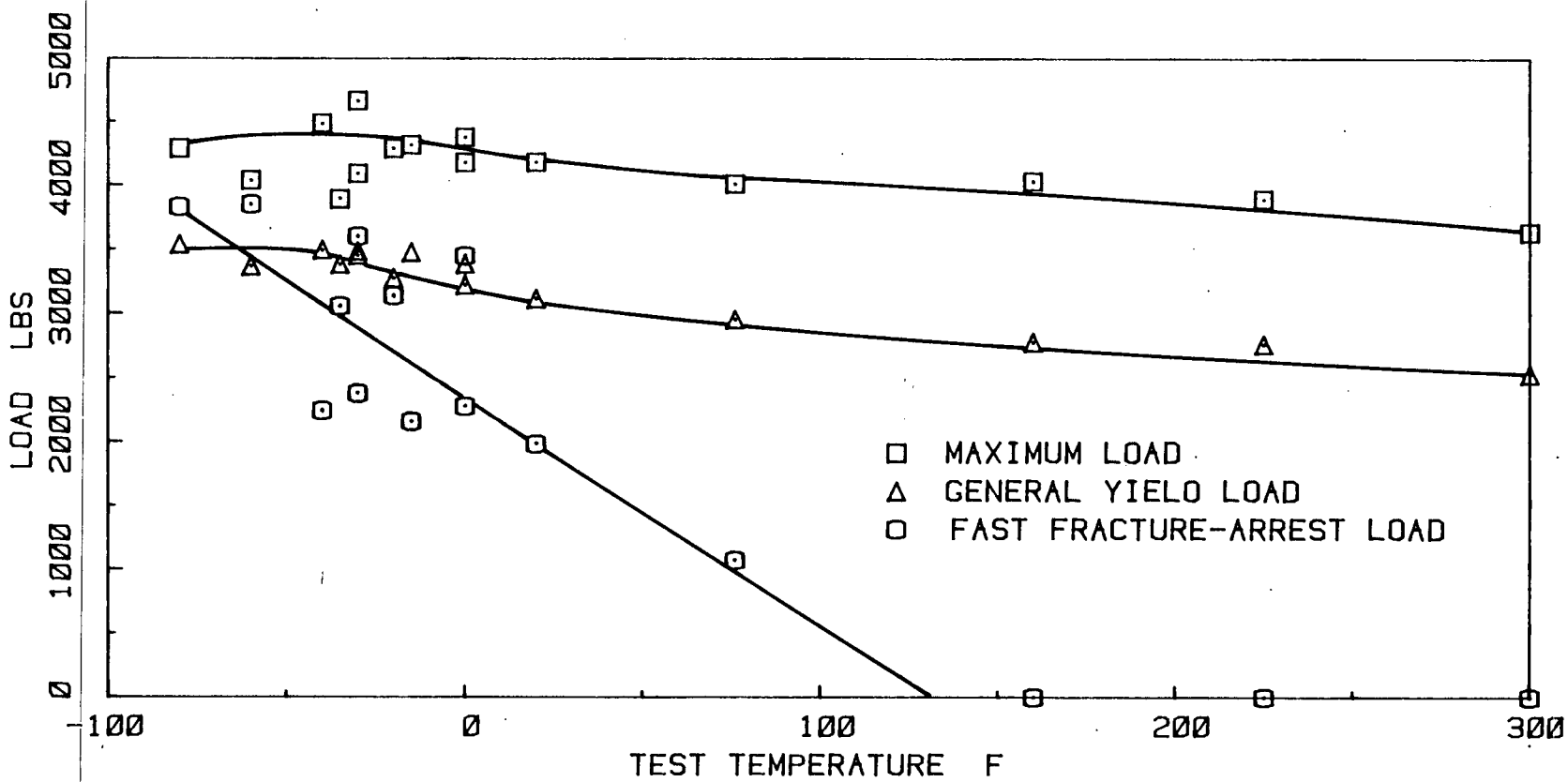

FIGURE A-9. INSTRUMENTD CHARPY LOAD VERSUS TEST TEMPERATURE FOR IRRADIATED WELD METAL SPECIMENS FROM THE MONTICELLO 30 DEGREE SURVEILLANCE CAPSULE

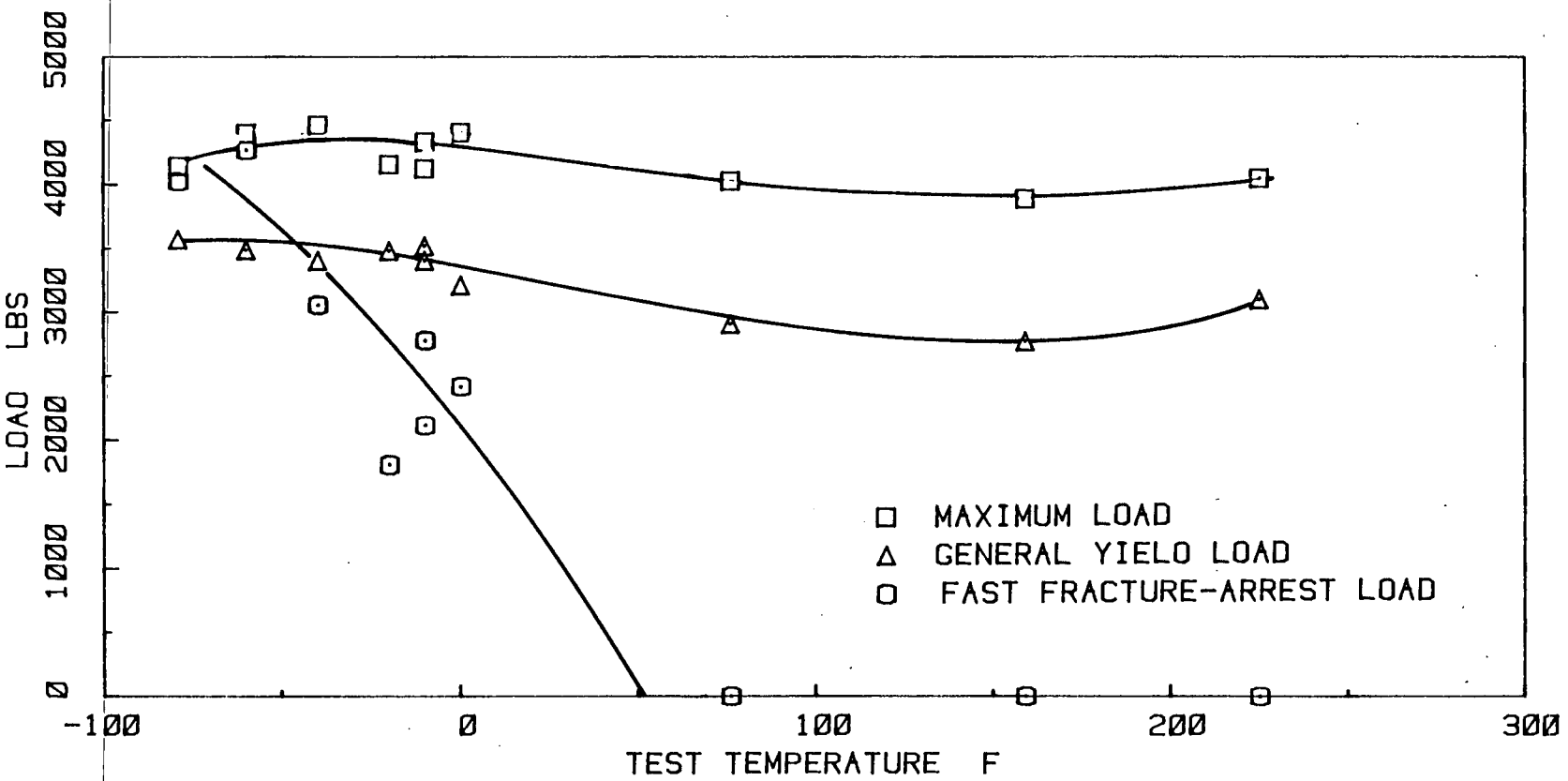

FIGURE A-10. INSTRUMENTED CHARPY LOAD VERSUS TEST TEMPERATURE FOR IRRADIATED HAZ METAL SPECIMENS FROM THE MONTICELLO 30 DEGREE SURVEILLANCE CAPSULE

APPENDIX A REFERENCES

(1) Wullaert, R. A., "Applications of the Instrumented Charpy Impact Test", in Impact Testing of Metals, American Society for Testing and Materials Special Technical Publication 466, p. 148 (1970).

(2) Perrin, J. S. and Sheckherd, J. W., "Current and Advanced Pressure Vessel Surveillance Specimen Evaluation Techniques", Proceedings of 21st Conference on Remote Systems Technology, American Nuclear Society (1973).

(3) Ireland, D. R., "Procedures and Problems Associated with Reliable Control of the Instrumented Impact Test", in Instrumented Impact Testing, American Society of Testing and Materials Special Technical Publication 563, p. 3 (1973).

(4) Server, W. L., "Impact Three-Point Bend Testing for Notched and Precracked Specimens", Journal of Testing and Evaluation, 6, 1, 29 (1978).

(5) Wullaert, R. A., editor, "C.S.N.I. Specialist Meeting on Instrumented Precracked Charpy Testing", Proceedings, Electric Power Research Institute (1980).

(6) Fearnehough, G. D. and Hoy, C. J., "Mechanism of Deformation and Fracture in the Charpy Test as Revealed by Dynamic Recording of Impact Loads", Iron and Steel Institute, 202, 912 (1964).

(7) Tetelman, A. S. and McEvily, A. J., Fracture of Structural Materials, John Wiley and Sons, Inc., New York (1967).

(8) Kobayashi, T., Takai, K., and Maniwa, H., "Transition Behavior and Evaluation of Fracture Toughness in Charpy Impact Test", Trans. Iron and Steel Institute of Japan, 7, 115 (1967).